# TRNSYS Modeling of A Hybrid Lighting System: Energy Savings and Colorimetry Analysis

by Frank Burkholder

A thesis submitted in partial fulfillment of the requirements for the degree of:

Master of Science

Mechanical Engineering

University of Wisconsin-Madison

2004

# Abstract

TRNSYS Modeling of a Hybrid Lighting System:
Building Energy Loads and Colorimetry Analysis

by Frank Burkholder
under the supervision of William Beckman, Sanford Klein, and Doug Reindl

The TRNSYS (TRaNsient SYstems Simulations) Hybrid Lighting Model was revised so that two colorimetric indices pertinent to indoor illumination, the correlated color temperature (CCT) and color rendering index (CRI), could be predicted by the model. For calculation of the CCT and CRI relevant to the hybrid lighting system, the spectral power density (SPD) of beam normal radiation was needed. Though TRNSYS provides algorithms to calculate the magnitude of beam normal radiation on any surface, no methods were provided in TRNSYS to determine the SPD of solar radiation. This thesis describes the inclusion of a spectral model in TRNSYS: Gueymard's SMARTS2 (Simple Model of the Atmospheric Radiative Transfer of Sunshine) algorithm. This algorithm was used to calculate the SPD of beam normal radiation as a function of solar position, atmospheric turbidity, moisture content, and other atmospheric parameters.

The TRNSYS hybrid lighting model, augmented by SMARTS2, was used to analyze building illumination and energy loads for a 2500 $m^2$ office building equipped with a hybrid lighting system (HLS). The HLS uses two-axis tracking collectors to collect beam normal radiation that is later divided into visible and infrared components. The visible radiation is piped to luminaires inside the building using optical fibers, while the infrared radiation is focused on thermal photovoltaic arrays and used to generate

electricity. The TRNSYS model calculated annual building energy loads (lighting, cooling, and heating) and energy savings in office buildings located in six U.S. cities: Honolulu, HI; Tucson, AZ; Reno, NV; Atlanta, GA; Seattle, WA; and Madison, WI; that were equipped with hybrid lighting systems. Using local utility rates and assuming 52 lm/W lamps efficacies (the commercial average in the U.S.), the annual energy savings per $m^2$ collector area in these cities were: \$240-Tucson, \$140-Reno, \$320-Honolulu, \$40-Atlanta, \$50-Madison, and \$60-Seattle.

For the colorimetry analysis, four representative lamp SPDs - warm white fluorescent, full spectrum fluorescent, tungsten incandescent, and halogen incandescent - were defined as standard indoor light source spectrums. Two cities were chosen to perform the analyses in: Tucson, which represented a clear climate with consistent beam normal radiation values, and Seattle, a cloudier climate. The CCT and CRI were calculated each hour during office working hours. When cloudy, the CCT and CRI of the illumination inside took on the values of the lamp providing it, but when beam normal radiation was available these values were influenced by the 5000-5500 K CCT and 80 CRI of the beam normal radiation transmitted though the HLS. Histograms showing the number of hours at varying CCT and CRI ranges for different locations and with different lamps are presented in Chapter 7.

# Acknowledgements

I would like to thank my advisors, Bill Beckman, Sandy Klein, and Doug Reindl for their support and interest in this research. I feel I've had the privilege to work with the best, and I look forward to working with them more in the future.

I would also like to thank my officemates - Charlie, Diego, Daniel, Adam, and Thomas - for the laughs, guidance, and perspective. And in the same vein I'd like to thank Tim Shedd for his interest in me and my research. He treated me like a colleague, and helped make me feel welcome and wanted here.

Thank you, Mom and Dad, Barbara and Val. I couldn't do it without you. And thank you Kahlil Gibran, wherever you are.

**Table of Contents**

**List of Figures**

# List of Tables

# Chapter 1

# **Introduction**

## 1.1 The Hybrid Lighting Project

Since 2000, Oak Ridge National Lab (ORNL) in Tennessee has spear-headed the Hybrid Lighting Project. Along with other academic, governmental, and private institutions, ORNL has attempted to demonstrate the feasibility of using the full spectrum of daylight to simultaneously provide illumination and energy savings to commercial buildings. A schematic of the system is shown in Figure 1.1.

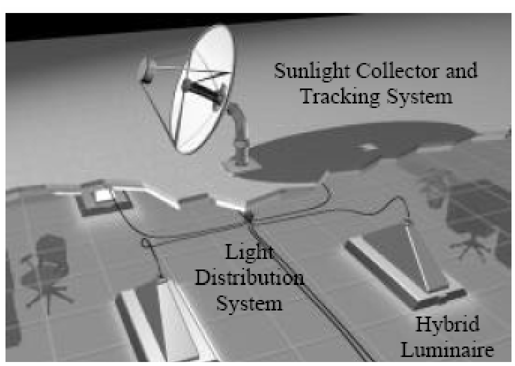


Figure 1.1: The hybrid lighting system

At this time a working prototype is providing lighting and energy savings at ORNL and another prototype at the University of Ohio is being used to grow algae in ongoing $CO_2$ mitigation research. Present goals include delivery of several more Hybrid Lighting Systems (HLS) to other industry partners as well as system redesign for better function, manufacturability, and decreased cost. ORNL estimates that commercialization of this technology could provide a significant fraction of the USA's four quadrillion kilojoule (4 Quad) commercial building lighting energy estimate , resulting in carbon reductions of up to 45 MtC per year by 2020 (EIA, 2000).

## 1.2 The University of Wisconsin's Role

The University of Wisconsin Solar Energy Laboratory specializes in thermodynamic modeling of energy systems. From the outset, the Solar Energy Lab's role in the HLS project has been to provide design assistance to ORNL by modeling the HLS in order to predict potential building energy savings using the transient systems simulation program TRNSYS (Klein et al., 2000) TRNSYS utilizes local weather and solar irradiance data with user-generated building models to calculate building lighting, heating, and cooling loads. The loads associated with a typical commercial building can be compared to the loads associated with the same building equipped with HLS. Utility rate schedules are then used in conjunction with differences in the buildings' energy usage to calculate monetary annual energy savings due to HLS technology.

But besides modeling building energy loads, the appearance of the illumination delivered and its ability to render colors are also important to quantify. Two colorimetric indices, the correlated color temperature (CCT) and color rendering index (CRI), estimate how "warm" or "cool" a light source appears and its ability to show different colors, respectively. Lighting designers need this type of information when designing a lighting system so that their clients' lighting expectations are met. A colorimetric model that utilizes the spectral model SMARTS2 (Simple Model of the Atmospheric Radiative Transfer of Sunshine) (Gueymard, 2000) was added to TRNSYS to predict CCT and CRI values.

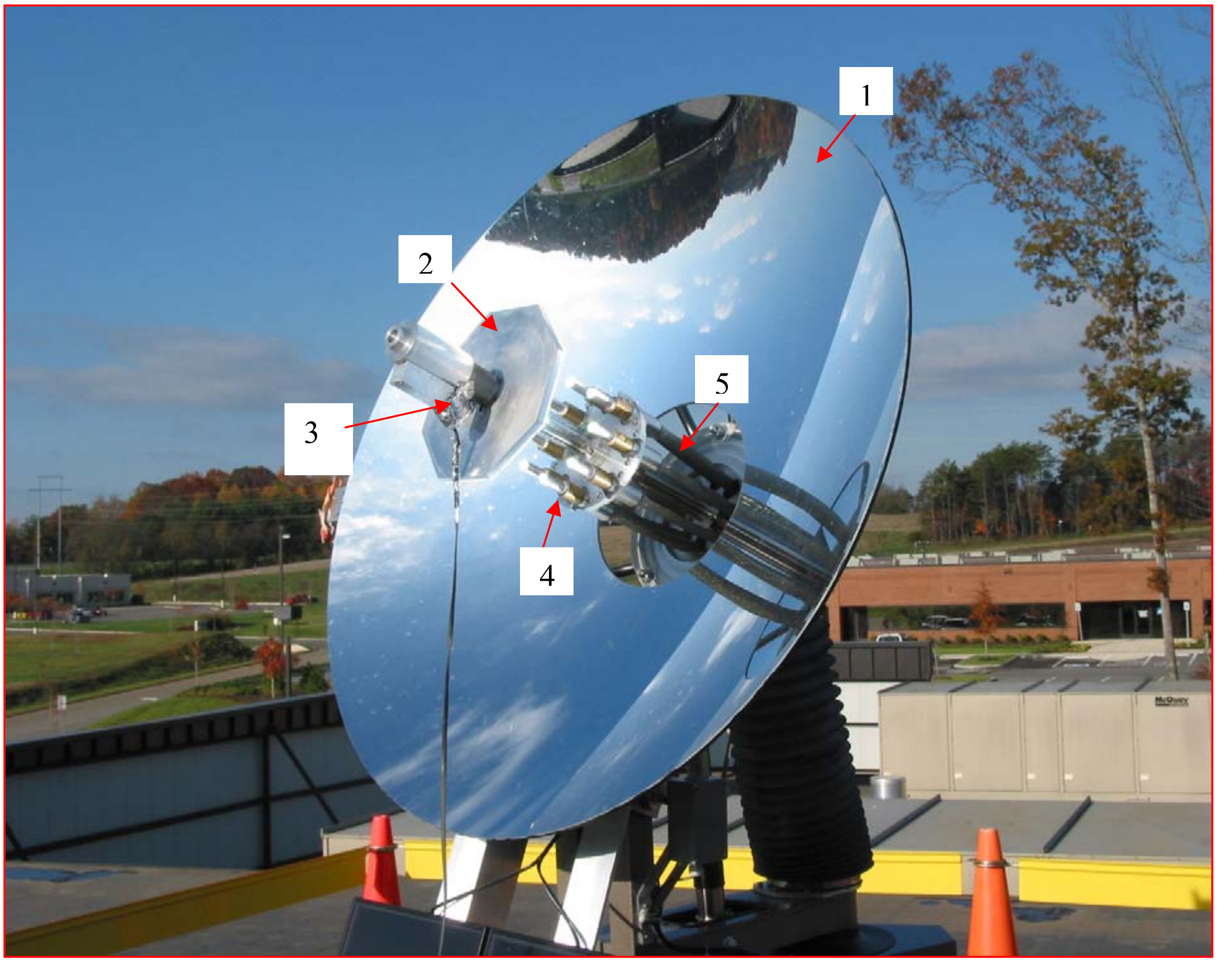

Figure 1.2 - Prototype system in Oak Ridge, TN

## 1.3 Description of the Hybrid Lighting System (HLS)

Though the HLS design continues to change, the following components can be found in all designs. Numbers in Figure 1.2 correspond to the numbered components below.

**1) A sun-tracking, focusing concave parabolic collector**

The collector gathers the terrestrial radiation and increases the power density of the sunlight by focusing it onto the smaller area of the receiving cold mirror. The reflectivity of the collector is wavelength dependent, though fairly constant (≥ 95%) across the visible spectrum. The prototype uses a 1 $m^2$ glass collector that was designed to transmit signals to trains down long stretches of railway. Other mirror options are being considered, including coated aluminum and coated plastic injection-molded mirrors.

**2) A receiving cold mirror**

The cold mirror lies near the focal point of the concentrating collector, and its two-fold purpose is to reflect the visible light into the fiber optic cable while allowing the infrared portion of the spectrum to pass through to a thermal photovoltaic array that converts the IR energy to electricity. The geometry of the cold mirror is not set; the prototype uses 8 flat off-axis mirrors to focus the visible light into 8 large core optical fibers, while another prototype under development uses one elliptical mirror to focus the sunlight into a bundle made of many fused small fibers. The advantage of the elliptical design is the reduced angle of the incoming light relative to the fiber face. However, some problems are being experienced with manufacturing the bundled fibers.

**3) A thermal photovoltaic array**

The thermal photovoltaic (TPV) array is a Gallium Antimonide (GaSb) photovoltaic device that is sensitive in the near infrared spectrum. The benefit of using the TPV array in the HLS is that energy in the near infrared spectrum, which would otherwise be wasted, can be used to generate electricity. A conventional silicon (Si) photovoltaic would not be as effective due to its sensitivity in the visible spectrum and insensitivity in the near infrared. The thermal photovoltaic voltaic array, manufactured by TX Crystals, is made up of 100 cells wired in series over an area of approximately 180 $cm^2$. Performance is limited by the least amount of IR radiation incident on one of these cells; therefore considerable work has attempted to provide uniform radiation flux to the array (Dye, 2003). The TPV and the necessary diffuser are not shown in Figure 1.2 but their intended location is indicated by 3.

**4) Quartz rod diffusers**

Early tests of the HLS that did not include quartz rods at the entrance to the fiber optic cables resulted in several spectacular failures associated with local heating of the fiber ends. The purpose of the quartz rods is to diffuse the incident light thereby providing uniform illumination to the fiber end. Unfortunately significant reflective losses occur at the air/quartz rod interface.

**5) The optical fibers**

The optical fibers are used to distribute the visible light collected by the HLS. Once the filtered sunlight passes through the quartz rods, it enters 8 flexible large core polymethylmethacrylate optical fibers that are run through a hole in the roof to the building below. Attenuation of the visible light is a function of the wavelength and entrance angle of the light, the presence of bends in the fiber, and most importantly the length of the fiber. Presently each of the 8 optical fibers is run to its own luminaire. Attempts to split the light from one fiber into others have resulted in heating and eventual melting of the splitter; this is another reason that small bundled fibers are being considered as an alternative.

**6) The luminaires and control system**

Hybrid luminaires that consist of fluorescent bulbs and scored light-emitting rods are used to distribute the visible light on to work surfaces within the building. Photosensors on the ceiling monitor the illumination level in the room and control the power to the fluorescent bulbs through dimmable electronic ballasts. When solar insolation does not meet desired illumination levels, power to the fluorescent system is increased accordingly. The photosensor reacts quickly to changes in illumination levels and is also sensitive to the reflective qualities of the work surface – so much so that the system adjusts itself when a book with white pages is opened on a table


Figure 1.3: Laboratory illuminated by HLS

underneath the photosensor. The differing color temperatures of the delivered sunlight and the light provided by the fluorescent bulbs make this change noticeable. Work is ongoing to determine the best luminaire (Earl, 2003) and photosensor (Pande-Rolfsen, 2003) fit for the HLS application.

# Chapter 2

# The Physics of Light

## 2.1 Light as Radiant Energy

Light is visually evaluated radiant energy. The importance of this definition is twofold: 1) it describes light as electromagnetic radiation and therefore part of the electromagnetic spectrum, and 2) it introduces the concept that an observer's spectrally defined visual response changes incident electromagnetic radiation into the perception of light. Because light is both radiation as well as an observer-derived quantity, two different systems of terms and units can be used to describe it: radiometric and photometric. "Radiometric" pertains to its fundamental electromagnetic character, while "photometric" pertains to the visual sensation of light.

Table 2.1 lists radiometric and photometric terms, symbols and units in the SI system. Analogous terms are grouped; e.g. Radiant flux is the radiometric quantity from which other radiometric quantities are derived, and Luminous flux is the photometric equivalent for photometric quantities.

Table 2.1 - Radiometric and Photometric terms, symbols, and units

| Term | Symbol | Defining Equation | Description | SI Unit |
|---|---|---|---|---|
| Radiant Flux | $F_e$ | $F_e = \frac{\partial Q}{\partial t}$ | Total quantity of radiation emitted from a source | Watt (*W*) |
| Luminous Flux | $F$ | $F = K_m \int F_e(\lambda)V(\lambda)d\lambda$ | Total quantity of light emitted from a source | lumen (*lm*) |
| Radiant Intensity | $I_e$ | $I_e = \frac{\partial F_e}{\partial \omega}$ | Total quantity of radiation emitted by a point source in a given solid angle | $\frac{W}{\omega}$ |
| Luminous Intensity | $I$ | $I = \frac{\partial F}{\partial \omega}$ | Total quantity of light emitted by a point source in a given solid angle | candela (*cd*)<br><br>*lm/ω* |
| Irradiance | $E_e$ | $E_e = \frac{\partial F_e}{\partial A_r}$ | Density of radiation incident on a surface or plane | $\frac{W}{m^2}$ |
| Illuminance | $E$ | $E = \frac{\partial F}{\partial A_r}$ | Density of light incident on a surface or plane | lux $(lm/m^2)$ |
| Radiance | $L_e$ | $L_e = \frac{\partial I_e}{\partial A_s \cos\theta}$ | Amount of radiation emitted or reflected from a source in a given direction | $\frac{W}{\omega \cdot m^2}$ |
| Luminance | $L$ | $L = \frac{\partial I}{\partial A_s \cos\theta}$ | Amount of light emitted or reflected from a source in a given direction | $cd/m^2$<br><br>$lm/\omega\text{-}m^2$ |

$\delta Q$ is the total energy emitted by a source (Joules)
$\delta t$ is the time interval (seconds)
*Km* is the maximum spectral luminous efficacy (683 lm/W photopic, 1700 lm/W scotopic)
$V(\lambda)$ is the relative spectral luminous efficiency curve (photopic or scotopic)
$\delta\omega$ is the solid angle of the source (steradians)
$A_r$ is the area of the receiving surface or plane
$A_s$ is the surface area of the source
$\theta$ is the angle between the given direction and the normal to the emitting surface

As indicated in the table, luminous flux is derived from radiant flux through the maximum spectral efficacy of the radiation and the relative spectral luminous efficiency curve.

Though readers are most likely comfortable with the Watt as the measure of radiative power, the candela (*cd*) and lumen (*lm*) as measures of luminous power are probably unfamiliar. Likewise, the reader may have little experience with quantities such as maximum spectral efficacy and the spectral luminous efficiency curve. For this reason, the following sections will describe these terms and relate them to the radiative character of light. In addition, the concepts of a blackbody and a spectral power distribution will be reviewed because their use is essential in deriving the lumen and relating it to the watt.

## 2.2 The Candela and Lumen

The candela (cd) emerged as a measure of luminous flux because whale and spermacetti candles were the major sources of light when the lighting standard was established in 1860 in the United States (Murdoch, 1985) In 1948 the lighting standard was refined to read "The candela is the unit of luminous intensity. The magnitude of the candela is such that the luminance of a blackbody radiator at the temperature of solidification of platinum is 60 candelas per square centimeter. (Murdoch, 1985)" Platinum solidifies at 2042 K. However, there was interest in having a luminous standard that depended only on radiometric quantities (watts). For this reason in 1979 the General Conference on Weights and Measures adopted the following definition "The candela is the luminous intensity in a given direction of a source which is emitting monochromatic radiation of frequency $540 \times 10^{12}$ Hz (555 nm) and whose radiant intensity in that direction is 1/683 W/sr. (Murdoch 1985)" The reasons for the use of 555 nm monochromatic radiation and the 1/683 value in this definition will become clear in Section 2.4 where the lumen is related to the watt.

With the candela defined, the lumen can be related to the candela through the use of a 1 candela spherically symmetric source at the center of a 1 meter radius sphere, shown in Figure 2.1. The lumen, also a measure of luminous flux, is defined as the rate at which luminous energy is incident on a 1 $m^2$ surface 1 meter away from a uniform point source of 1 cd. The total luminous flux emitted by a uniform 1 cd source is 4π lumens.

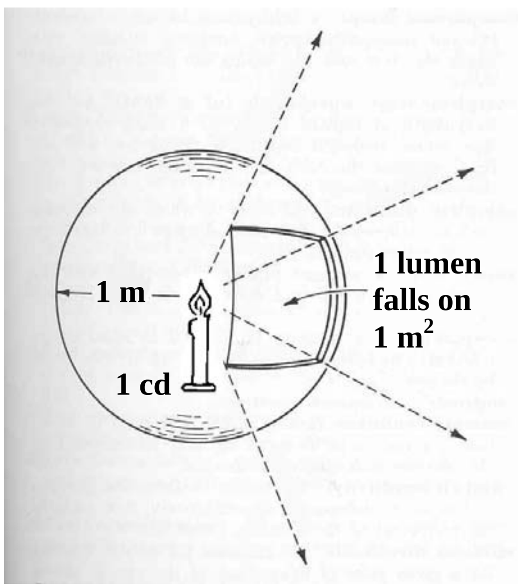


Figure 2.1 - Definition of 1 lumen (IESNA, 2000)

## 2.3 Blackbody Radiation

Light from current day sources, particularly incandescent sources, can often be described by likening the light source to a blackbody radiator operating at a given temperature.

A blackbody is defined as a body that absorbs all radiation incident upon it. Because it is a perfect absorber, it is also a perfect radiator. A blackbody radiates more power at each wavelength and more total power than any other incandescent radiator of the same surface area operating at the same temperature.

Planck developed the following equation to relate the power radiated by a blackbody at each wavelength to its temperature:

$$L_{e,\lambda} = c_1 \lambda^{-5} (e^{c_2/\lambda T} - 1)^{-1} \qquad 2.1$$

$$c_1 = 3.742 \times 10^{20} \quad (W - nm^4/m^2)$$
$$c_2 = 1.439 \times 10^{7} \quad (nm - K)$$
$$\lambda = \text{wavelength}(nm)$$
$$T = \text{temperature}(K)$$

Equation 2.1 was used to create the spectral power distribution for a blackbody at 2042 K. Figure 2.2 shows the radiance, $L_{e,\lambda}$, calculated at 5 nm intervals. In this spectral power distribution (SPD), the radiant power of each 5 nm band is plotted versus the wavelength at which it occurs. The total power of this SPD can be found by integrating the area underneath the curve. In this case, the integrated power is 972 kW/m$^2$.

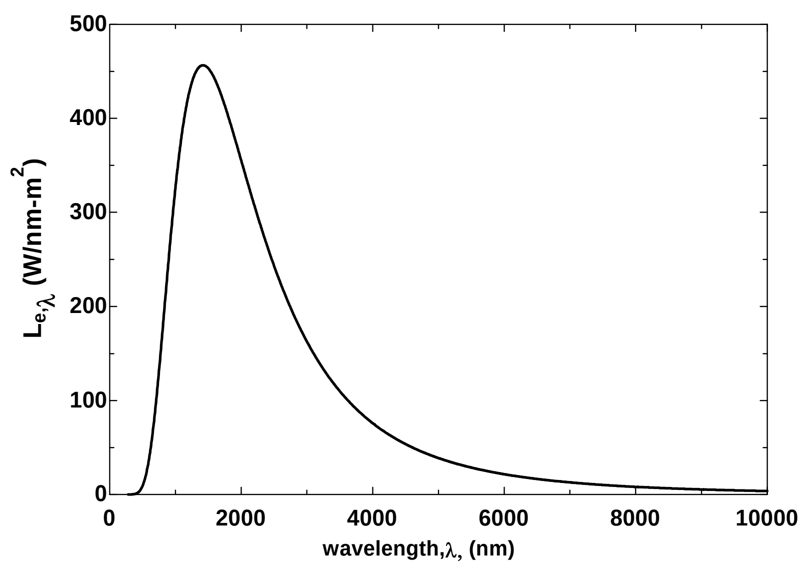

Figure 2.2 - Blackbody spectral power density, 2042 K

## 2.4 Relating the Lumen to the Watt

The human eye shows varying sensitivity to different wavelengths of light. For the purpose of eliciting a visual sensation, these sensitivity differences can be summarized by the photopic and scotopic luminous efficiency curves shown in Figure 2.3. Figure 2.3 was created in the following manner. In the 1920's K.S. Gibson and E.P.T. Tyndall reasoned that the sensation of luminance (brightness) could be separated from that of color in a comparison test of two radiation sources whose wavelength differed by only 10 nm. During the period from 1921 to 1923, Gibson and Tyndall had 52 observers make luminance comparisons over the entire visible spectrum (380 nm to 770 nm). They found that the minimum power required to achieve a prescribed constant luminance level occurred at 555 nm (Murdoch, 1985). All other wavelengths required more power to achieve a desired luminance level. They then defined the spectral luminous efficiency as

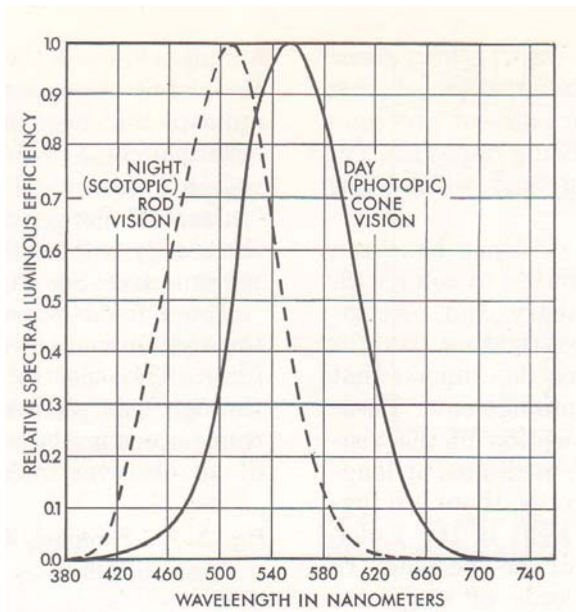


Figure 2.3 - Photopic and Scotopic *V(λ)*

$$V(\lambda) = \frac{L_{555}}{L_{\lambda}} \quad 2.2$$

where $L_{555}$ is the luminance at 555 nm, and $L_{\lambda}$ is the luminance at another wavelength in the visible range that appears to give the same luminance as $L_{555}$.

Equation 2.2 defines the photopic visibility curve. As will be described further in Chapter 5, the rods and cones in the human eye are responsible for the human visual response, and their response is partially dependent on luminance levels. For luminance levels greater than 3.4 cd/m$^2$, the cones dominate the visual response, yielding the photopic *V(λ)* curve. For luminance levels less than 0.034 cd/m$^2$, the rods dominate, yielding the scotopic *V(λ)* curve. As will be shown later, the rods, which are more prevalent in the perimeter of the retina, are more sensitive than the cones. For this reason, under low illumination levels at night a star can often be glimpsed out of the corner of one's eye but disappears when focused on.

The photopic V(λ) curve, the 1948 blackbody standard, and the spectral power distribution of a blackbody at 2042 K (the melting point of platinum) are necessary to relate the lumen (luminous flux) to the watt (radiant flux). The calculation proceeds as follows. The spectral power distribution of a blackbody at 2042 K (Figure 2.2) is multiplied by the photopic *V(λ)* curve (Figure 2.3). This yields the spectral light power density, Figure 2.4, where the ordinate is the luminous power density in light watts per m$^2$ (lW/m$^2$). The photopic *V(λ)* curve peaks at 555 nm. This is the only wavelength where 1 watt = 1 light watt. The area

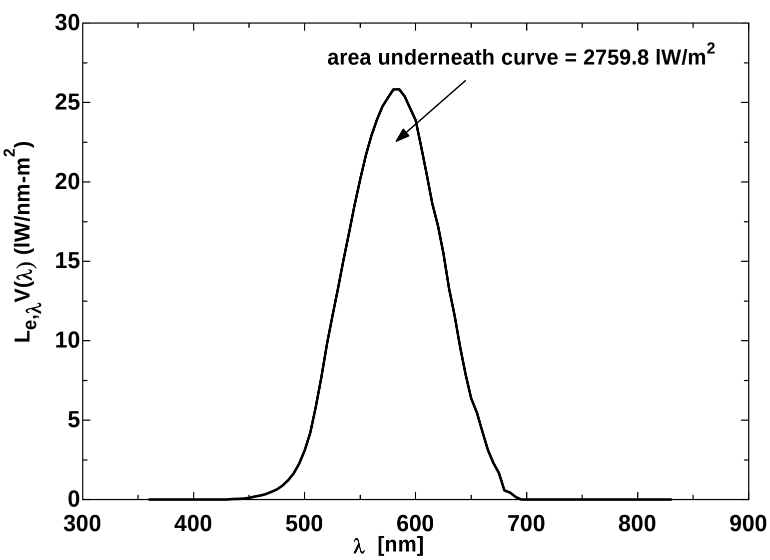


Figure 2.4 - Spectral Light Power Density

underneath the curve, 2759.8 $lW/m^2$, indicates the total luminous spectral power density present in the 2042 K blackbody spectrum.

From the definition of the 1948 luminous standard, platinum at 2042 K emits 60 $cd/cm^2$. Assuming it is perfectly diffusing, the luminance is $60\pi$ $lm/cm^2$, or $1.88495\times10^6$ $lm/m^2$. Dividing the luminance by the total luminous spectral power density means that each light watt must create $1.88495\times10^6$ $lm/m^2$ / 2759.8 $lW/m^2$ = 683 lumens (lm).

## 2.5 Luminous efficacy

Luminous efficacy is defined as the amount of luminous power in a given amount of radiative power. The value calculated above, 683 lm/W, is the maximum spectral luminous efficacy radiant power can have under photopic viewing conditions. Put another way, 1 W of radiant power at 555 nm gets multiplied by the photopic $V(\lambda)$ curve, which at 555 nm = 1. The 1 W of radiant power in this case gets converted to 1 lW of luminous power. Light watts are converted to lumens by the constant 683 lumens/lW. So 1 W of radiant power at 555 nm became 683 lm, hence a luminous efficacy of 683 lm/W. But because the photopic $V(\lambda)$ is less than 1 at all other wavelengths, the efficacy for conversion of radiant power to luminous power at these other wavelengths will always be less than 683 lm/W. In Table 2.1, the *Km* value for photopic vision is 683 lm/W. For night vision, the scotopic *Km* is calculated in a similar manner yielding 1700 lm/W.

Chapter 3

# Review of Full Spectrum and Daylighting Literature

## 3.1 Full spectrum lighting - better quality light?

One selling point for the hybrid lighting system (HLS) is that it will generate energy savings that will, over time, justify the expense of the system. The energy load analyses presented in Chapter 7 generally support this statement. Another more debated and controversial benefit of a HLS, is that the light provided is "better" than that provided by conventional lamps. Some contend that full spectrum light makes it easier for us to see (Blackwell, 1985), improves mood (Rosenthal, 1984), increases productivity, increases retail sales (Heschong Mahone Group, 1999), and offers other positive health effects (Jewet et al.,1986 and Mayron et al.,1974).

Advocates for daylighting and full spectrum lighting generally start with the assumption that sunlight is better than conventional light sources because humans evolved under its influence and have various physiological reactions that are dependent on it. Differences in the spectral power distribution (SPD) of sunlight and conventional fluorescent bulbs are offered as physical reasons for differences in visual and physiological response. Figure 3.1 shows the relative SPD of beam normal radiation (air mass 1.5), a full spectrum fluorescent bulb, and a warm white fluorescent bulb across the visible spectrum.

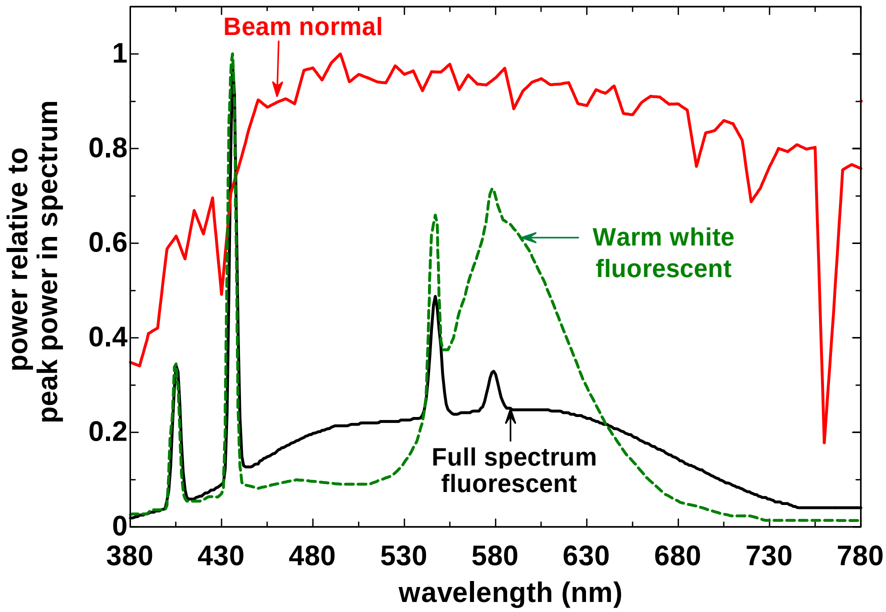


Figure 3.1: Spectral power distributions of three light sources in the visual range

As Figure 3.1 illustrates, sunlight provides substantial power in all wavelengths across the visible range with significant power in wavelengths below 500 nm. The full spectrum fluorescent shares these characteristics to some extent, and for this reason there is some overlap in claimed benefits of daylighting and full spectrum fluorescent bulbs. However, the warm white fluorescent SPD is markedly different: it does not have a smooth distribution of power across wavelengths in the visible and near UV ranges. Instead, most of its power is in the yellow and green parts of the spectrum with a few isolated spikes at shorter wavelengths.

The purpose of this chapter is to investigate the previously mentioned claims of the benefits of daylighting and full spectrum lighting that are relevant to the HLS. First, generally accepted physiological responses of the human body to light are reviewed. Next, studies that attribute more controversial benefits are discussed. The chapter concludes by summarizing the results of the studies and notes that, except for a few possible exceptions, HLS lighting will not deliver the dramatic positive effects on human behavior or health that could be inferred from some studies.

## 3.2 Physiological Responses to Light

Light plays an important role in many of the physiologic processes of plants and mammals. In this section, some of the relationships that light has with our health are explored. Where applicable, the adverse health effects of excessive light exposure will be highlighted as well.

The tanning process is driven by dermal exposure to solar radiation in both the UVB radiation (290 nm - 320 nm) and UVA (320 nm - 400 nm) wavelengths. Unfortunately, prolonged exposure to UVB radiation has been linked to skin cancer (FDA, 2000).

Some chemical reactions in the skin and blood are stimulated by light absorption. The chemical precursor of vitamin D absorbs ultraviolet radiation in the skin and underlying subcutaneous tissue and is transformed into vitamin D. Rickets, the vitamin D deficiency disease, is curable through exposure to sunlight (Wurtman, 1975).

Light is also used to treat neonatal jaundice, a disorder common to premature babies. The livers in these babies are not developed enough to metabolize bilirubin, but phototherapy can be used to bleach the bilirubin into a form that can be excreted (Wurtman, 1975).

The process of vision is also a physiological response to light. Light enters the eyes through the pupil and strikes the retina where photoreceptive cells change the light stimulus into a neural signal. The neural signal pathway for visual information leaves the retina through the optic nerve and terminates in visual cortex where electrical impulses from the retina are interpreted.

A second neural pathway exists in mammals. In this pathway, the neural signal travels from the retina to the suprachiasmatic nucleus in the anterior hypothalamus. The biological process affected by this secondary pathway are not completely understood (Wurtman, 1975). The suprachiasmatic nucleus sends signals to the brain, the spinal cord, and the pineal gland. This pathway may influence circadian rhythms.

Light activation of the pineal gland inhibits its release of melatonin, a hormone that has many physiological effects. Melatonin induces sleep and causes the release of serotonin, a neurotransmitter believed to be responsible for some depressions (Kalat, 1984). Melatonin shows some role in the regulation of circadian rhythms (Hill, 1992), which are 24 hour cyclic regulatory processes found in many organisms. Melatonin also influences the secretions of the pituitary, adrenal glands, and gonads. It is believed that this is the means by which light and dark cycles influence other periodic biological processes, such as ovulation (Wurtman, 1975).

## 3.3 Discussion of Daylighting and Full Spectrum Lighting Studies

Currently there are no studies that have investigated the effect the HLS has on visual performance and health. Application of daylighting and full spectrum lighting studies to the HLS must be done with care. First, HLS light is not exactly sunlight. The "sunlight" referred to in daylighting studies is usually a combination of diffuse and beam radiation like that seen on a horizontal surface. The total radiation incident on a horizontal surface (global horizontal) around noon under an air mass of 1.5 is plotted in Figure 3.2. The HLS cannot collect diffuse radiation. Its SPD is that of beam normal radiation attenuated by the spectrally dependent transmission characteristics of its components. Figure 3.2 shows the SPDs of beam normal and the HLS delivered beam normal to the interior of the building. The HLS light is still distributed relatively evenly over the visual range with significant spectral power at shorter wavelengths, but differences between the global horizontal and HLS SPDs are evident.

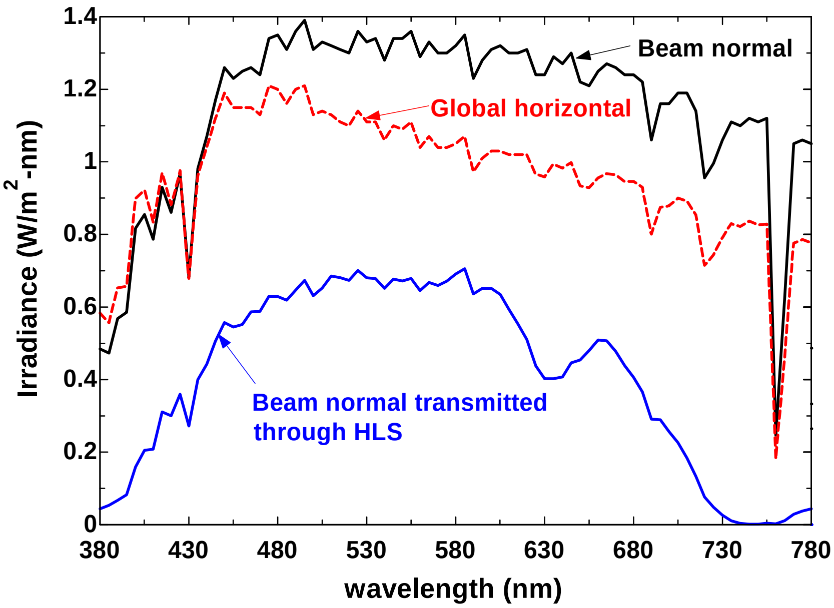


Figure 3.2: Comparison of beam normal (AM 1.5), global horizontal (AM 1.5) and HLS attenuated beam normal SPDs

Daylighting studies are often not relevant to the HLS because many involve windows that permit a view of the outdoors and increased illumination levels in the windowed space. The HLS doesn't provide views of the outdoors, and increased illumination levels would result only if the HLS was designed to provide it. One daylighting study that seemed relevant to this author investigated the effect of skylights on retail sales. It is discussed later. Full spectrum lighting studies are more applicable, but a major concern with these studies is that they are often conducted with full spectrum fluorescent bulbs with varying SPDs, none of which perfectly matches the SPD of sunlight or HLS light. Therefore if a physiologic response is claimed under full spectrum fluorescent bulbs, it cannot be assumed that sunlight or HLS light will elicit the same response.

Nevertheless the fact that sunlight, full spectrum fluorescent light, and HLS light have distributed power over the entire visual range and share continuous power at shorter wavelengths allows some generalizations about the applicability of research to be made.

### 3.3.1 Visual Performance

A common claim by proponents of full spectrum lighting is that it decreases visual fatigue and makes things easier to see. Under tightly controlled conditions there is some evidence to support such claims (Blackwell, 1985). Blackwell compared four light sources, one of which was a full spectrum lamp. Test subjects participated in a standard visual performance test, the Landolt ring test, under each lamp. Best results were achieved under the full spectrum lamp.

Berman (1992) explains the results of this test through his theory of scotopic sensitivity. In this theory, the dilation of the pupil is controlled by the rods, not the cones, even at light levels typical of building interiors. The rods are more sensitive to light at shorter wavelengths than the cones, and therefore light sources with power shifted toward shorter wavelengths, such as HLS light, would cause the pupil to contract more. Berman claims that pupil contraction increases depth of field and visual acuity which more than offsets the small reduction of illuminance on the retina due to a smaller iris.

Some studies do not support the theory of scotopic sensitivity. Boyce and Rea (1993) examined visual, cognitive, color, and mood assessments of 28 subjects under cool white and full spectrum lighting fluorescent lighting. Illumination levels were set at 470 lux (normal) and 170 lux (dim). There was little effect seen at normal illumination levels, though slightly better visual performance at the low illumination level was performed under full spectrum lighting.

### 3.3.2 Color Rendering

As will be further described in Chapter 5, full spectrum sources are defined as having good color rendering abilities. Warm white and cool white fluorescent bulbs generally do not render colors well, having color rendering indices (CRI) between 50 and 70. Boyce and Simons (1977) compared color discrimination under different lamp types in a series of experiments. The full spectrum source (5000 K, 90 CRI) produced the fewest errors. However, when the full spectrum source was compared to a 4100 K source with a high CRI (most likely an incandescent source), there was no difference in error rate.

### 3.3.3 Preference to Color Temperature

As will shown in Chapter 7**,** the HLS raises the correlated color temperature (CCT) of the indoor light when it is paired with bulbs that have color temperature less than about 5000 K. The literature shows no clear preference for higher or lower color temperatures

(Boray et al. 1989 and Kuller et al., 1993), though electronic assembly workers showed a preference for 5000 K full spectrum light over 4100 K fluorescent lighting (Berry, 1983). This preference is not necessarily due to the higher color temperature of the full spectrum bulb. It could be due its better color rendering ability, or the perceived increase in illumination level due to Berman's scotopic sensitivity hypothesis.

**3.3.4 Effect on Arousal**

As described previously, light inhibits secretion of melatonin by the pineal gland. The level of melatonin in the blood is the primary measure of the body's circadian rhythm, with higher levels of arousal and performance associated with lower levels of melatonin (Rea, 2002).

Figueiro (2002) states that the spectral sensitivity of the circadian system is different than the visual system, with a peak sensitivity at 460 nm instead of photopic's 555 nm. For this reason, two light sources that appear to have the same brightness would not necessarily inhibit melatonin secretion the same way. Full spectrum light sources have power in this part of the spectrum and would be better at regulating rhythms than 3000 K fluorescents (Figueiro 2002). It is hypothesized that 3000 K fluorescents at illumination levels typical of building interiors do not supply the stimulus required to tell a person's body that it's daytime. However, experiments with young adults under either full spectrum, warm white, or cool white fluorescent bulbs did not show any differences in reports of arousal during 35 minute exposure sessions (Boray et al, 1989). Veitch et al. (1991) reports similar results for one hour sessions.

### 3.3.5 Effect on Mood

Veitch (1993) has documented that many people feel happier under light that simulates sunlight. The use of full spectrum lamps in the treatment of some psychological disorders, such as Seasonal Affective Disorder (SAD), reinforces the idea that full spectrum lamps should be used more generally for the public's well being.

The exact cause of SAD is not known. Its main symptom is depression. Changes in total daily light exposure appear to trigger this disorder (Hill, 1992). The circadian rhythms in those affected by SAD are disrupted, and such a change implicates problems secreting melatonin correctly. However, studies of hormone levels in control and test subjects with SAD have not shown significant differences (Hill, 1992).

Hellekson et al. (1986) reported that full spectrum light treated depressive symptoms in Alaskan patients with SAD. Whether the two hour treatment was done in the morning, in the evening, or split one hour in each appeared irrelevant.

A significant number have studies have shown that full spectrum lighting is not necessary for treatment. Early experiments examining treatment efficacy compared full spectrum fluorescents to dim controls, leaving open the possibility that light intensity was also responsible for treatment effectiveness (Hellekson et. al., 1986). Lewy et al. (1987) saw full spectrum and cool white fluorescent lamps give similar results. Treatment of SAD has been achieved with a wide variety of bright white lights and colored lights (Bielski et al.,1992, Eastman et al.,1998 and Brainard et al.,1990).

### 3.3.6 Effect on Productivity and Sales

In 1999 the Heschong Mahone Group submitted a report to Pacific Gas and Electric studying the daylighting's affect on sales in a retail chain in California. Sales over an eighteen month period for 108 stores were analyzed. Two-thirds of these stores were equipped with skylights and photosensors controlling dimming fluorescents. The other third of the stores were primarily lit using fluorescent bulbs. The stores were otherwise similar.

The retailer insisted on anonymity and sales figures were normalized to a non-descriptive sales index. Multivariate regression analysis was used to isolate other variables the study authors believed might influence sales until just the effect of skylights could be determined. The study concluded that, all other factors being equal, a store equipped with skylights would sell 40% more than a store without them (Heschong Mahone Group, 1999).

However, a 2003 follow up study by the same group reports markedly different results. This study focused on another retailer in the same state, and used an analysis methodology influenced by a panel of experts recruited by Lawrence Berkeley National Laboratory. Data from the 1999 study was reanalyzed and included in the results of this study. The effect of light on retail sales was amended from 40% to 0-6% (Heschong Mahone Group, 2003).

## 3.4 Conclusion

The benefits of full spectrum lighting, if they exist, are subtle and difficult to quantify. When fine color discrimination is required, there is no substitute for full spectrum lighting.  Under low illuminance levels, there is a possibility that full spectrum lighting induces a better visual response than cool or warm white fluorescent bulbs.  This effect is not clear under illumination levels typical of interior environments.  There is not a preference for the higher color temperature of full spectrum light.  The response of the circadian system may be weighted towards wavelengths found in full spectrum light, but the magnitude and significance of this effect is not clear.  Many SAD studies show that full spectrum light is not necessary for treatment.  Studies that attempt to show increased performance under full spectrum light by analyzing schools and other buildings are often plagued by confounding factors as well as vague definitions of productivity and performance.  Results of these studies are inconclusive.

# Chapter 4

# Lamps

## 4.1 Introduction

The hybrid lighting system (HLS) is designed to supplement illumination provided by conventional lamps. The energy savings, the color of the indoor illumination, and the color rendering ability of the indoor illumination predicted by the TRNSYS model are dependent on the amount of HLS delivered light as well as the amount of light provided by the conventional lamps. Lamp characteristics relevant to TRNSYS results are the lamp's spectral power density (SPD), its efficacy, and how it performs when dimmed. This chapter describes these characteristics for the four different lamps evaluated with the HLS: incandescent, tungsten-halogen, full-spectrum fluorescent, and energy efficient fluorescent. It begins by describing the physics behind incandescence and luminescence.

## 4.2 Incandescence

All objects emit radiation as a function of their temperature. The amount of radiation an object emits at a given wavelength is based on Planck's equation for emission from a blackbody (equation 2.1) and the spectral emissivity of the object. Temperatures below 873 K (600 C) do not have significant power in visible wavelengths; most of the radiation emitted at these temperatures is in the invisible infrared. Electronic transitions in atoms and molecules at temperatures above 600 C result in the release of visible radiation along with heat. In an incandescent lamp, electric current is passed through a small diameter, highly resistive filament. As the filament is heated past 600 C, visible wavelength radiation (i.e. light) is produced (IESNA, 2000).

## 4.3 Luminescence and Fluorescence

The fundamental cause of light emission from incandescent and luminescent sources is the same: photons are emitted as electrons move from higher to lower energy states. In the case of incandescence, the thermal energy associated with heating many atoms gives rise to radiation of all wavelengths, forming a continuous spectrum. The process of luminescence is different in that it results from the excitation of single valence electrons. Figure 4.1 describes the processes of luminescence and phosphorescence.

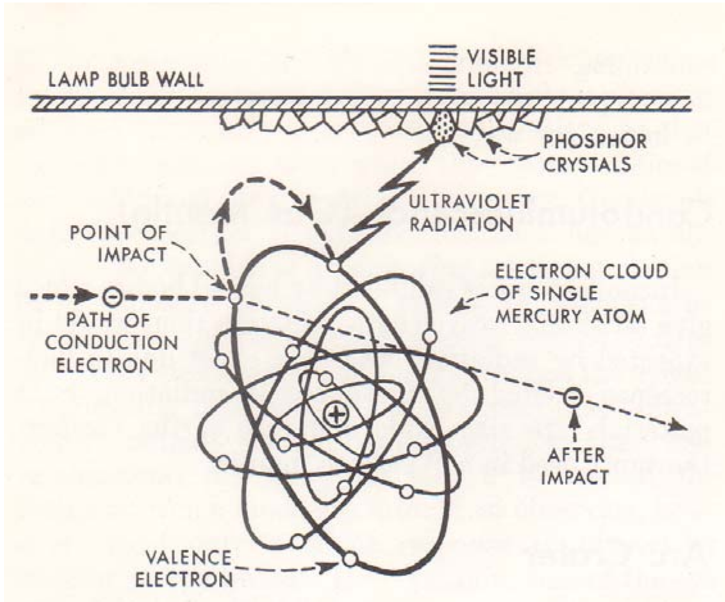


Figure 4.1: The processes of luminescence and phosphorescence (IESNA, 2000)

The process that emits visible light from a moving electron begins at the left side of the figure. A free electron, in this case emitted by the cathode of a fluorescent bulb, collides with a valence electron of a mercury atom. Kinetic energy is imparted to the valence electron and raises its energy level. After a short delay the valence electron returns to its base energy state, either in a series of jumps or one single jump At each of these jumps an ultraviolet photon is emitted. The conduction electron continues on its way down the bulb to the anode, gaining energy from the electric field to excite more mercury valance electrons in its path.

The ultraviolet photon eventually impacts a phosphor crystal coating on the inside of the fluorescent bulb. The phosphor transmits the photon through the crystal until it reaches an activator ion. If the photon's wavelength is in the activation band of the phosphor, the photon will be absorbed and re-emitted as a photon of longer wavelength in the near ultraviolet or visible spectrum. This is the light produced by the bulb.

## 4.4 Incandescent Lamps

Figure 4.2 shows a cross-section of a typical incandescent bulb.

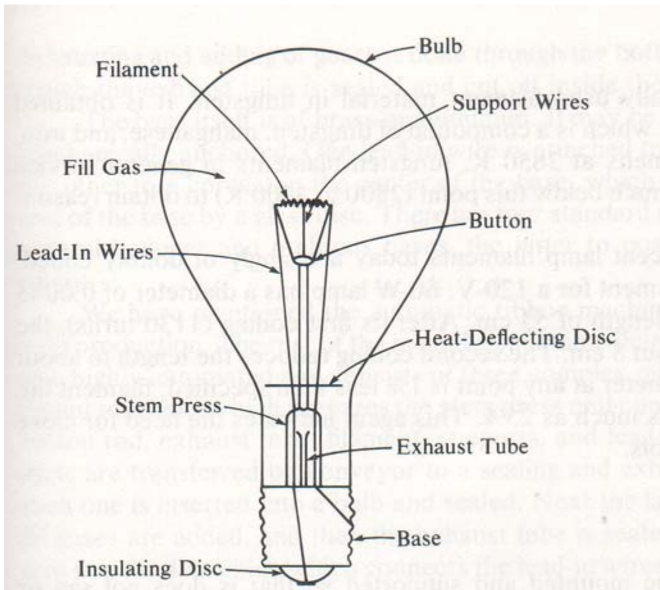


Figure 4.2: The components of an incandescent bulb (Murdoch, 1985)

During operation, electricity travels up one of the lead-in wires, resistively heats the filament, and then travels back down the other wire. Light is emitted from the filament as a function of its temperature; the filament acts as a blackbody radiator with selective emission. The maximum luminous efficacy of a blackbody radiator is 95 lm/W and occurs at 6800 K (Murdoch, 1985). However, practical luminous efficacies for incandescent lamps are limited by the melting temperature of the filament material. The most commonly used filament material is tungsten, which has a melting temperature of

3650 K. At this temperature, the efficacy of a tungsten filament is at its maximum of 52 lm/W. A filament at this temperature would burn out immediately, so to extend life temperatures in the filament are decreased to 2770 K in the case of a 60 W bulb (Murdoch, 1985). At this temperature the efficacy of the bulb is about 15 lm/W, which accounts for losses due to heat conduction away from the filament by the lead-in wires, the gas in the bulb, and direct radiation absorbed by the bulb and base (Murdoch, 1985).

Figure 4.3 shows the SPDs of a blackbody and a tungsten filament operating at 3000 K. The SPD is necessary to determine the correlated color temperature and the color rendering ability of the lamp. The calculation procedures for these photometric quantities will be discussed in detail in Chapter 5. In general, incandescents provide good color rendering abilities as well as warm pleasing light but with low luminous efficacies, which range between 10 and 20 lm/W. The incandescent lamp used in this study had a CCT of 2850 K, a CRI of 99+, and a luminous efficacy of 15 lm/W.

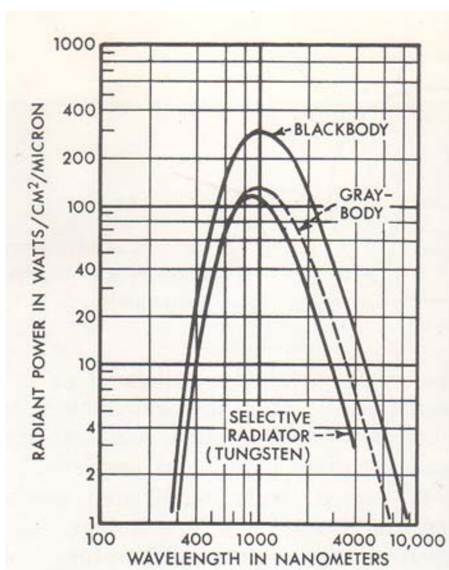


Figure 4.3: SPDs of a blackbody and tungsten filament at 3000 K (IESNA, 2000)

## 4.5 Tungsten-Halogen Lamps

Tungsten halogen lamps are incandescent lamps that use a halogen gas to take advantage of the halogen cycle described below. One factor affecting the life and luminous efficacy of incandescent bulbs is the evaporation of the tungsten filament. Over time, tungsten particles are transported from the filament to the inside of the bulb by gas convection currents. This weakens the filament and decreases the efficacy of the bulb. One way to circumvent this process lies in the halogen regenerative cycle, shown in Figure 4.4.

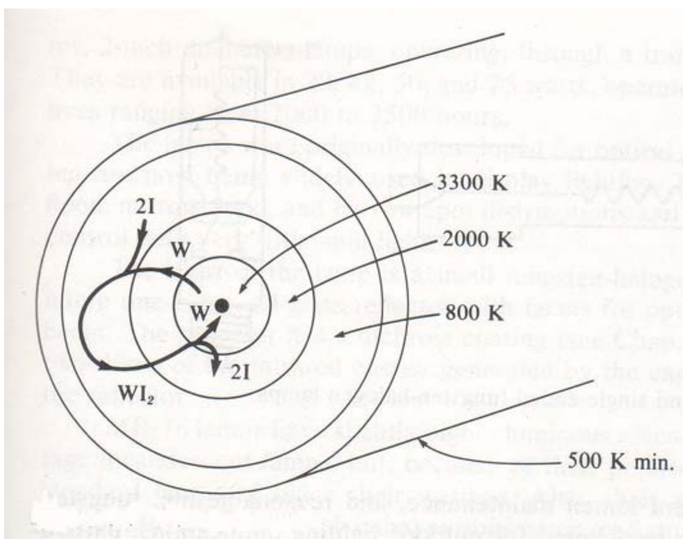


Figure 4.4: The halogen cycle. W represents tungsten; I is iodine, $WI_2$ is tungsten iodide. (Murdoch, 1985)

When iodine is added to the fill gas, typically a mixture of argon and nitrogen, the evaporating tungsten particles combine with the iodine vapor to form tungsten iodide. Convection carries the tungsten iodide away from the filament to the bulb wall, but if the bulb temperature is high enough (500-1500 K) the tungsten is not deposited on the bulb wall. Instead, it drifts back towards the filament. Near the filament, if the temperature is at least 2800 K, tungsten iodide is reduced back to tungsten and iodide. In the process the tungsten is re-deposited on the filament. The tungsten is never deposited in the same place it evaporates from. If it did, the bulb would theoretically have an infinite life span.

Figure 4.5 shows the SPD of a specific type of tungsten-halogen lamp, the MR-16. MR-16 lamps were originally developed for optical projection equipment but are now used in display lighting. They have a slightly higher luminous efficacy than incandescents and use reflectors to better focus their light. The tungsten-halogen lamp used in this study was the Solux MR-16. It has a CCT of 4185 K, a CRI of 98, and an efficacy of 22 lm/W.

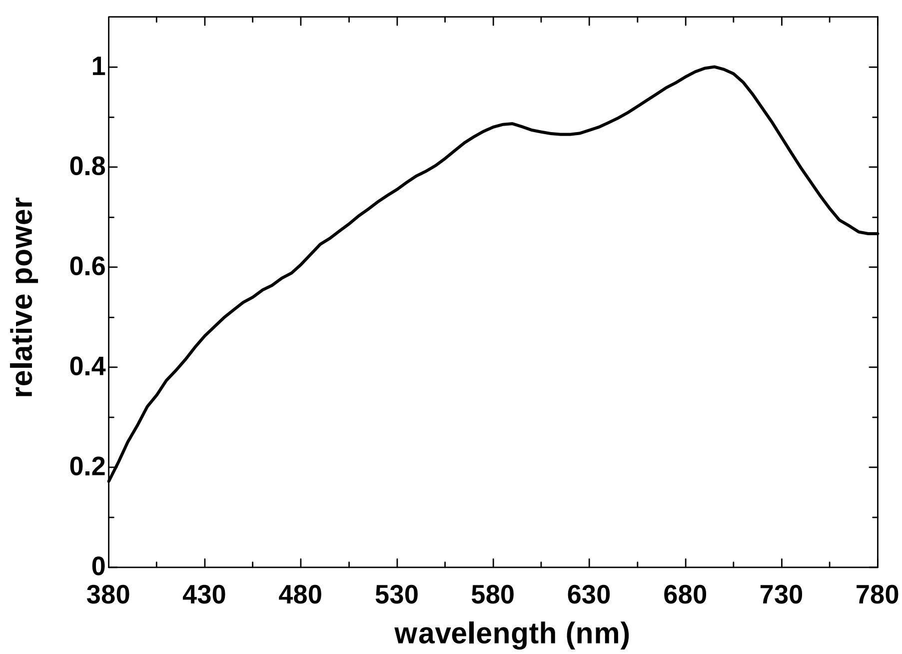


Figure 4.5: SPD of Solux Halogen MR-16

## 4.6 Fluorescent Lamps

Figure 4.6 shows a cut-away view of the end of a fluorescent lamp. The electrode assembly is similar to the stem press assembly of incandescent lamps. The filament serves double duty as cathode and anode because of the applied alternating current. The filament is dipped in a mixture of electron-rich materials so that when the filament serves as a cathode it has a large supply of easily obtainable electrons.

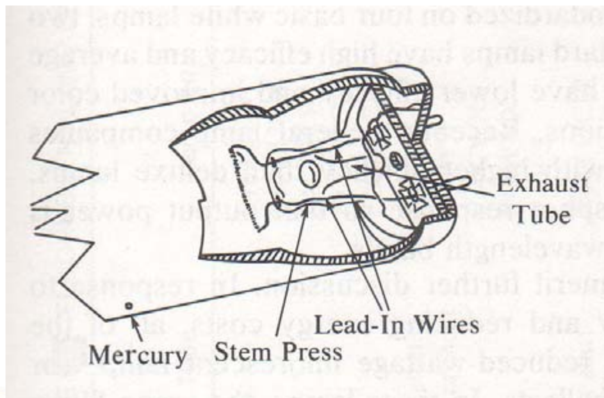


Figure 4.6: The end of a fluorescent lamp

The fluorescent lamp provides light by the processes of luminescence and phosphorescence described previously, i.e. current applied to the filament causes the release of electrons that travel down the bulb to the anode, exciting mercury valence electrons along the way that release UV photons which the phosphor coating on the inside of the bulb transforms into visible light.

Efficient conversion of electrical power to light results if a low current density is used to produce only one spectral line from mercury vapor emission at 253.7 nm. Phosphors with peak sensitivities near 253.7 nm are used to convert the ultraviolet spectral line to light at visible wavelengths. Different phosphors are mixed to create the desired color and SPD of the visible light emitted from the lamp.

Figure 4.7 shows the SPDs of the two Sylvania fluorescent bulbs used in this study.

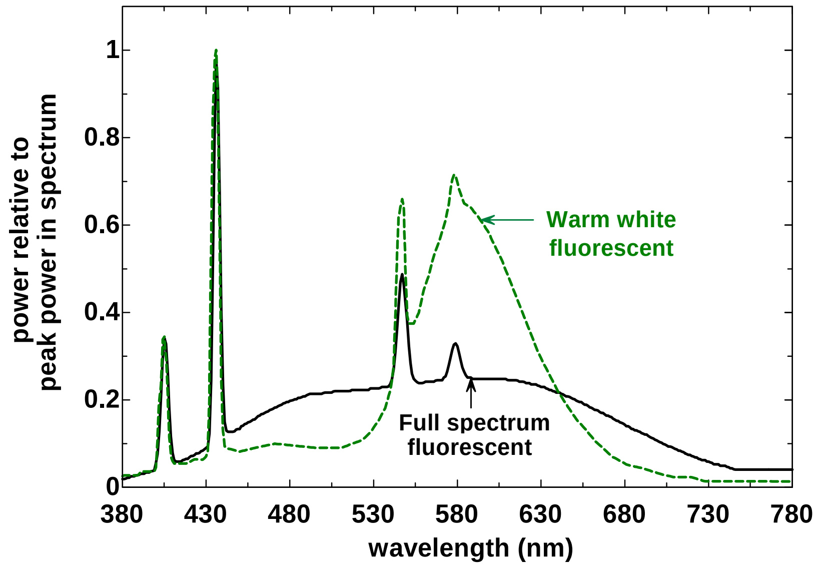


Figure 4.7: SPDs of Sylvania warm white and full spectrum fluorescent bulbs in the visible spectrum (Sylvania, 2003)

Because the full spectrum fluorescent has more relative power at wavelengths less than 500 nm, its CCT of 5000 K is higher than the warm white fluorescent's CCT of 3000 K. It has a more equal distribution of power across the visible spectrum as well, and for this reason its CRI of 90 is better than the warm white fluorescent's CRI of 52.

However, a lower luminous efficacy is often the penalty for providing the broad distribution of power necessary for good color rendering. The warm white SPD better concentrates its total power at wavelengths near the maximum sensitivity of the eye, yielding luminous efficacies between 80 and 95 lm/W (Murdoch, 1985). The efficacy used in this study was 89 lm/W. The full spectrum fluorescent's efficacy of 52 is less because it provides power at wavelengths that, while necessary for good color rendering, are farther away from the eye's maximal sensitivity at 555 nm. These efficacies include take into account the power consumed by the electronic ballasts that change the 60 Hz input voltage to direct current and then to 20-25 kHz (Murdoch, 1985).

## 4.7 Dimming

Both fluorescent and incandescent bulbs can be dimmed automatically using controls that monitor the illumination level inside a room. The bulbs are dimmed by decreasing the amount of power available to them. In an ideal dimming system, a power reduction of 50% would correspond to a light reduction of 50%. Figure 4.8 shows how the relative light output is affected by relative power for incandescent and fluorescent bulbs (Lutron, 2003 and Advance, 2003). As shown in the figure, neither incandescent systems nor fluorescent systems dim ideally. Instead, reductions in power cause more dramatic reductions in light output. If an incandescent bulb is dimmed to 25% of its full light output, it still requires 40% of full output energy. Dimming fluorescents is a little worse: at 40% of full output energy, the fluorescent bulb will put out only 20% of its full light output. These dimming effects are included in the TRNSYS model.

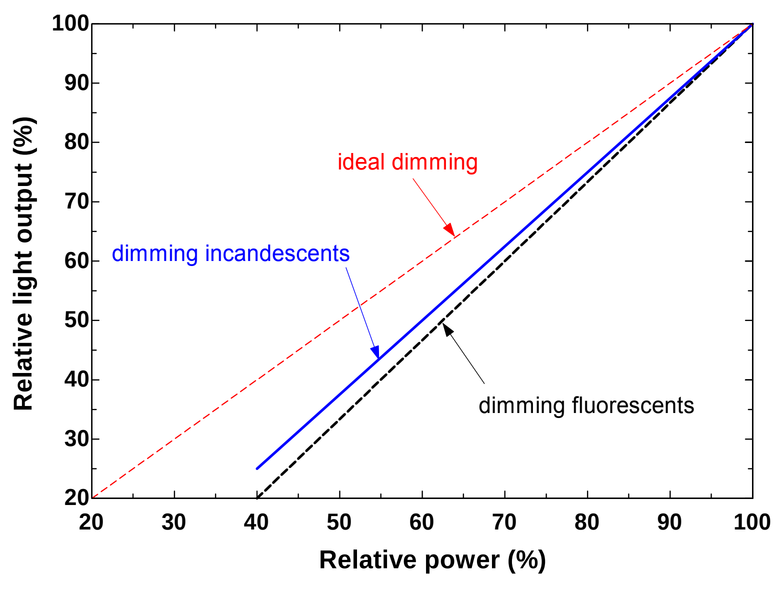


Figure 4.8: Affect of bulb energy usage on illumination provided

# Chapter 5

# Colorimetry

## 5.1 Introduction

Colorimetry is the branch of color science concerned with quantifying the color of a visual stimulus. It is also concerned with the specification of small color differences due to differences in the spectral power distributions (SPDs) of visual stimuli.
Two colorimetric indices described previously, the correlated color temperature (CCT) and the color-rendering index (CRI), are used to quantify the color and the color-rendering abilities of light sources, respectively. The Illumination Engineering Society of North America (IESNA) uses these indices as lighting design guidelines (IESNA, 2000). For example, in hospital surgery areas IESNA recommends that light sources have CCT values between 3500 K and 6700 K and that all light sources are of the "color-improved type only" (IESNA, 2000). In museums, IESNA states, "In interior spaces, a lower color temperature or (warmer) source than daylight is usually preferred" and that light sources should have "good to excellent" color rendering abilities.

The addition of the HLS to a conventional lighting system will affect the CCT and CRI of the delivered light. Beam normal radiation attenuated by the HLS has a CCT around 5000 K, much larger than the 3000 K of warm white fluorescent or incandescent bulbs. Its ability to render color, quantified by the CRI, is better than many lamps but not as good as sunlight. For these reason, the CCT and CRI of the delivered light are calculated in the TRNSYS model so that lighting designers can be better informed about the effect of the HLS on the delivered illumination of a lighting system.

The calculation of the CCT and the CRI for a given light source is a lengthy process that involves many colorimetric concepts. This chapter begins by explaining colorimetric concepts relevant to the calculation of the CCT and CRI and then describes how each index is calculated. Example calculations are performed throughout to facilitate understanding.

## 5.2 Colorimetric Concepts

### 5.2.1 The trichromatic generalization

The trichromatic generalization states that most color stimuli can be matched in color completely by additive mixtures of three fixed primary stimuli whose radiant powers have been suitably adjusted. The choice of the three primary stimuli is arbitrary with the restriction that none of them can be color matched by a mixture of the other two (e.g. red, blue, and green are valid because red and blue mixed do not make green, etc.). The primary stimuli do not have to be red, blue, and green. The three primary stimuli, called primaries, can be mixed in different ratios to make other colors in the visible spectrum. The proper combination of these three primaries produces white light. Figure 5.1 shows additive color mixing using red, green, and blue as the primaries.


Figure 5.1: Additive color mixing using red, green, and blue primaries (Finbury, 2004)

### 5.2.2 The Color Matching Functions

In the 1920's color matching experiments were performed that led to the "chromaticity characteristics of the standard observer" adopted by the CIE in 1931 (Murdoch, 1985). The experiment used the colorimeter shown in Figure 5.2.

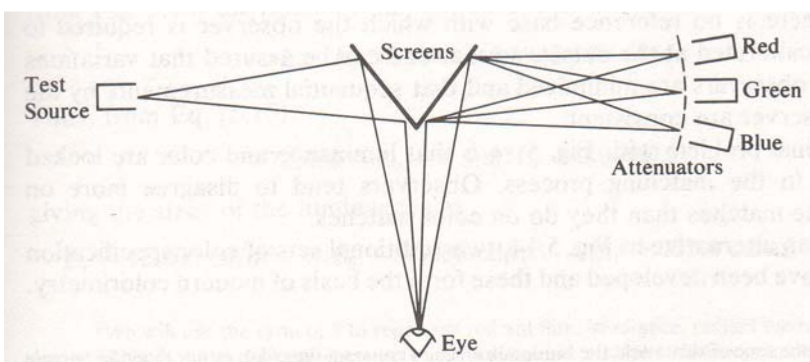


Figure 5.2: Schematic of a colorimeter (Murdoch, 1985)

In a procedure similar to the one used by Gibson and Tyndall to quantify the eye's photopic luminous efficiency curve described in Chapter 2, seventeen observers adjusted red (700 nm), blue (435.8 nm), and green (546.1 nm) attenuators on the colorimeter until the color that appeared in the right hand field of the colorimeter matched the color appearing in the left hand field. The radiant power of the test source and each of the primaries was recorded for each color match. For some spectral colors, it was necessary to transfer a primary from the right-hand field to the left-hand field to get a color match. In such cases, this corresponded to a "negative" addition of that primary color.

Figure 5.3 shows the spectral sensitivity curve obtained from these tests.

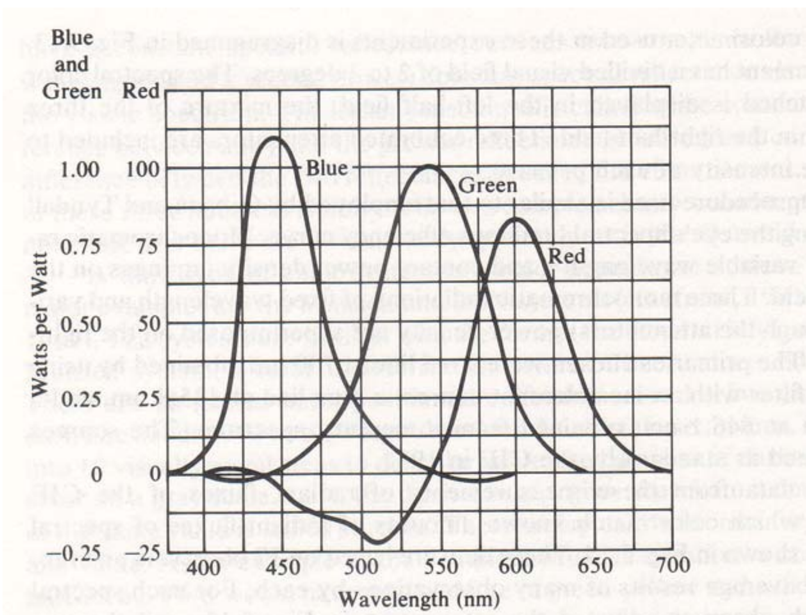


Figure 5.3: Spectral sensitivity curve for color matching (Murdoch, 1985)

To illustrate how to use these curves, imagine that you wanted to match 1 W of pure spectral color at 475 nm. This would require about 0.625 W of blue, 0.125 W of green, and -12.5 W of red, meaning that 12.5 W of red had to be added to the 475 nm spectral color for a color match.

Although this method of color matching is simple it has several deficiencies. By comparing the scales on the left side of Figure 5.3, one can see that the required power of red light is often ten times larger than the power of the other primaries. Because the total color derived is based on summing the product of the red, green, or blue sensitivity with the SPD of the light in question, the large red values tend to obscure the affects of the blue and green sensitivities, leading to error. Another problem with Figure 5.3 is that the total luminous power (brightness) and color are inextricably linked. Observers have more problems with luminance matches than color matches (Murdoch, 1985). Finally, it's odd that an acceptable color match derives from "negative" color addition.

To address these deficiencies the CIE (Commission Internationale de l'Eclairage, International Commission on Illumination) adopted a different system for quantifying color in 1931. Instead of using primaries that have a physical basis (red, green, and blue), non-physical primaries X, Y, Z derived from a linear transformation of red, green, and blue primaries are used. The scales of these primaries are chosen so that one unit of each primary yields equal energy white, which is equal power across all wavelengths in the visible range. Figure 5.4 shows the color matching functions $\bar{x}, \bar{y}, \bar{z}$ that are used with a light source SPD to find the tristimulus values X, Y, and Z that completely define the color and luminance of the SPD.

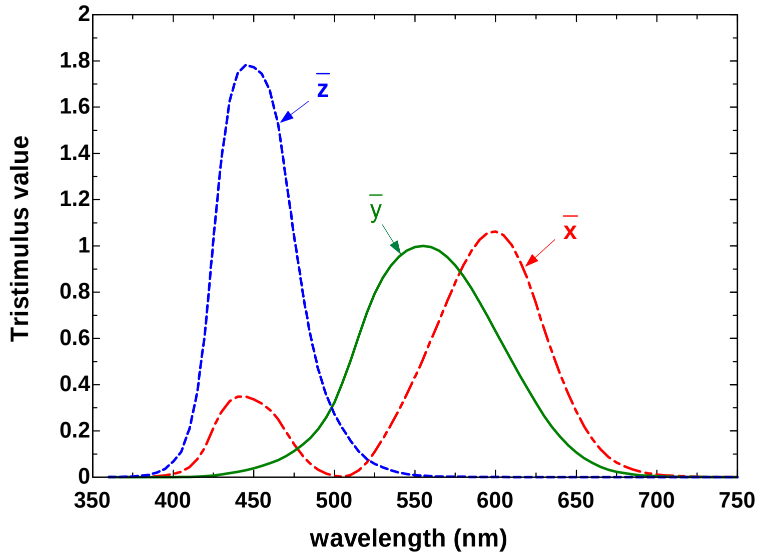


Figure 5.4: 1931 CIE color matching functions

### 5.2.3 Tristimulus values and chromaticity coordinates

The tristimulus values X, Y, and Z are calculated from the SPD of a light source and the color matching functions in the following manner (IESNA, 2000)

$$X = k\sum_{\lambda=360}^{\lambda=830} S(\lambda)\rho(\lambda)\bar{x}(\lambda)\Delta\lambda \qquad (5.1)$$

$$Y = k\sum_{\lambda=360}^{\lambda=830} S(\lambda)\rho(\lambda)\bar{y}(\lambda)\Delta\lambda \qquad (5.2)$$

$$Z = k\sum_{\lambda=360}^{\lambda=830} S(\lambda)\rho(\lambda)\bar{z}(\lambda)\Delta\lambda \qquad (5.3)$$

where

$S(\lambda)$ is the SPD of the light source at a given wavelength.

$\rho(\lambda)$ is the reflectivity of an object at a given wavelength with values ranging from 0 (all radiation at that wavelength absorbed) to 1 (all radiation at that wavelength reflected). If the color of the light source is under study, then $\rho(\lambda) = 1$ at all wavelengths. Otherwise, the tristimulus values calculated will be the color of light reflected from the object.

$\bar{x}, \bar{y}, \bar{z}$ are the non-physical color matching functions defined in Figure 4.4

$\Delta\lambda$ is the wavelength interval. For the TRNSYS model, $\Delta\lambda = 5$ nm which is sufficient for colorimetric applications (Wyszecki, 1982) k is a normalizing factor. If k = 683 lm/W and S(λ)'s units are W/nm, then Y will equal the luminous power in lumens of the SPD because $\bar{y}(\lambda)$ is defined to be the photopic efficiency curve, V(λ) introduced in Chapter 2. When calculating the color rendering index, k is defined as

$$k = \frac{100}{\sum_{\lambda=360}^{\lambda=830} S(\lambda)\bar{y}(\lambda)\Delta\lambda} \quad (5.4)$$

In the calculation of the CRI, this normalization is used to set the Y values of the light source under study and the reference source to 100, meaning equalizing their luminances before color rendering calculations take place. This will be discussed in more detail in the color rendering section that follows.

Though the tristimulus values X, Y, and Z completely describe the color derived from a given SPD, more often chromaticity coordinates are used to describe the color instead. These chromaticity coordinates, x and y, are calculated from the tristimulus values X, Y, and Z in the following manner (IESNA, 2000)

$$x = \frac{X}{X + Y + Z} \quad (5.5)$$

$$y = \frac{Y}{X + Y + Z} \quad (5.6)$$

It is unnecessary to calculate z because x + y + z = 1.

### 5.2.4 The chromaticity diagram

These chromaticity coordinates are used with the 1931 chromaticity diagram shown in Figure 5.5 to visually define the color of the SPD of interest. Disregard for now the dark line that runs through the white, yellow, and red area on the diagram. This line will be explained in the correlated color temperature section.

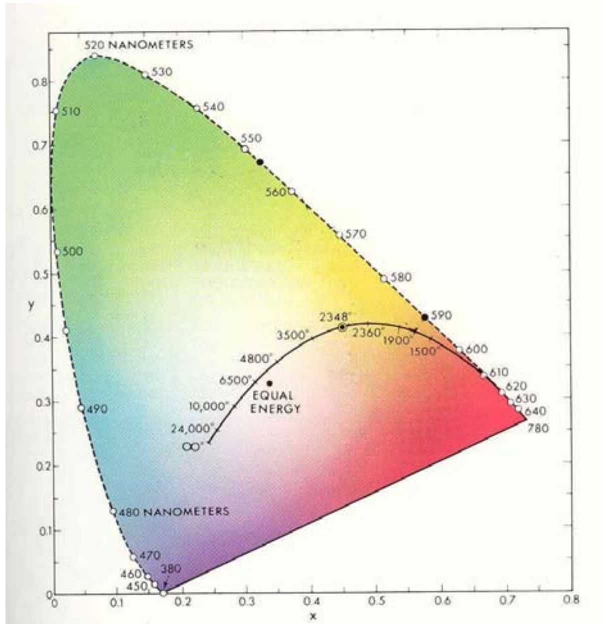

Figure 5.5: 1931 CIE chromaticity diagram (IESNA, 2000)

The use of tristimulus values, chromaticity coordinates, and Figure 5.5 to determine the color of a SPD is probably best explained by example. Consider the SPD of the warm white fluorescent bulb introduced in Chapter 4 and the color matching functions plotted together in Figure 5.6.

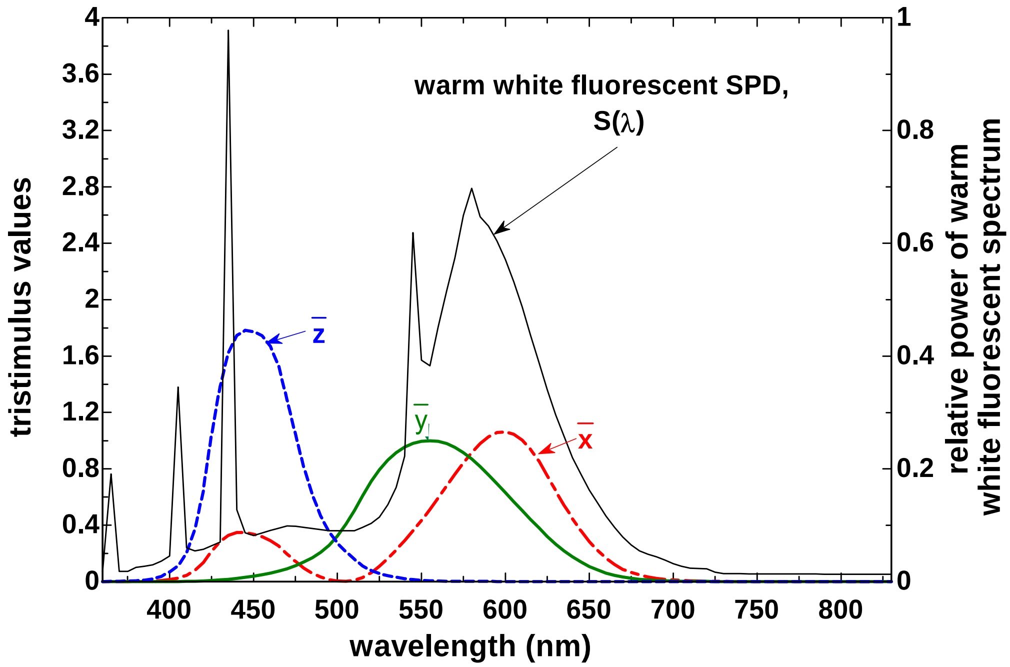


Figure 5.6: Color matching functions and SPD of warm white fluorescent SPD

Using equations 5.1 through 5.3 with $\rho(\lambda) = 1$ at all wavelengths, $\Delta\lambda = 5$ nm, and $k = 2.481$ defined by equation 5.4, the tristimulus values for the fluorescent bulb are

$$X = 108.9$$
$$Y = 100 \quad \text{(scale factor k = 2.481 defined by equation 5.4 assured this value)}$$
$$Z = 42.12$$

The chromaticity coordinates are defined by equations 5.5 and 5.6:

$$x = \frac{108.9}{108.9 + 100 + 42.12} = 0.4338$$
$$y = \frac{100}{108.9 + 100 + 42.12} = 0.3984$$

The chromaticity coordinates (0.4338, 0.3984) for the warm white fluorescent bulb are plotted on the 1931 CIE chromaticity diagram to determine the color of its SPD. The x chromaticity coordinate is located on the abscissa, the y chromaticity coordinate on the ordinate, and the point specified by these x,y coordinates indicates the color of the

SPD. Figure 5.7 shows the plotted chromaticity coordinates of the warm white fluorescent lamp as well as the other lamp sources described in Chapter 4. The chromaticity coordinates of beam normal sunlight (air mass 1.5), described further in chapter 6, is also shown.

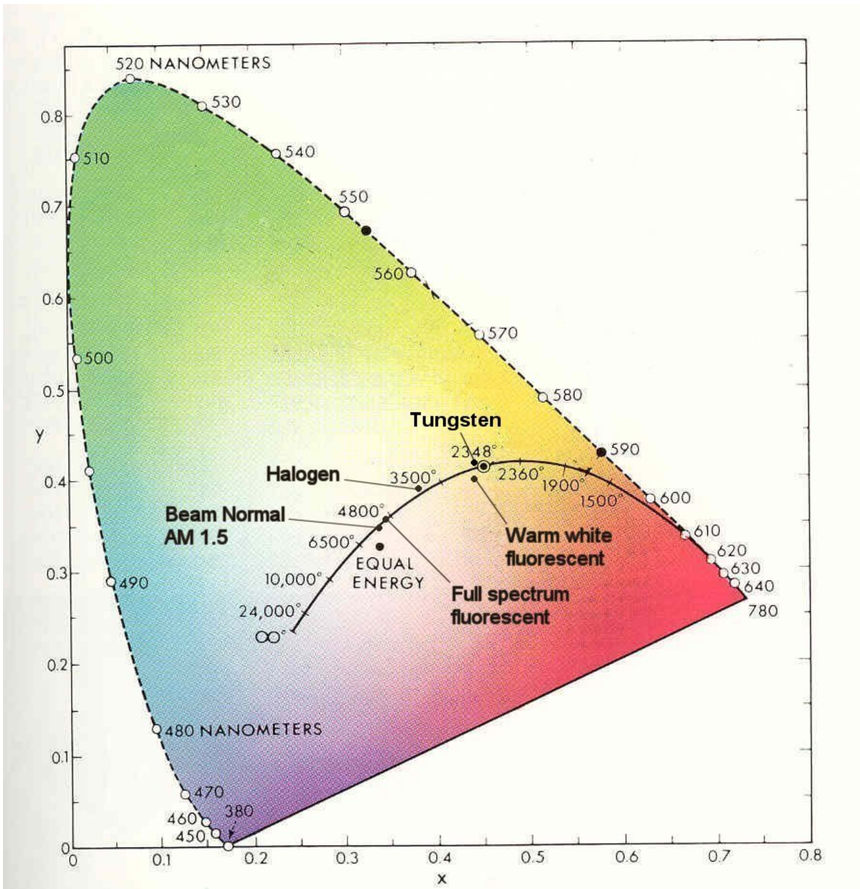


Figure 5.7: Chromaticity of lamps used in study and beam normal radiation, AM 1.5 on CIE 1931 chromaticity diagram

In Figure 5.7, the color of each of the lamps used in this study is specified by its respective chromaticity coordinates. Starting near the right side of Figure 5.7, the tungsten incandescent lamp's color would be yellowish-white, which is often associated with a "warm" appearance. Moving to the left, the warm white fluorescent's appearance is similar. The halogen appears whiter than either the tungsten or warm white fluorescent because it has very little yellow tint in its color. The full spectrum fluorescent is whiter still, and it has a white-blue tint that is often associated with "cooler" appearing lamps. The beam portion of sunlight around noon appears even cooler than the full spectrum fluorescent lamp.

## 5.3 Correlated color temperature

Though lamps differ in how "warm" or "cool" they appear, they are predominantly white in appearance. This means that there are roughly equal amounts of the tristimulus values (X, Y, and Z) in their SPDs. Blackbody radiators at large enough temperatures share this characteristic. The dark black line that starts at the right and moves to the left in Figures 5.5 and 5.7 is the chromaticity coordinate curve created by the SPDs of blackbodies operating at increasing absolute temperature (K). The temperature of a blackbody, when used in Planck's equation 2.1, creates a SPD unique to that temperature with a unique set of chromaticity coordinates that correspond to colors along this line. For this reason, the colors that intersect this curve, called the Planckian locus, can be described by their x,y chromaticity coordinates or by the blackbody temperature (K) that creates those same chromaticity coordinates. In the latter case, the color of the SPD is described by its **color temperature**.

None of the chromaticity coordinates of the light sources in Figure 5.7 fall exactly on the Planckian locus. For this reason, technically it's incorrect to define any of them by a color temperature. However, they are relatively close to this line and specifying a color temperature that specifies a color approximately the same as the color of the lamp is a useful way to describe its color. The **correlated color temperature** (CCT) is defined as the temperature of a blackbody radiator whose perceived color most closely resembles that of a given selective radiator (Wyszecki, 1982).

By visual inspection of Figure 5.7, one might say that the CCT of the tungsten incandescent lamp is greater than 2400 K but less than 3500 K. The CCT of the warm white fluorescent is probably slightly larger than the tungsten lamp's CCT. The halogen's CCT is definitely greater than 3500 K but less than 4800 K. The CCTs of the beam normal and full spectrum fluorescent lamp are both larger than 4800 K but less than 6500 K.

A more systematic approach is used to calculate the CCTs of these lights sources, but the method is similar to the approximating method described above. It involves the interpolating between 31 pre-generated isotemperature lines that intersect the Planckian locus, as shown in Figure 5.8.

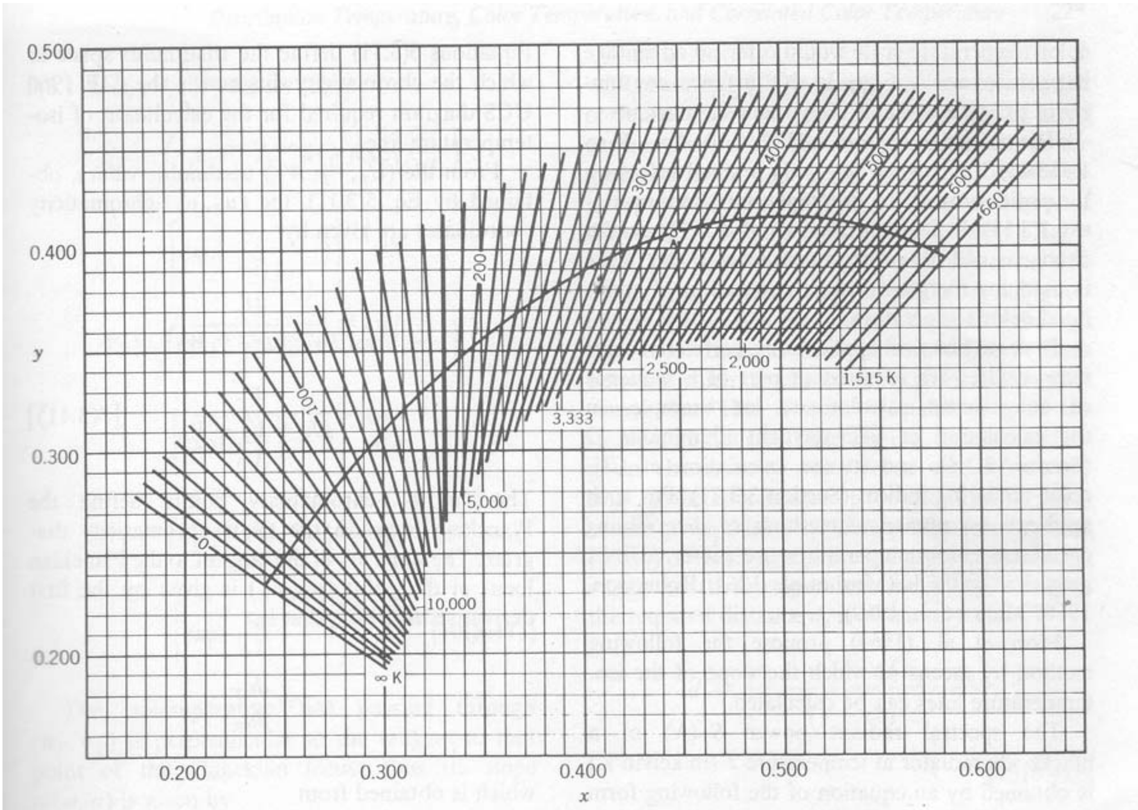


Figure 5.8: Isotemperature lines and the Planckian locus (Wyszecki, 1982)

An isotemperature line is a line along which all chromaticity coordinates have the same correlated color temperature. The temperature of a given isotemperature line is defined where it intersects the Planckian locus. Wyszecki (1982) describes the method for generating these lines. The lines' color temperature values, slopes, and intersection points with the Planckian locus are shown in Table 5.1 in both CIE 1931 x,y and 1960 UCS (uniform color space) u,v notation. These two notations are related through the simple relations:

$$u = \frac{4X}{X + 15Y + 3Z} \tag{5.7}$$

$$v = \frac{6Y}{X + 15Y + 3Z} \tag{5.8}$$

where X, Y, and Z are the tristimulus values of the SPD under study defined by equations 5.1, 5.2, and 5.3.

Table 5.1 Isotemperature lines of Figure 5.8 in CIE 1931 x,y and CIE 1960 u,v notations (Wyszecki, 1982)

| | Reciprocal Megakelvin | Temperature | Chromaticity Coordinates in CIE 1960 UCS Diagram | | Slope | Chromaticity Coordinates in CIE 1931 Diagram | | Slope |
|---|---|---|---|---|---|---|---|---|
| $i$ | ($MK^{-1}$) | $T$(K) | $u_T$ | $v_T$ | $t_T(u,v)$ | $x_T$ | $y_T$ | $t_T(x,y)$ |
| 1 | 0 | ∞ | 0.18006 | 0.26352 | −0.24341 | 0.23987 | 0.23404 | −0.68705 |
| 2 | 10 | 100,000 | 0.18066 | 0.26589 | −0.25479 | 0.24258 | 0.23802 | −0.72797 |
| 3 | 20 | 50,000 | 0.18133 | 0.26846 | −0.26876 | 0.24560 | 0.24240 | −0.77926 |
| 4 | 30 | 33,333 | 0.18208 | 0.27119 | −0.28539 | 0.24890 | 0.24714 | −0.84248 |
| 5 | 40 | 25,000 | 0.18293 | 0.27407 | −0.30470 | 0.25251 | 0.25222 | −0.91976 |
| 6 | 50 | 20,000 | 0.18388 | 0.27709 | −0.32675 | 0.25645 | 0.25763 | −1.01403 |
| 7 | 60 | 16,667 | 0.18494 | 0.28021 | −0.35156 | 0.26070 | 0.26333 | −1.12891 |
| 8 | 70 | 14,286 | 0.18611 | 0.28342 | −0.37915 | 0.26526 | 0.26930 | −1.26959 |
| 9 | 80 | 12,500 | 0.18740 | 0.28668 | −0.40955 | 0.27011 | 0.27547 | −1.44313 |
| 10 | 90 | 11,111 | 0.18880 | 0.28997 | −0.44278 | 0.27524 | 0.28182 | −1.65981 |
| 11 | 100 | 10,000 | 0.19032 | 0.29326 | −0.47888 | 0.28063 | 0.28828 | −1.93507 |
| 12 | 125 | 8,000 | 0.19462 | 0.30141 | −0.58204 | 0.29518 | 0.30477 | −3.08425 |
| 13 | 150 | 6,667 | 0.19962 | 0.30921 | −0.70471 | 0.31101 | 0.32116 | −6.18336 |
| 14 | 175 | 5,714 | 0.20525 | 0.31647 | −0.84901 | 0.32775 | 0.33690 | −39.34888 |
| 15 | 200 | 5,000 | 0.21142 | 0.32312 | −1.0182 | 0.34510 | 0.35162 | 11.17883 |
| 16 | 225 | 4,444 | 0.21807 | 0.32909 | −1.2168 | 0.36276 | 0.36496 | 5.34398 |
| 17 | 250 | 4,000 | 0.22511 | 0.33439 | −1.4512 | 0.38045 | 0.37676 | 3.68730 |
| 18 | 275 | 3,636 | 0.23247 | 0.33904 | −1.7298 | 0.39792 | 0.38690 | 2.90309 |
| 19 | 300 | 3,333 | 0.24010 | 0.34308 | −2.0637 | 0.41502 | 0.39535 | 2.44455 |
| 20 | 325 | 3,077 | 0.24702 | 0.34655 | −2.4681 | 0.43156 | 0.40216 | 2.14300 |
| 21 | 350 | 2,857 | 0.25591 | 0.34951 | −2.9641 | 0.47464 | 0.40742 | 1.92863 |
| 22 | 375 | 2,677 | 0.26400 | 0.35200 | −3.5814 | 0.46262 | 0.41121 | 1.76811 |
| 23 | 400 | 2,500 | 0.27218 | 0.35407 | −4.3633 | 0.47701 | 0.41368 | 1.64291 |
| 24 | 425 | 2,353 | 0.28039 | 0.35577 | −5.3762 | 0.49059 | 0.41498 | 1.54240 |
| 25 | 450 | 2,222 | 0.28863 | 0.35714 | −6.7262 | 0.50338 | 0.41525 | 1.45962 |
| 26 | 475 | 2,105 | 0.29685 | 0.35823 | −8.5955 | 0.51541 | 0.41465 | 1.39021 |
| 27 | 500 | 2,000 | 0.30505 | 0.35907 | −11.324 | 0.52669 | 0.41331 | 1.33101 |
| 28 | 525 | 1,905 | 0.31320 | 0.35968 | −15.628 | 0.53723 | 0.41131 | 1.27989 |
| 29 | 550 | 1,818 | 0.32129 | 0.36011 | −23.325 | 0.54712 | 0.40882 | 1.23522 |
| 30 | 575 | 1,739 | 0.32931 | 0.36038 | −40.770 | 0.55640 | 0.40593 | 1.19579 |
| 31 | 600 | 1,667 | 0.33724 | 0.36051 | −116.45 | 0.56508 | 0.40271 | 1.16074 |

In table 5.1, each isotemperature line (i = 1 through 31) corresponds to a color temperature (K). The chromaticity coordinates of the source in question ($u_s$,$v_s$ derived from X, Y, and Z in 5.7 and 5.8) will be located between two isotemperature lines ( i -1 and i ) defined by their temperatures ($T_{i-1}$ and $T_i$), their slopes ($t_{Ti-1}$ and $t_{Ti}$), and their location on the Planckian locus ($u_{Ti-1}$, $v_{Ti-1}$ and $u_{Ti}$, $v_{Ti}$). Based on the relative normal distance ($d_{i-1}$ and $d_i$) from each isotemperature line to the chromaticity point ($u_s$,$v_s$), the interpolated CCT value can be calculated from equations 5.9 and 5.11. These equations are slightly modified from Wyszecki (1982). Figure 5.9 illustrates the variables described above and the interpolation method as well.

$$d_i = \frac{(v_s - v_{Ti}) - t_{Ti}(u_s - u_{Ti})}{\sqrt{1 + t_{Ti}^{\,2}}} \qquad (5.9)$$

$$T_{CCT} = \left[\frac{1}{T_{i-1}} + \frac{\theta_1}{\theta_1 + \theta_2}\left(\frac{1}{T_i} - \frac{1}{T_{i-1}}\right)\right]^{-1} \qquad (5.10)$$

but $\theta_1$ and $\theta_2$ are small so $\theta_1 / \theta_2 \approx \sin\theta_1 / \sin\theta_2$ changing (5.10) into

$$T_{CCT} = \left[\frac{1}{T_{i-1}} + \frac{d_{i-1}}{d_{i-1} - d_i}\left(\frac{1}{T_i} - \frac{1}{T_{i-1}}\right)\right]^{-1} \qquad (5.11)$$

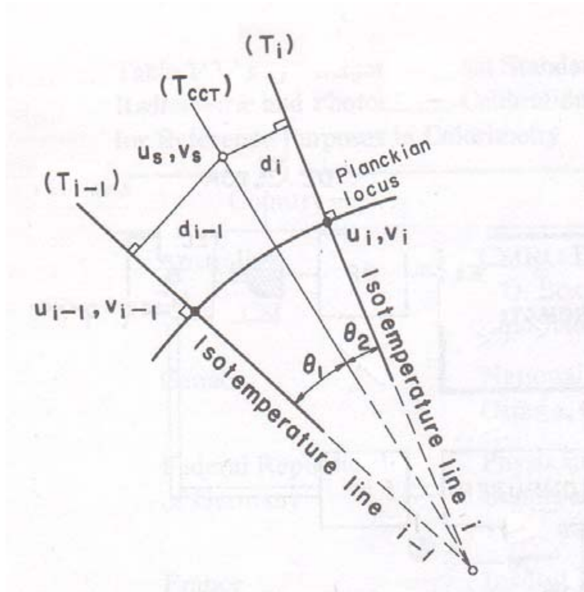


Figure 5.9: Method of interpolation to find the CCT of a light source with chromaticity coordinates $u_s$, $v_s$. Adapted from Wyszecki (1982)

A separate computer code (EES, Klein, et al., 2004) that solves for CCT was developed and then incorporated into the TRNSYS HLS model. A print out of this code is in the Appendix. CCT results for the lamps described in Chapter 4 are presented in Table 5.2. The CCT results calculated by TRNSYS are compared with manufacturer specifications and CIE specified values, in the case of the tungsten incandescent and daylight 6500 K spectrum.

Table 5.2: Comparison of CCT specified by bulb manufacturer or CIE (*) and TRNSYS results calculated according to procedure above.

| light source spectrum | manufacturer specification | TRNSYS value | difference |
|---|---|---|---|
| tungsten incandescent | 2850* | 2828 | 0.8% |
| warm white fluorescent | 3000 | 2992 | 0.3% |
| halogen | 4100 | 4133 | 0.8% |
| full spectrum fluorescent | 5000 | 5001 | 0.0% |
| daylight 6500 K (D65) | 6500* | 6507 | 0.1% |

The values predicted by TRNSYS are close to manufacturer specification. The slight differences are most likely explained by the use of varying wavelength intervals used for the calculation. The color matching functions are defined at 1 nm, 5 nm, and 10 nm wavelength intervals and any can be used to calculate the CCT (Wyszecki, 1982). The analysis presented here uses 5 nm wavelength intervals, which is sufficient for most practical applications (Wyszecki, 1982). Another explanation for the difference may be that, besides the D65 spectrum, all other light source spectrums were digitized from the web or scanned diagrams. Finally, this author has never seen a CCT reported that is not an interval of 50. It is not known if rounding to this interval is common in the industry. In any case, the algorithm calculates values with enough accuracy to be useful in this analysis.

## 5.4 Color rendering index

The CCT defines the perceived color of a light source. It does not indicate how well the light source will render the color of objects it illuminates. For that, another colorimetric index is needed: the color rendering index (CRI). The CRI of a light source is a measure of the color shift of objects illuminated by a light source in comparison to the same objects illuminated by a reference illuminant of comparable correlated color temperature. A CRI of 100 means that the light source in question renders the color of eight color samples in the same manner as the reference illuminant. The CRI has been defined so that the color differences seen between a 3000 K fluorescent bulb and a 3000 K blackbody spectrum yield a CRI of 50.

There are eight color samples used in the calculation of the general CRI. These color samples, numbered 1 through 8, are defined by different spectral reflectances, $\rho(\lambda)$. Samples are selected to yield a range of colors in the visible spectrum. Figures 5.10 through 5.18 show these reflectance curves (Kruschwitz, 2004). The caption of each figure describes the color the sample has under sunlight.

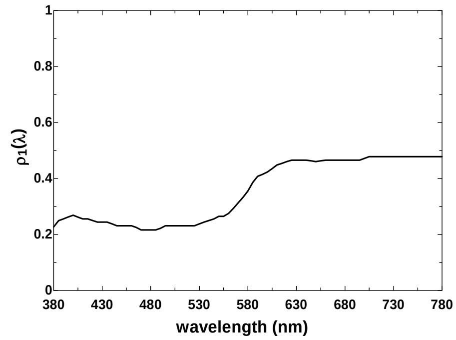

Figure 5.10: Sample 1, light greyish red

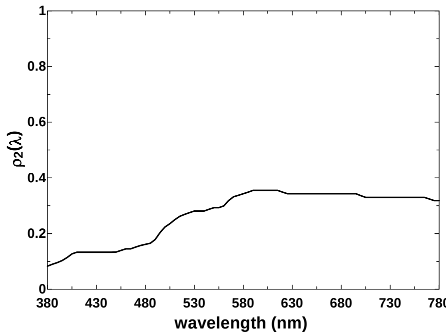

Figure 5.11: Sample 2, dark greyish yellow

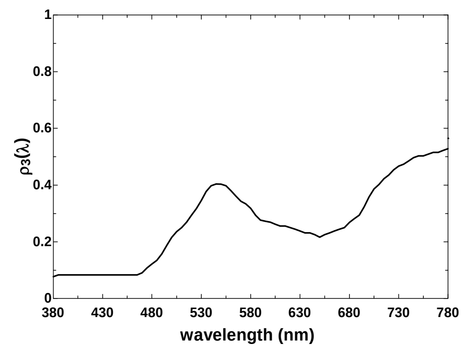

Figure 5.12: Sample 3, strong yellow green

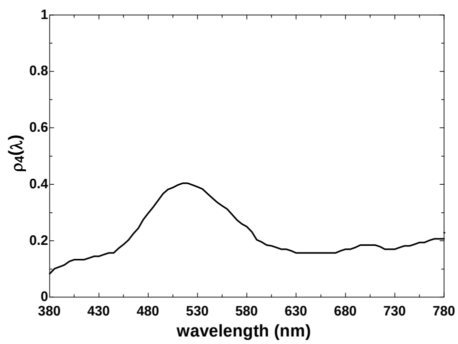

Figure 5.13: Sample 4, medium yellowish green

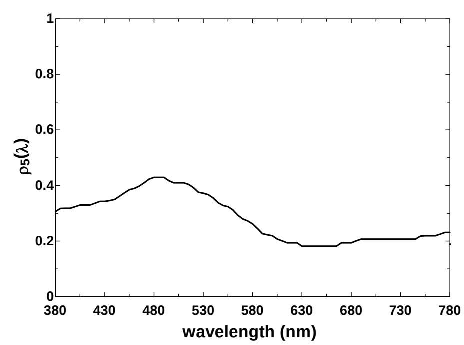

Figure 5.14: Sample 5, light bluish green

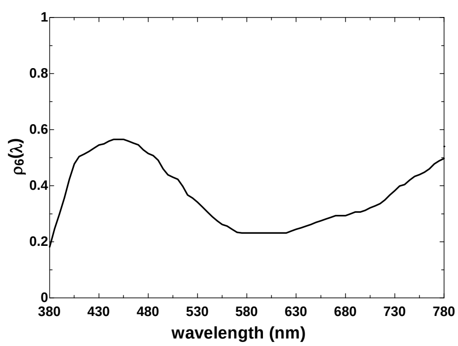

Figure 5.15: Sample 6, light blue

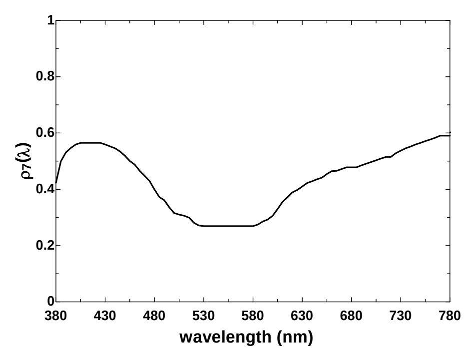

Figure 5.16: Sample 7, light violet

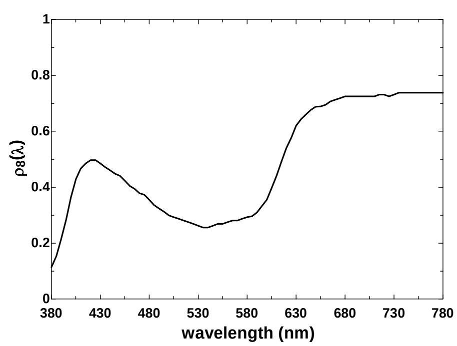

Figure 5.17: Sample 8, light reddish purple

The color of light reflected from an object is found the same way as the color of a light source, i.e. the utilization of equations 5.1 through 5.6 to find the tristimulus values and chromaticity coordinates of the SPD. However, the $\rho(\lambda)$ term in equations 5.1 through 5.3 is no longer 1 at all wavelengths as when the color of the light source was under study, but becomes the wavelength dependent reflective characteristics of the object illuminated. As an example, consider the eight color samples defined by Figures 5.10 through 5.17 illuminated by the SPD of 6500 K daylight (the D65 standard) shown below in Figure 5.18.

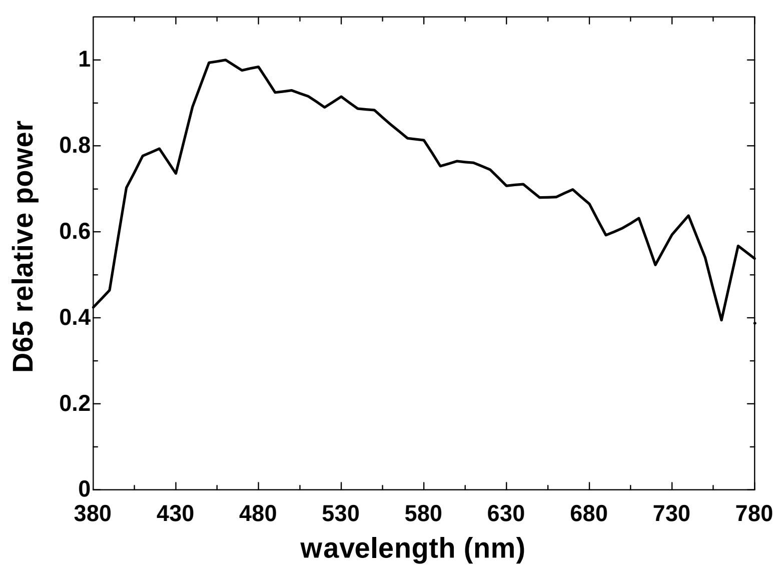


Figure 5.18: SPD of the 6500 K daylight standard (Wyszecki, 1982)

The chromaticity coordinates for each color sample illuminated by $S(\lambda)$ defined by Figure 5.18 are shown in Table 5.3. GretaMacbeth, a color systems and software company, distributes a color conversion program for PCs that transforms chromaticity coordinates into a colored patch on the computer screen. This program is available from

<http://standards.gretagmacbeth.com/Munsell/Color%20Conversion.htm> and was last accessed in January 2004. Its interface is shown in Figure 5.19. The colors rendered by this program on this author's computer screen were close, but not exact, to the color of physical swatches in "The New Munsell Student Color Set" (Long, 2001). The reader may compare the colors to the descriptions in Table 5.2 to decide if the colors are accurate. A better check requires the Munsell Book of Color (Munsell Color Corporation, 1980) and the Munsell notation of the color samples. The notations of the samples are available from Kruschwitz (2004).

Table 5.3: Chromaticity coordinates of the CRI color samples illuminated by D65

| color sample number | description | Chromaticity Coordinates x | Chromaticity Coordinates y | Color from Munsell program |
|---|---|---|---|---|
| 1 | light greyish red | 0.3772 | 0.3420 | |
| 2 | dark greyish yellow | 0.3822 | 0.4016 | |
| 3 | strong yellow green | 0.3678 | 0.4677 | |
| 4 | moderate yellowish green | 0.2840 | 0.4060 | |
| 5 | light bluish green | 0.2597 | 0.3175 | |
| 6 | light blue | 0.2460 | 0.2555 | |
| 7 | light violet | 0.2908 | 0.2571 | |
| 8 | light reddish purple | 0.3316 | 0.2776 | |

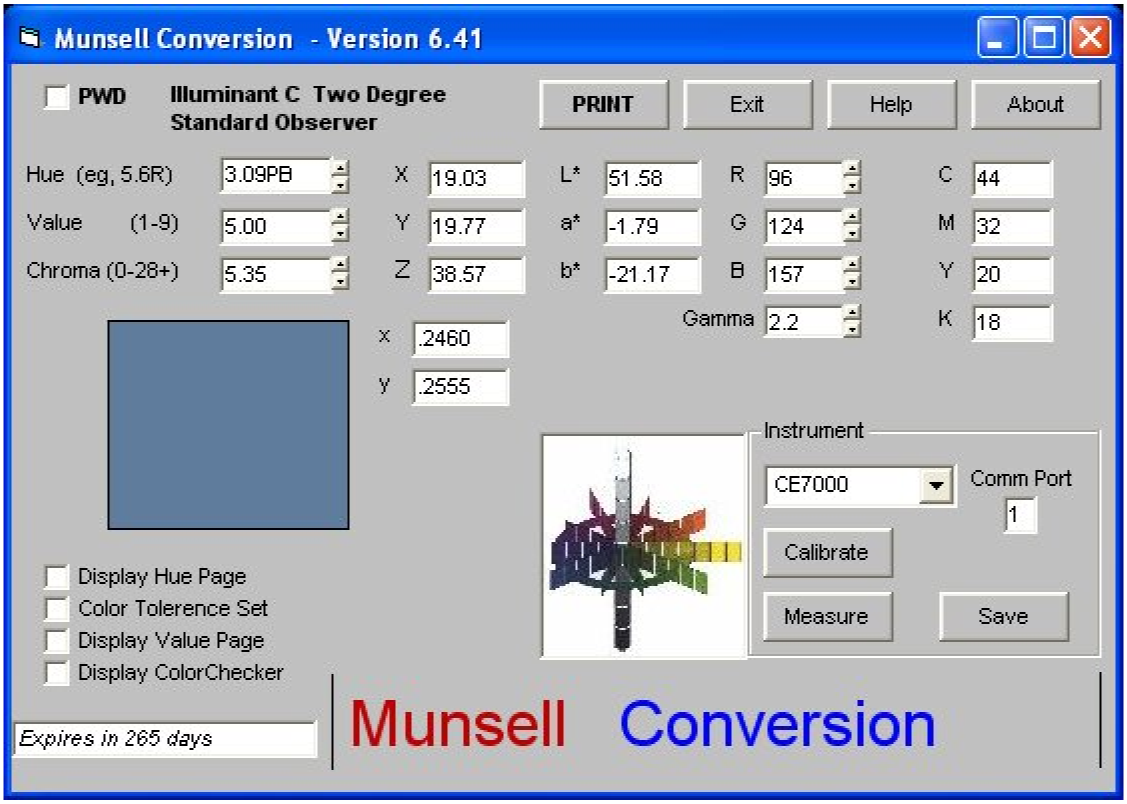


Figure 5.19: Munsell Conversion program used to generate color patches in Table 5.2

The CRI of a light source is a measure of how well a light source under study renders color compared to a reference light source. Selection of the correct reference source is important. To illustrate this point, let's choose the warm white fluorescent lamp detailed in Chapter 4 as the light source under study. Because daylight renders colors well, D65 is one choice for a reference illuminant. For reasons that will be described shortly, the spectrum created by a blackbody at 2992 K (the CCT of the warm white fluorescent bulb) is another choice for a reference illuminant. Figure 5.20 shows the colors of the samples rendered by the Munsell program for the SPDs of these color samples illuminated by these three light sources.

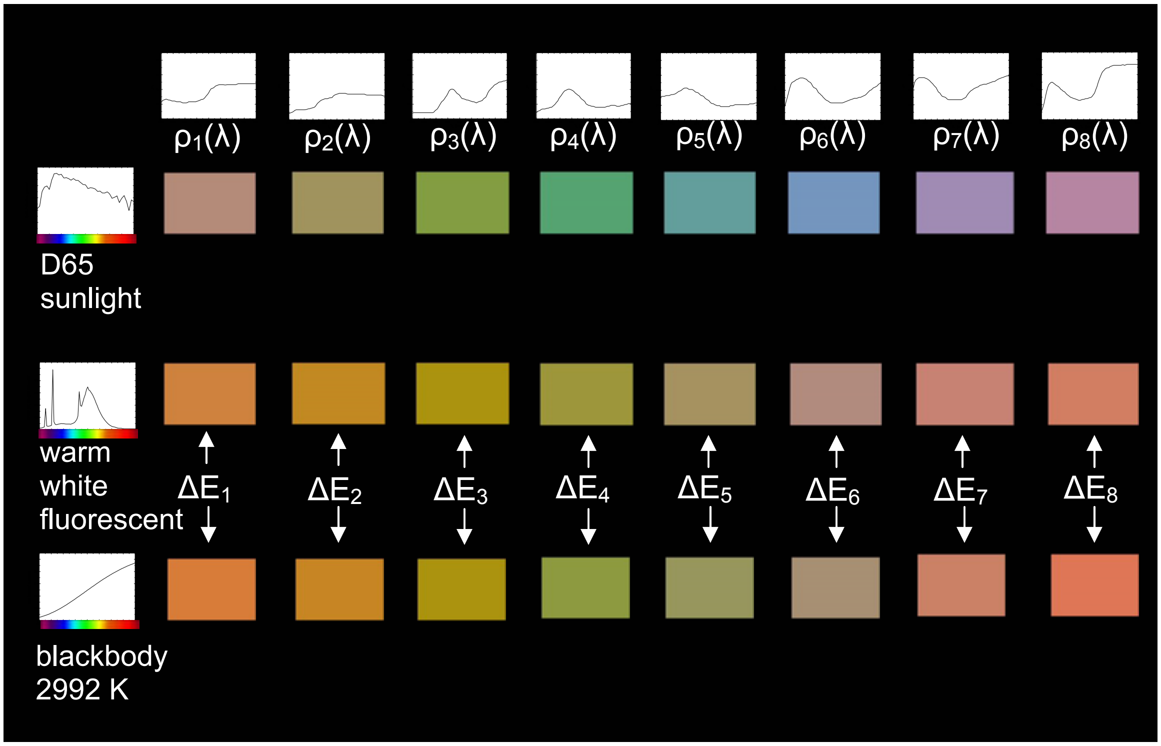


Figure 5.20: The color of the eight color samples, $\rho(\lambda)$, illuminated in turn by D65, the warm white fluorescent lamp described in Chapter 4, and a 2992 K blackbody spectrum. $\Delta E$ indicates the color difference for a given color sample between two illuminants.

The sunlight renders the color of the samples best, especially the blue sample, but the choice of sunlight as the reference illuminant is not ideal because of a phenomenon known as chromatic adaptation. Chromatic adaptation is a process that occurs in the photoreceptors and the brain that attempts to maximize discernment of colors under a given light source. As part of this process, the brain decides that the illumination provided by the illuminant under study is "white", even if it is not. As a result, the perception of color is based not only on the SPD of the light source, the reflective characteristics of the object, and the eye's color matching functions but also on an individual's chromatic adaptation to the light source under study. Using sunlight as a reference would be a non-sensical comparison: the eye adapts to the spectrum of the illuminant under study. However, if the light source has no color at certain wavelengths, then the ability of the eye to discern differences in color between those two wavelengths is limited. What the CRI measures is how well a light source allows the discernment of different colors relative to a light source whose SPD allows the maximum discernment of color under a given state of chromatic adaptation.

For this reason the reference illuminant must be picked to give the closest state of chromatic adaptation to the illuminant under study. The SPD of a blackbody operating at the CCT of the illuminant under study is the chosen reference for CCT values ≤ 5000 K, and a daylight spectrum closest in CCT to the illuminant under study is chosen as the reference for CCT values larger than 5000 K.

The calculation of the CRI is a multi-step process. The purpose of most of the equations is to get to a color difference value, $\Delta E_{i=1 \text{to } 8}$, for each of the color samples lit by the illuminant under study, *k*, and the reference illuminant, *r*. A graphical example of these color difference values was shown in Figure 5.20. The procedure is broken down into 10 steps below:

I. Find CCT (section 5.3) of light source under study, *k*. Generate reference spectrum, *r*.
If $CCT_k < 5000$ K use Planckian distribution (equation 2.1) as reference.
If $CCT_k \geq 5000$ K use appropriate phase of CIE daylight D spectrum as reference.

II. Scale *r* and *k* spectrums to same luminous intensity using equations below.

$$k_r = \frac{100}{\sum_{\lambda=360}^{\lambda=830} S_r(\lambda)\bar{y}(\lambda)\Delta\lambda} \tag{5.12}$$

$$k_k = \frac{100}{\sum_{\lambda=360}^{\lambda=830} S_k(\lambda)\bar{y}(\lambda)\Delta\lambda} \tag{5.13}$$

$k_r$ and $k_k$ are scaling factors so that when Y tristimulus values are calculated:

$$Y_r = k_r \sum_{\lambda=360}^{\lambda=830} S_r(\lambda)\bar{y}(\lambda)\Delta\lambda \quad (5.14)$$

$$Y_k = k_k \sum_{\lambda=360}^{\lambda=830} S_k(\lambda)\bar{y}(\lambda)\Delta\lambda \quad (5.15)$$

$Y_r = Y_k = 100$. The scaling factors are used to scale the *k* and *r* light source spectrums according to equations 5.16 and 5.17

$$S_r(\lambda) = k_r S_r(\lambda) \quad (5.16)$$

$$S_k(\lambda) = k_k S_k(\lambda) \quad (5.17)$$

The result of equations 5.12 through 5.17 is shown in Figure 5.21 for the warm white fluorescent bulb and its reference and the halogen bulb and its reference.

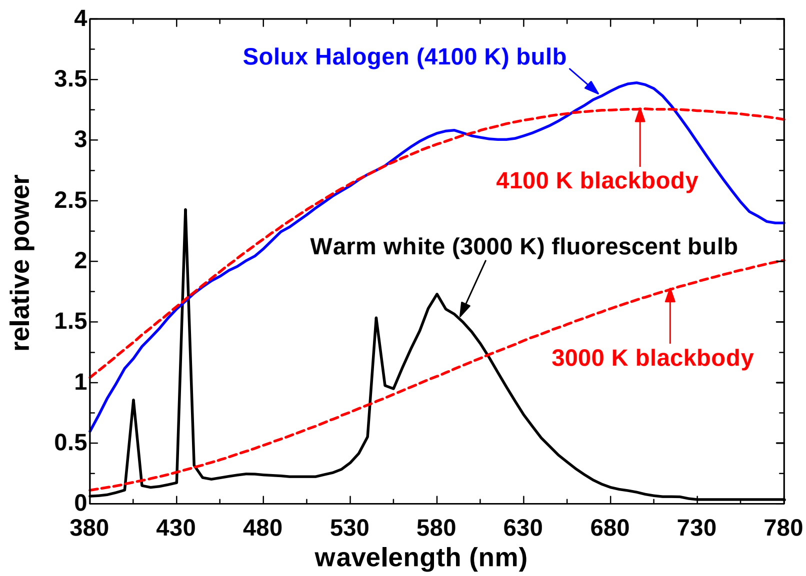


Figure 5.21: Results or scaling light source spectrums and their references for CRI calculation.

From visual inspection, one can see already that the CRI of the halogen bulb will be greater than the warm white fluorescent bulb's CRI because its character is closer to that of its reference.

III. Find the tristimulus values (X, Y, and Z) and chromaticity coordinates (u,v) of the scaled *r* and *k* spectrums.

$$X_r = \sum_{\lambda=360}^{\lambda=830} S_r(\lambda)\bar{x}(\lambda)\Delta\lambda \tag{5.18}$$

$$Y_r = \sum_{\lambda=360}^{\lambda=830} S_r(\lambda)\bar{y}(\lambda)\Delta\lambda \tag{5.19}$$

$$Z_r = \sum_{\lambda=360}^{\lambda=830} S_r(\lambda)\bar{z}(\lambda)\Delta\lambda \tag{5.20}$$

$$X_k = \sum_{\lambda=360}^{\lambda=830} S_k(\lambda)\bar{x}(\lambda)\Delta\lambda \tag{5.21}$$

$$Y_k = \sum_{\lambda=360}^{\lambda=830} S_k(\lambda)\bar{y}(\lambda)\Delta\lambda \tag{5.22}$$

$$Z_k = \sum_{\lambda=360}^{\lambda=830} S_k(\lambda)\bar{z}(\lambda)\Delta\lambda \tag{5.23}$$

$$u_r = \frac{4X_r}{X_r + 15Y_r + 3Z_r} \tag{5.24}$$

$$v_r = \frac{6Y_r}{X_r + 15Y_r + 3Z_r} \tag{5.25}$$

$$u_k = \frac{4X_k}{X_k + 15Y_k + 3Z_k} \tag{5.26}$$

$$v_k = \frac{6Y_k}{X_k + 15Y_k + 3Z_k} \tag{5.27}$$

IV. Calculate values necessary to account for slight differences in chromatic adaptation between *k* and *r* light sources.

$$c_r = \frac{4 - u_r - 10v_r}{v_r} \tag{5.28}$$

$$d_r = \frac{1.708v_r + 0.404 - 1.481u_r}{v_r} \tag{5.29}$$

$$c_k = \frac{4 - u_k - 10v_k}{v_k} \quad (5.30)$$

$$d_k = \frac{1.708v_k + 0.404 - 1.481u_k}{v_k} \quad (5.31)$$

$$u'_k = \frac{10.872 + 0.404\frac{c_r}{c_k}c_k - 4\frac{d_r}{d_k}d_k}{16.518 + 1.481\frac{c_r}{c_k}c_k - \frac{d_r}{d_k}d_k} \quad (5.32)$$

$$v'_k = \frac{5.52}{16.518 + 1.481\frac{c_r}{c_k}c_k - \frac{d_r}{d_k}d_k} \quad (5.33)$$

The $u'_k$ and $v'_k$ that result in 5.32 and 5.33 equal $u_r$ and $v_r$, respectively.

V. Calculate the tristimulus values (X,Y,Z) and chromaticity coordinates (u,v) for each of the color samples (i = 1 through 8) lit by *r* and *k*.

$$X_{ri} = \sum_{\lambda=360}^{\lambda=830} S_r(\lambda)\rho_i(\lambda)\bar{x}(\lambda)\Delta\lambda \quad (5.34)$$

$$Y_{ri} = \sum_{\lambda=360}^{\lambda=830} S_r(\lambda)\rho_i(\lambda)\bar{y}(\lambda)\Delta\lambda \quad (5.35)$$

$$Z_{ri} = \sum_{\lambda=360}^{\lambda=830} S_r(\lambda)\rho_i(\lambda)\bar{z}(\lambda)\Delta\lambda \quad (5.36)$$

$$X_{ki} = \sum_{\lambda=360}^{\lambda=830} S_k(\lambda)\rho_i(\lambda)\bar{x}(\lambda)\Delta\lambda \quad (5.37)$$

$$Y_{ki} = \sum_{\lambda=360}^{\lambda=830} S_k(\lambda)\rho_i(\lambda)\bar{y}(\lambda)\Delta\lambda \quad (5.38)$$

$$Z_{ki} = \sum_{\lambda=360}^{\lambda=830} S_k(\lambda)\rho_i(\lambda)\bar{z}(\lambda)\Delta\lambda \quad (5.39)$$

$$u_{ri} = \frac{4X_{ri}}{X_{ri} + 15Y_{ri} + 3Z_{ri}} \tag{5.40}$$

$$v_{ri} = \frac{6Y_{ri}}{X_{ri} + 15Y_{ri} + 3Z_{ri}} \tag{5.41}$$

$$u_{ki} = \frac{4X_{ki}}{X_{ki} + 15Y_{ki} + 3Z_{ki}} \tag{5.42}$$

$$v_{ki} = \frac{6Y_{ki}}{X_{ki} + 15Y_{ki} + 3Z_{ki}} \tag{5.43}$$

VI. Change chromaticity coordinates defined by 5.42 and 5.43 slightly to account for differences in chromatic adaptation between *r* and *k*.

$$c_{ki} = \frac{4 - u_{ki} - 10v_{ki}}{v_{ki}} \tag{5.44}$$

$$d_{ki} = \frac{1.708v_{ki} + 0.404 - 1.481u_{ki}}{v_{ki}} \tag{5.45}$$

$$u'_{ki} = \frac{10.872 + 0.404\frac{c_r}{c_k}c_{ki} - 4\frac{d_r}{d_k}d_{ki}}{16.518 + 1.481\frac{c_r}{c_k}c_{ki} - \frac{d_r}{d_k}d_{ki}} \tag{5.46}$$

$$v'_{ki} = \frac{5.52}{16.518 + 1.481\frac{c_r}{c_k}c_{ki} - \frac{d_r}{d_k}d_{ki}} \tag{5.47}$$

VII. Transform all color sample chromaticity coordinates (i=1 through 8 and *r*, *k*) into U,V,W coordinates which take into account chromatic adaptive shift.

$$W^*_{ri} = Y^{1/3}_{ri} - 17 \tag{5.48}$$

$$U^*_{ri} = 13W^*_{ri}(u_{ri} - u_r) \tag{5.49}$$

$$V^*_{ri} = 13W^*_{ri}(v_{ri} - v_r) \tag{5.50}$$

$$W^*_{ki} = Y^{1/3}_{ki} - 17 \tag{5.51}$$

$$U^*_{ki} = 13W^*_{ki}(u'_{ki} - u'_k) \tag{5.52}$$

$$V^*_{ri} = 13W^*_{ki}(v'_{ki} - v'_k) \tag{5.53}$$

VIII. Calculate color difference for each color sample, $\Delta E_i$. This is the color difference illustrated in Figure 5.21.

$$\Delta E_i = \sqrt{(U^*_{ri} - U^*_{ki})^2 + (V^*_{ri} - V^*_{ki})^2 + (W^*_{ri} - W^*_{ki})^2} \quad (5.54)$$

IX. Calculate color rendering index for each color sample, $R_i$.

$$R_i = 100 - 4.6\Delta E_i \quad (5.55)$$

X. Calculate the color rendering index.

$$CRI = \frac{1}{8}\sum_{i=1}^{8} R_i \quad (5.56)$$

Table 5.4 lists manufacturer specified and TRNSYS calculated results using the procedure above for calculating the CRI. The TRNSYS results agree well enough to be useful in the analysis of the HLS. Reasons for differences are similar to those explained for the CCT.

Table 5.4: Comparison of manufacturer and CIE(*) specified CRI values with calculated TRNSYS results

| light source spectrum | manufacturer specification | TRNSYS value | difference |
|---|---|---|---|
| tungsten incandescent | >99* | 99.7 | 0.2% |
| warm white fluorescent | 52 | 53.0 | 1.9% |
| halogen | 98 | 97.9 | 0.1% |
| full spectrum fluorescent | 90 | 88.3 | 1.9% |
| daylight 6500 K (D65) | 100* | 100 | 0.0% |

The TRNSYS code that calculates CCT and CRI values is included in the appendix.

# Chapter 6

# The Solar Irradiance Model

## 6.1 SMARTS2 (Simple Model of the Atmospheric Radiative Transfer of Sunshine)

In a building equipped with a hybrid lighting system (HLS), the light delivered to an illuminated space will be a combination of light provided by the conventional electric lamps and the light delivered the HLS. The spectral power distribution (SPD) of this "hybrid" light is a combination of the SPD of the electric lamps and the SPD of the attenuated beam normal solar radiation collected by the HLS. The SPD of the hybrid light is necessary to calculate its correlated color temperature (CCT) and color-rendering index (CRI). Unfortunately, neither TRNSYS nor the Typical Meteorological Year (TMY2) data set it uses has SPD information about solar insolation; consequently this information has to be derived from other sources.

SMARTS2 (*Simple Model of the Atmospheric Radiative Transfer of Sunshine rev. 2*) (Gueymard, 2000) is a Fortran-based spectral model that calculates clear sky beam normal, diffuse, and global irradiance on a terrestrial surface. It creates a SPD of the near ultraviolet (280-380 nm), visible (380-780 nm), and near infrared bands (780-4000 nm) at user-defined wavelength intervals based on an input file that describes the atmospheric conditions for the location of interest (Gueymard, 2000).

Table 6.1 shows the SMARTS2 two-column input data file for the United States terrestrial solar irradiance standards ASTM E891-87, ASTM E892-87, ASTM G159-99 and ISO 9845-1 (Gueymard, 2000). This data file serves as the basis for the input files used in the TRNSYS simulations.

Table 6.1: SMARTS2 input file

| Input file Column 1 Data read by SMARTS2 | Input file Column 2 Data Comment | Description |
|---|---|---|
| 'ASTM_Standards' | !Card 1 Comment | represents the ASTM Standard irradiance |
| 1 | !Card 2 ISPR | directive to read site pressure on card 2a |
| 1013.25 0. | !Card 2a Pressure & altitude | surface pressure (mbar), altitude (km) |
| 1 | !Card 3 IATMOS | directive to use a reference atmosphere defined by card 3a |
| 'USSA' | !Card 3a Atmosphere | use U.S. standard atmosphere |
| 0 | !Card 4 IH2O | directive to read water vapor data on card 4a |
| 1.42 | !Card 4a W | precipitable water (cm) |
| 0 | !Card 5 IO3 | directive to read ozone altitude correction and ozone abundance on card 5a |
| 0 0.34 | !Card 5a IALT, AbO3 | IALT = 0 bypasses altitude correction , abundance of ozone set to 0.34 (atm-cm) |
| 1 | !Card 6 IGAS | conditions for atmospheric gaseous absorption and pollution based on USSA standard atmosphere |
| 370 | !Card 7 qCO2 | average $CO_2$ concentration (ppmv) |
| 1 | !Card 7a ISPCTR | selection of Gueymard's extra-terrestrial spectrum |
| 'S&F_RURAL' | !Card 8 Aeros | selection of aerosol model |
| 0 | !Card 9 ITURB | directive to read Tau5 on card 9a |
| 0.27 | !Card 9a TAU5 | aerosol optical depth at 500 nm |
| -1 | !Card 10 IALBDX | directive to read broadband Lambertian albedo on card 10a |
| 0.2 | !Card 10a RHOX | broadband Lambertian albedo |
| 0 | !Card 10b ITILT | no tilted surface calculations (use air mass, card 17a instead) |
| 280 4000 1.0 1367.0 | !Card 11 Input wavelengths; solar spectrum | spectrum generated from 280-4000 nm, sun-earth distance = 1, solar constant = 1367 $W/m^2$ |
| 2 | !Card 12 IPRT | print spectrum to external file |
| 280 4000 5 | !Card12a Print limits | print from 280-4000 nm at 5 nm intervals |
| 4 | !Card12b # Variables to Print | number of output variables to print to external file |
| 1 2 3 4 | !Card12c Variable codes | print extraterrestrial, beam normal, diffuse horizontal, and global horizontal irradiances respectively |
| 0 | !Card 13 ICIRC | do not simulate radiometer |
| 0 | !Card 14 ISCAN | do not smooth results |
| 0 | !Card 15 ILLUM | no illuminance calculations |
| 0 | !Card 16 IUV | no broadband uv calculations |
| 2 | !Card 17 IMASS | directive to read air mass on card 17a |
| 1.5 | !Card 17a Air mass | air mass value of 1.5 |

SMARTS2 uses the inputs described in Table 6.1 to create the SPD of beam normal radiation in Figure 6.1. The extraterrestrial spectrum used by SMARTS2 is a synthetic spectrum created by previously measured and modeled values (Gueymard, 2000).

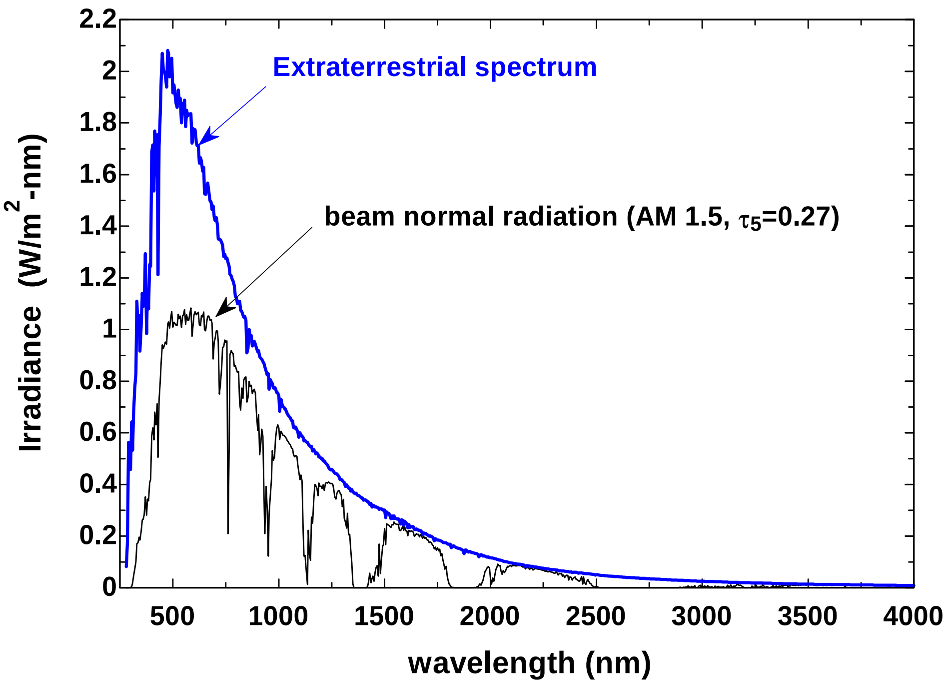


Figure 6.1: The extraterrestrial (ET) and terrestrial SPDs created by the SMARTS2 input file detailed in Table 6.1

As shown by Figure 6.1, as beam radiation passes through the atmosphere it is significantly attenuated. The attenuation is caused by scattering by dust, air and water molecules and absorption by ozone, water and carbon dioxide. Ångstrom's turbidity coefficient, SMARTS2 input card 9a, models scattering by dust and water while Rayleigh scattering by air molecules is significant at wavelengths less than 600 nm. As an aside, Rayleigh scattering is responsible for the blue color of the sky. Ozone in the upper atmosphere strongly absorbs radiation below 290 nm, but absorption decreases with increasing wavelengths until at 350 nm there is no absorption. Water vapor and carbon dioxide absorb radiation in bands mostly in the infrared (Duffie and Beckman, 1991).

In a previous analysis of using SMARTS2 with TRNSYS, Schlegel (2003) found that turbidity and air mass, cards 9a and 17a respectively, had the most significant effect on the beam normal SPD produced by SMARTS2. These two parameters as well as other atmospheric values appearing in the TMY2 weather file were incorporated into the TRNSYS model as described in Section 6.3.

Using 5 nm intervals, the integrated power in the extraterrestrial spectrum of Figure 6.1 is 1352.4 $W/m^2$. The total power defined by the beam normal curve of Figure 6.1 from 280 nm to 4000 nm is 755.2 $W/m^2$ (56%). If the analysis is only carried from 280 nm to 2500 nm, then the area under the beam normal curve is 747.5 $W/m^2$ (55%). The reason for this second calculation is to show that the wavelength range from 280 nm to 2500 nm captures 98.98% of beam normal radiation power, and therefore this wavelength range can be used with confidence in the TRNSYS model. This sentiment is consistent with Table 2.6.1 of Duffie and Beckman (1991). A scale factor of 98.98% is used in Equation 6.3 to slightly increase the integrated beam normal value to account for power beyond 2500 nm.

## 6.2 TMY2 Data (Typical Meteorological Year 2)

SMARTS2 calculates only clear sky SPDs and solar insolation values. In reality, not all days are clear days and a different method must be used to find the magnitude of beam normal radiation in a given hour. The TMY2 is a data set of hourly values of solar radiation and meteorological elements for a 1-year period in a particular geographic location. The TMY2 dataset do not consist of data from one single year, but rather an attempt based on a 30 year history to make one representative year. The actual month of data best reflecting the long-term average for that month forms the basis for selection and inclusion in the TMY2 set. TMY2 data are available for 239 locations in the U.S. Their intended use is for computer simulations of solar energy conversion systems and building systems (NREL, 1995) in order to estimate long-term performance.

The TMY2 data set contains several atmospheric values that are used in the SMARTS2 input file. It contains the atmospheric pressure (SMARTS2 card 2a), precipitable water (4a), and broadband atmospheric turbidity (9a). This last value is especially important as Schlegel (2000) showed that turbidity has a significant affect on the SPD created by SMARTS2. Since atmospheric values change hourly, provisions must be made to change the SMARTS2 input file per hour to accept these variations.

Another significant atmospheric value that changes hourly is the air mass. Air mass is a relative measure of the amount of atmosphere that radiation has to travel through in order to reach the earth's surface. The minimum air mass value is unity, corresponding to the amount of atmosphere that radiation travels through when the sun is directly overhead. Though air mass is not included in the TMY2 data file, it is easily calculated from the sun's zenith angle according to

$$\text{Air mass} = \frac{1}{\cos\theta_z} \quad (6.1)$$

where $\theta_z$ is the zenith angle (radians) calculated by TRNSYS in a given hour. The air mass value calculated by TRNSYS is used in card 17a of the SMARTS2 input file.

When the substitutions for site pressure, precipitable water, turbidity, air mass, and site altitude are made into SMARTS2 input files for Tucson, the SPDs shown in Figure 6.2 are created. These spectrums provide a general sense for how the SPD of clear day beam normal radiation changes throughout a day.

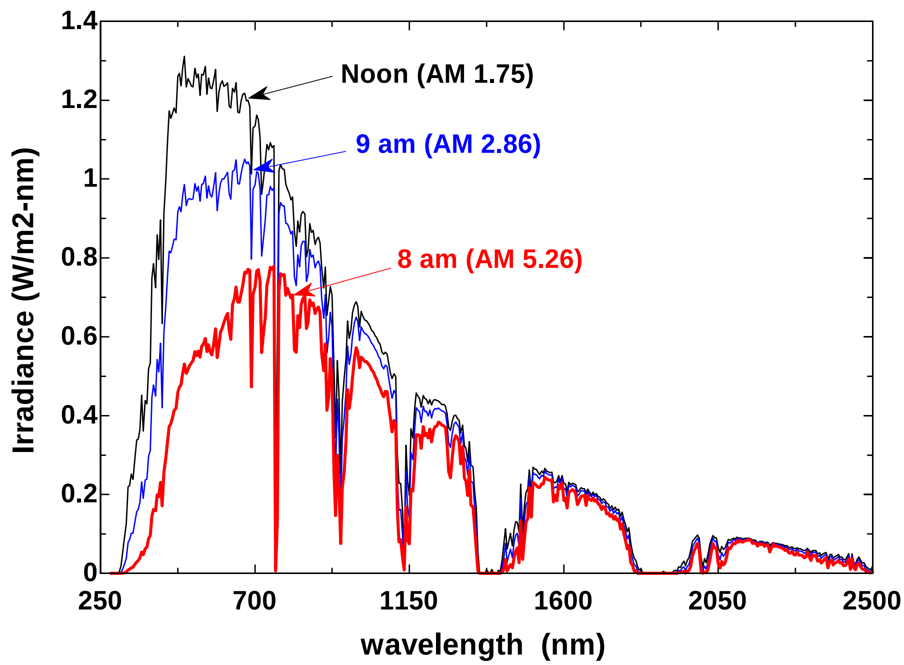


Figure 6.2: SMARTS2 generated SPDs of a clear winter day in Tucson
($\beta$=0.04, w = 0.6 in., P = 917.3 mbar)

Note: care was taken to supply SMARTS2 with correct units. In several cases, e.g. precipitable water and atmospheric pressure, the TMY2 manual's units are not the units used in the data file. Required input units are listed in Table 6.1. Also, the broadband turbidity values in the TMY2 data correspond to Beta in SMARTS2, not Tau5. These changes are further explained below.

## 6.3 Incorporation of SMARTS2 into TRNSYS

Based on the discussion above, parts of the SMARTS2 input file of Table 6.1 are modified to incorporate hourly changing values from TRNSYS and TMY2 data. Table 6.2 details the modifications made to the input file. This modified input file is read by SMARTS2 on an hourly basis to create a SPD for the hour and location of interest.

Table 6.2: Changes made to the SMARTS2 input file to accommodate changing values from TRNSYS and TMY2

| Input file Column 1 Data read by SMARTS2 | Input file Column 2 Data Comment | Description |
|---|---|---|
| 'SMARTS2_input' | !Card 1 Comment | |
| PMBAR ELEV | !Card 2a Pressure & altitude | surface pressure (mbar) from TMY2,<br>altitude (km) from city information |
| W | !Card 4a W | precipitable water (cm) from TMY2 |
| 1 | !Card 9 ITURB | directive to read BETA (turbidity) on card 9a |
| TURB | !Card 9a BETA | broadband turbidity (aerosol optical depth at 1000 nm) from TMY2 |
| 280 2500 1.0 1367.0 | !Card 11 Input wavelengths; solar spectrum | spectrum generated from 280-2500 nm, sun-earth distance = 1, solar constant = 1367 $W/m^2$ |
| 280 2500 5 | !Card12a Print limits | print from 280-2500 nm at 5 nm intervals |
| 1 | !Card12b # Variables to Print | number of output variables to print to external file |
| 2 | !Card12c Variable codes | print beam normal only |
| Air mass | !Card 17a Air mass | Air mass calculated from TRNSYS according to equation 6.1 |

One final modification of the SPD created by SMARTS2 is necessary to make it consistent with TMY2 data for a given location and hour. TMY2 data files contains the magnitude of beam normal radiation for a given hour, not its spectral distribution. The SPD created by SMARTS2 must be scaled so that its integrated value is equal to the beam normal magnitude specified by TMY2. This is accomplished through a scaling factor defined below.

$$G_{SMARTS2,int} = 3.6\left(\frac{kJ/hr - m^2}{W/m^2}\right)\cdot\sum_{\lambda=280nm}^{\lambda=2500nm} G_\lambda \Delta\lambda \quad (6.2)$$

$$ScaleFactor = \frac{G_{TMY2}}{k \cdot G_{SMARTS2,int}} \quad (6.3)$$

$$\text{for each } G_\lambda \text{ (280 nm} - \text{2500 nm at 5 nm intervals):}$$

$$G_{\lambda,scaled} = ScaleFactor \cdot G_\lambda \quad (6.4)$$

where

| | |
|---|---|
| $G_\lambda$ | is the SPD created by SMARTS2 at a given wavelength, $\lambda$ ($W/m^2$-nm) |
| $G_{SMARTS2,int}$ | is the integrated SPD created by SMARTS2 (kJ/hr-$m^2$) |
| k | is a correction factor that slightly increases the $G_{SMARTS2,int}$ value to account for power in the spectrum beyond 2500 nm. $k = 1/0.9898 = 1.01$ |
| $G_{TMY2}$ | is the beam normal value in SMARTS2 data file (kJ/hr-$m^2$) |
| $\Delta\lambda$ | is the wavelength interval, 5 nm |

The scale factors for annual simulations (8760 hours) in Tucson and Seattle are plotted in Figures 6.3 and Figure 6.4, respectively.

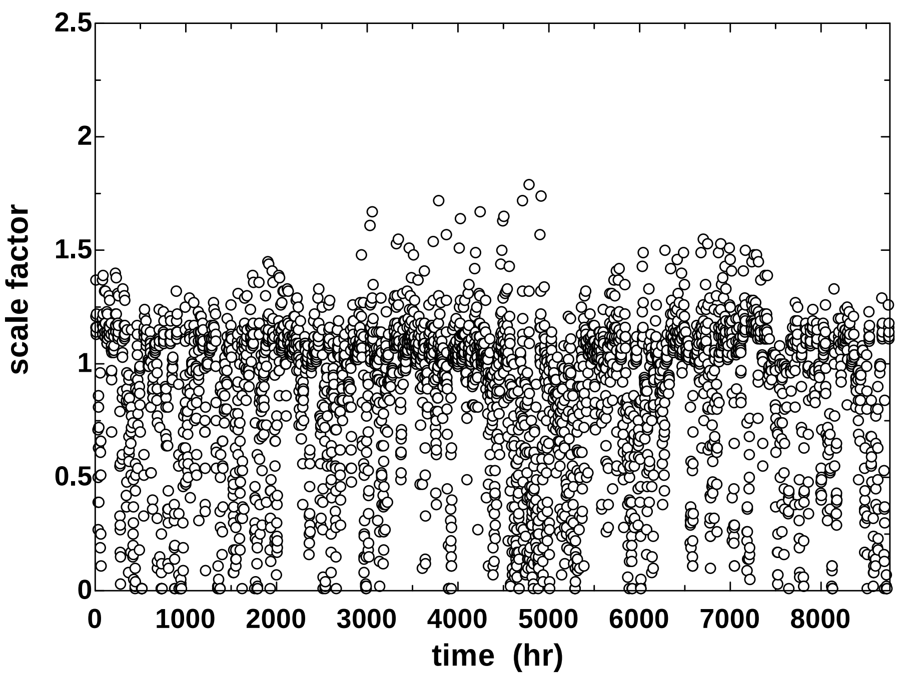


Figure 6.3: Scale factors generated for annual simulation in Tucson. Scale factor defined by equation 6.3.

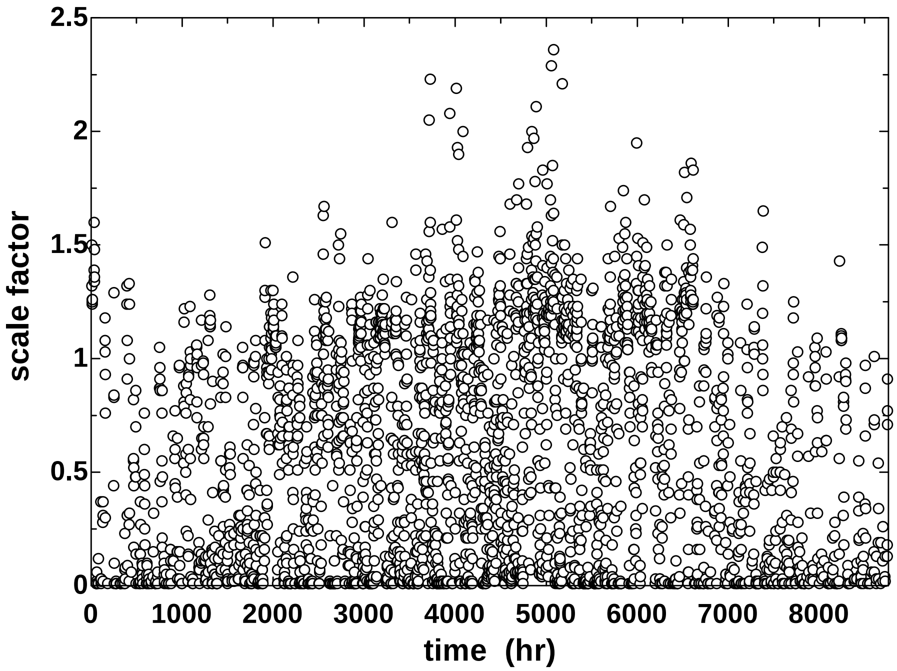


Figure 6.4: Scale factors generated for annual simulation in Seattle.
Scale factor defined by equation 6.3.

For a clear hour, the scale factor defined by equation 6.3 should be approximately one. In other words, the SMARTS2 predicted value for clear sky beam normal radiation should match the measured TMY2 beam normal radiation value. For a cloudy hour, the scale factor will be less than one; SMARTS2 is always a clear sky value so the TMY2 measured value will be less than SMARTS2 if there were any clouds present during that hour.

Figures 6.3 and 6.4 show these general trends. In Figure 6.3 the average scale factor appears to be about 1.1; the average scale factor is more difficult to determine in Figure 6.4 because there are more cloudy hours with corresponding small scale factors. At first thought, a scale factor greater than one may seem impossible: how can more beam normal radiation be measured than the SMARTS2 atmospheric model predicts? There are two possible answers: 1) the data set provided in Table 6.1 amended by values in Table 6.2 consistently causes SMARTS2 to underpredict (≈10-25%) beam normal radiation values or 2) the recorded beam normal radiation value in the TMY2 data set is slightly larger than what was physically available at that hour. To gain better insight, scale factors and lumens delivered as functions of hour in Tucson and Seattle are plotted on shorter timescales in Figures 6.5 and 6.6 below.

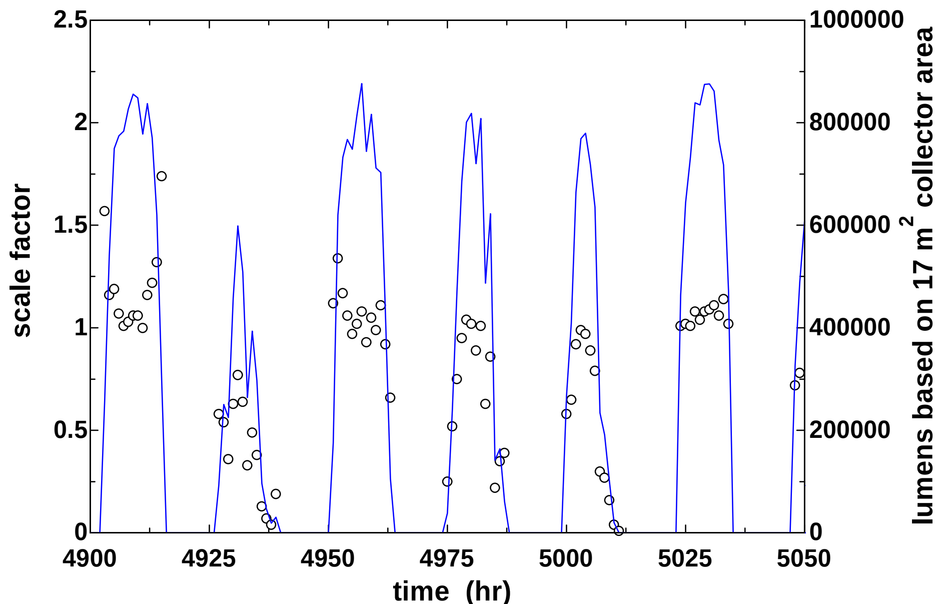


Figure 6.5: Scale factor and delivered lumens in Tucson based on 17 $m^2$ collecting area

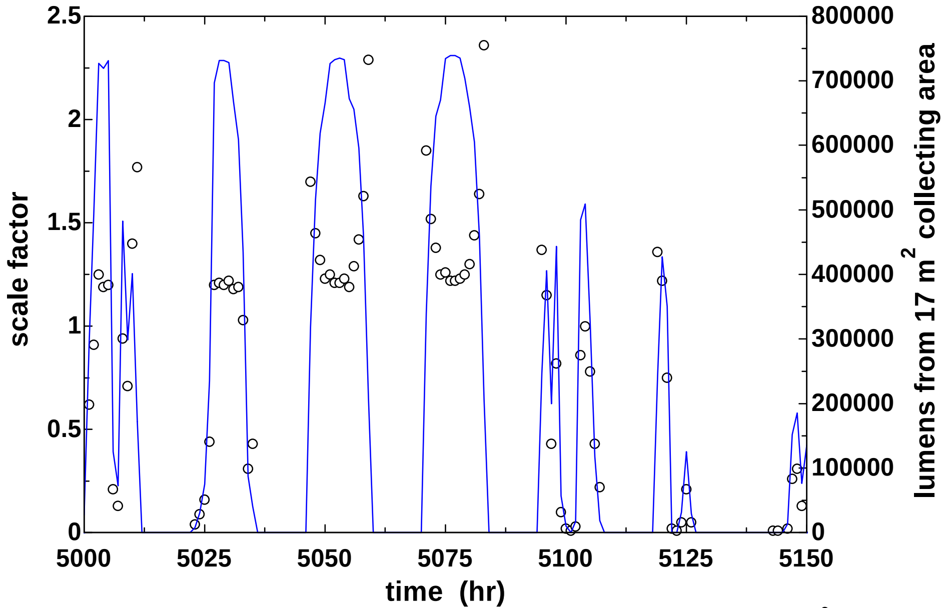


Figure 6.6: Scale factor and delivered lumens in Seattle based on 17 $m^2$ collecting area

Large lumen-delivered values for a given hour in Figures 6.5 and 6.6 indicate a clear hour when the scale factor should be around one. In Tucson this is generally the case. In Seattle, clear hours tend to have slightly larger scale factors of about 1.25. In both figures, scale factors around 2 exist near the beginning and end of the day. A review of the scale factors in Figure 6.3 and 6.4 leads to a similar conclusion: scale factors much greater than one, if they occur, always occur near sunrise or sunset where the effect on the delivered lumens is negligible. Most likely they are due to occasional over-approximations of beam normal radiation in the TMY2 data set due to cloud reflectance around sunrise and sunset. These sunrise/sunset scale factors are not affecting results.

An explanation for larger scale factors in Seattle on clear days involves the length of atmosphere the beam normal radiation travels through, quantified by the air mass. For clear days in both Figures 6.5 and 6.6, the scale factors closest to one correspond to the smallest air mass values that occur around noon. However, in Seattle the smallest air mass value in the summer is about 1.1, while in Tucson the smallest air mass value is about 1. As hours move away from noon on clear days, the scale factor increases. This symmetric behavior excludes the possibility of a time shift error. It suggests that the SMARTS2 model attenuates beam normal radiation at a slightly faster rate as function of air mass than is occurring physically. Then again, it is possible with different atmospheric parameters in Table 6.1 (for each hour) that the clear day scale factors at larger air mass values could get closer to unity. The amount of light coming in to the building is based on the TMY2 measured value, and that SMARTS2 is used to approximate its spectrum. The lumens delivered to the delivered space are a function of that spectrum, but as Figure 6.2 indicates large differences in air mass are required to get spectrums that yield significantly different amounts of light. Therefore scale factors slightly larger than one should not be of concern.

# Chapter 7

# The TRNSYS Model

## 7.1 Description of TRNSYS Model

"TRNSYS is a TRaNsient SYstems Simulation program with a modular structure. It recognizes a system description language in which the user specifies the components that constitute the system and the manner in which they are connected. The TRNSYS library includes many of the components commonly found in thermal and electrical energy systems, as well as component routines to handle input of weather data or other time-dependent forcing functions and output of simulation results. The modular nature of TRNSYS gives the program tremendous flexibility, and facilitates the addition to the program of mathematical models not included in the standard TRNSYS library." (TRNSYS website, 2004).

Schlegel (2003) created the first iteration of the TRNSYS hybrid lighting system (HLS) model and described its implementation in detail. The description of the system below is meant to give the reader a thorough overview of the TRNSYS HLS model, but for added detail the reader should consult Schlegel. There are significant differences between Schlegel's model and the current model, and these differences will be described after the overview.

The TRNSYS HLS model consists of interconnected component models that include a weather file, a radiation processor, a hybrid lighting model, a building model, building schedules, utility rate schedules, and output components. Simulation results include annual energy and monetary savings gained from the hybrid lighting system as well as colorimetric indices, the CCT and the CRI.

As described in Chapter 6, the TMY2 weather file is used with SMARTS2 to generate the spectral power density (SPD) of incident radiation on the collector for each hour of the year. This SPD is attenuated by either the spectral or wideband transmittances of the collecting and cold mirrors, the fiber entrance region, the fiber itself, and the luminaires. Some of these transmittances will be documented shortly.

Within TRNSYS, the light output from the hybrid lighting system model is sent to the building model. The building is modeled using the Type 56 multi-zone building model. Type 56 is a FORTRAN subroutine which is designed to provide detailed thermal models of buildings. The model consists of two windowless 2500 $m^2$ zones. During the simulation, one zone uses one of the lamps described in Chapter 4 to provide all the building lighting needs while the other zone pairs the selected lamp with light delivered by the HLS. Identical schedules in the two zones simulate the heating, cooling, and ventilation of a typical mixed-use environment. Additional gains in the model account for the people, equipment (e.g. computers), and lights in the building. Cooling in the building is supplied using a chiller with a constant COP of 3 and heating loads are met using an 80 % efficient natural gas furnace. Using local utility rate schedules, energy costs are calculated for the two zones of the building model with the difference representing the energy savings due to the hybrid lighting system.

The simulation uses a heating set point of 20 C with a night setback of 17 C. Cooling is active at 26 C and above. Relative humidity within the building is allowed to float between 30 and 60%. Illumination levels within the building are set to 500 Lux over the entire floor space, which is the IESNA recommended lighting level for general office work (IESNA, 2000). Occupancy schedules model a typical 8 am to 5 pm work week. Infiltration and ventilation rates are based on information provided in ASHRAE 62–2001. Rate schedules from utilities near the various locations are used to determine the time variant prices of natural gas and electricity (EIA, 2003).

## 7.2 Revisions to the original HLS model

There have been two major changes and one addition to Schlegel's model. The atmospheric spectral model was changed from a simplified SMARTS2 fit to the fully incorporated SMARTS2 algorithm. The second change was the inclusion of incidence angle effects and fiber bending effects in the fiber attenuation portion of the model. Finally, a colorimetric model capable of calculating the correlated color temperature (CCT) and the color rendering index (CRI) was added so that the appearance of the light delivered by the HLS and its ability to render colors could be quantified.

Chapter 6 has already described how SMARTS2 was added to the TRNSYS model. The simplified fit (Schlegel, 2003) estimated lighting and cooling savings within 10% of the TRNSYS model incorporating the full SMARTS2 algorithm but the spectrum it delivered was a generalized global horizontal spectrum that was insufficient for meaningful colorimetric calculations. When the colorimetric model was first added to the TRNSYS model and the simplified atmospheric model was used, incorrect CCT values as high as of 6000 K resulted for clear sky beam radiation. Though the lumens delivered by 6000 K and 5000 K blackbody spectrums scaled to give equal power in the visible range do not differ by more than a few percent, the spectrums appear quite different: the 6000 K spectrum appears bluer than the 5000 K spectrum. For accurate CCT and CRI calculations, the full SMARTS2 algorithm was required and consequently added.

In the original HLS model, the attenuation of light in the fiber was wavelength and fiber length dependent. Subsequent work by the Renssellaer Lighting Research Center and Oak Ridge National Lab showed that attenuation was a function of two other factors: the incidence angle of the entering light relative to the fiber centerline and the minimum radius bend present over the fiber length. Figure 7.1 shows the transmissivity of a one meter length of the PMMA (polymethyl-methacrylate) optical fiber as functions of these two effects.

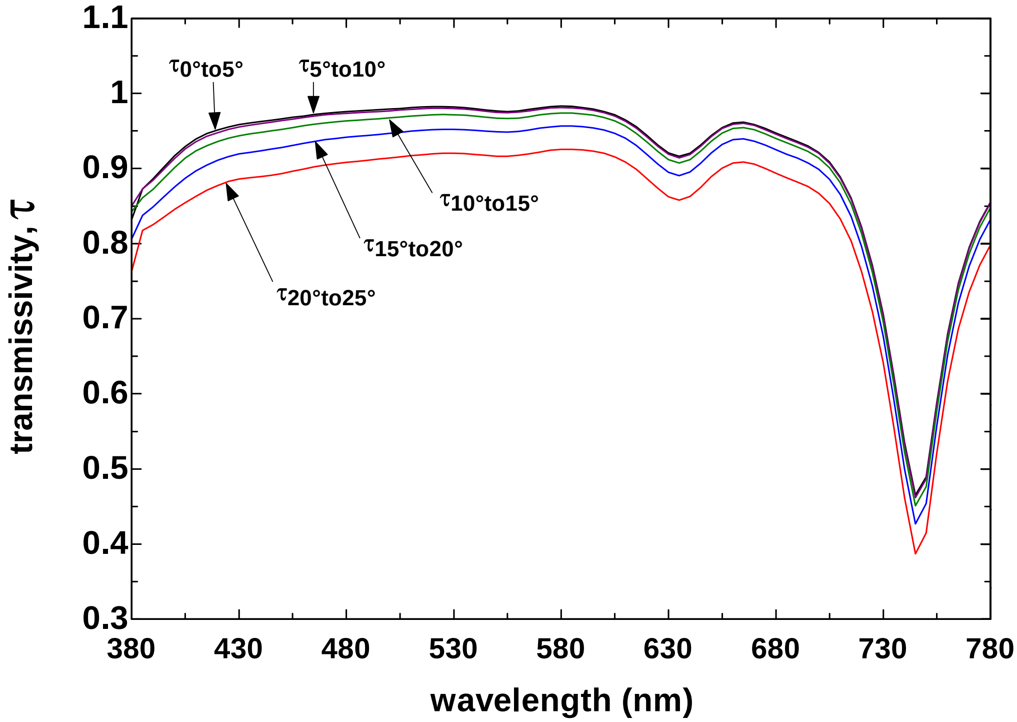


Figure 7.1: Transmissivity of one meter PMMA fiber as a function of wavelength and incidence angle. The incidence angle is defined as the angle between the centerline of the fiber and the incoming light from the cold mirror. Incidence angles are grouped in 5˚ intervals (Renssellaer, 2003).

As shown in Figure 7.1, larger entrance angles lead to smaller transmissivities at all wavelengths and correspondingly higher light attenuation per meter. Though the fiber does not transmit 700-750 nm radiation very well, the effect on the amount of visible light transmitted is small because the photopic visibility curve is close to zero in this wavelength range anyway.

Figure 7.2 shows how the relative transmission in a five meter length of fiber is affected by the incidence angle of the incoming light and the presence of the smallest radius bend in the fiber. Decreasing fiber radius and increased incidence angles decrease transmission.

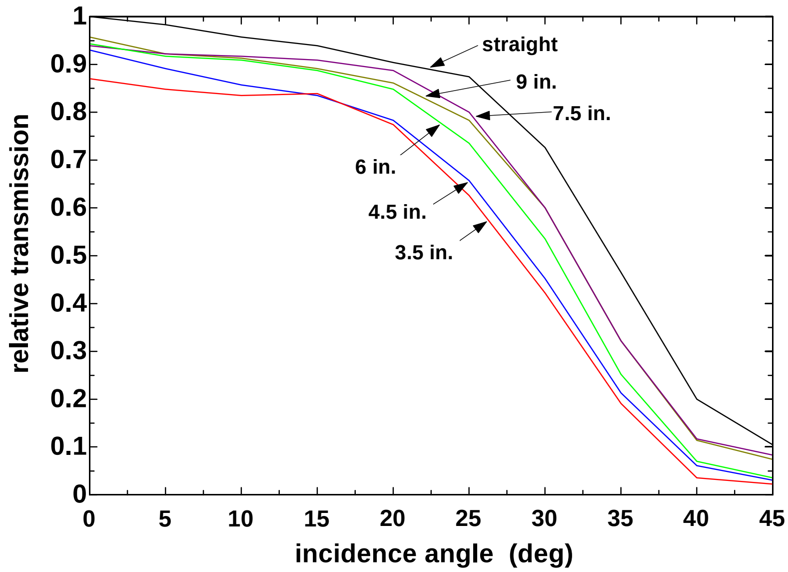

Figure 7.2: Relative transmission of a five meter length of PMMA fiber as a function of incidence angle and bend radius in fiber (ORNL, 2002).

Transmission data from Figure 7.2 must be changed into absolute transmissivity values. Furthermore, incidence angle effects are better quantified by Figure 7.1 than Figure 7.2 because Figure 7.1 shows wavelength attenuation dependence. The important information in Figure 7.2 is the effect of bend radius on the transmissivity of the fiber. This information was obtained by taking the ratio of the relative transmission for a specified bend radius to the straight relative transmission at a given incidence angle, yielding the absolute transmissivity for that incidence angle and bend radius. The absolute transmissivity for the same bend radius was then found in the same way at other incidence angles, yielding transmissivities that were at all times within 5% of each other except for larger incidence angles (20˚-25˚). The present design of the HLS has little light entering at these larger flux angles so the curve fit shown in Figure 7.3 is used to approximate the amount of light transmitted as a function of the smallest radius in the fiber length. A bend with a radius of 12" or more is considered straight.

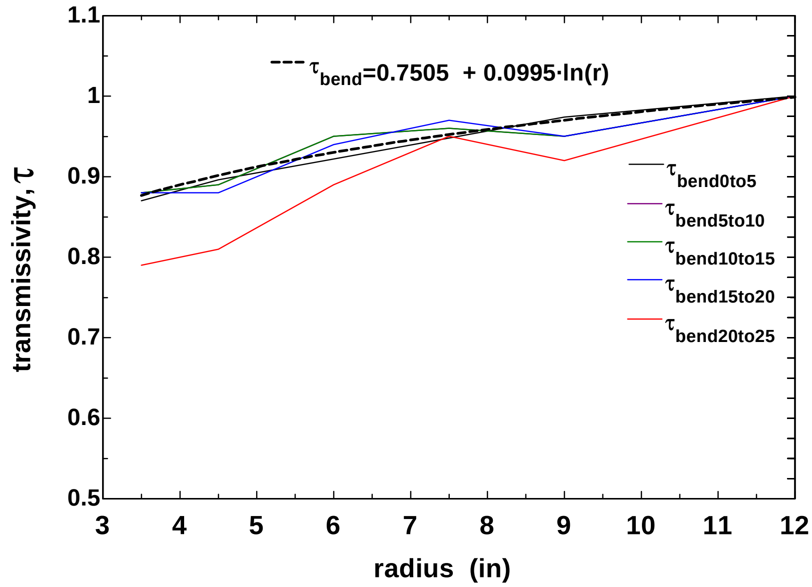

Figure 7.3: Effect of bend radius on fiber transmissivity. The curve fit shown is used in the fiber transmission equation 7.1 below.

Transmissivity values from Figures 7.1 and 7.3 are used to calculate the transmissivity of fiber at a given wavelength according to the equation 7.1:

$$\tau_{\lambda} = \left[ \begin{array}{l} \text{flux}_{0^o-5^o}(\tau_{\lambda,1m,0^o-5^o})^L + \text{flux}_{5^o-10^o}(\tau_{\lambda,1m,5^o-10^o})^L + \text{flux}_{10^o-15^o}(\tau_{\lambda,1m,10^o-15^o})^L + \\ \text{flux}_{15^o-20^o}(\tau_{\lambda,1m,15^o-20^o})^L + \text{flux}_{20^o-25^o}(\tau_{\lambda,1m,20^o-25^o})^L \end{array} \right] \times \tau_{bend} \quad (7.1)$$

where

| | |
|---|---|
| $\tau_{\lambda}$ | is the fiber transmissivity at a given wavelength, λ |
| $\text{flux}_{\text{angle interval}}$ | is the percentage of light, expressed as a decimal (i.e. 10% = 0.1), entering the fiber in the given incidence angle interval |
| $\tau_{\lambda,1m,\text{angle interval}}$ | is the transmission of 1 m length of fiber for a given wavelength and incidence angle interval plotted in Figure 7.1 |
| L | is the length of the fiber in meters |
| $\tau_{bend}$ | is the transmission in the fiber as a function of the minimum radius bend in its length from the curve fit in Figure 7.3 |

The total transmissivity of the fiber is the ratio of the visible light leaving it to the amount of light entering it. When a beam normal spectrum generated by SMARTS2 for summer in Oak Ridge (Knoxville), TN around noon is reflected by the primary and secondary mirrors and then passed through different length fibers, the total transmissivity curve in Figure 7.4 is created. These transmissivities were calculated using equation 7.1.

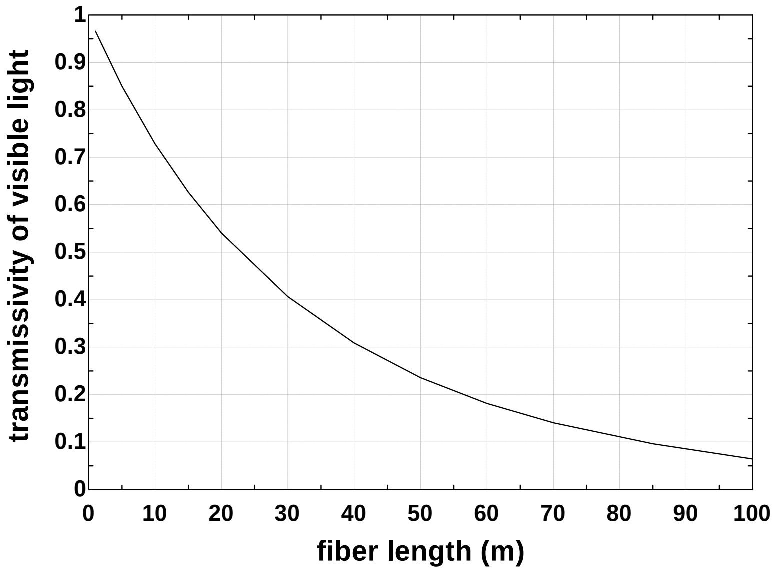


Figure 7.4: Fiber transmission of visible light as a function of its length. Assumed straight fiber and following fluxes: 0˚-5˚: 12%, 5˚-10˚: 34%, 10˚-15˚: 48%, 15˚-20˚: 6%, and 20˚-25˚: 0%. Incident beam normal SPD was summer noon Knoxville, TN generated by SMARTS2.

The last major change to the original TRNSYS HLS model was the addition of a colorimetric model. For each hour that the simulated building is operated, the colorimetric model calculates the CCT of the incident beam normal radiation as well as the CCT and CRI of the delivered light indoors. The indoor SPD is usually a combined SPD of the light delivered by the HLS and the SPD of the conventional lamp selected in the simulation. The colorimetric model uses the calculation methods described in Chapter 5 and the lamp spectrums mentioned in Chapter 4.

## 7.3 Selection of Model Inputs

As described in Chapter 1, the hybrid lighting system has numerous components that affect the overall performance of the system. Many of these components change as the design process continues, and the TRNSYS model must be flexible enough to accommodate changing component performance values. For this reason, the user of the TRNSYS simulation is given control over many parameters affecting the performance of the system.

Figures 7.5a and 7.5b show the TRNSYS HLS model user interface. The results section that follows is based on these component inputs. The parameters that change from simulation to simulation presented in the results section are: the city selection and corresponding altitude and utility rate schedule, the number of systems, the length of fiber, and the selection of the indoor light source.

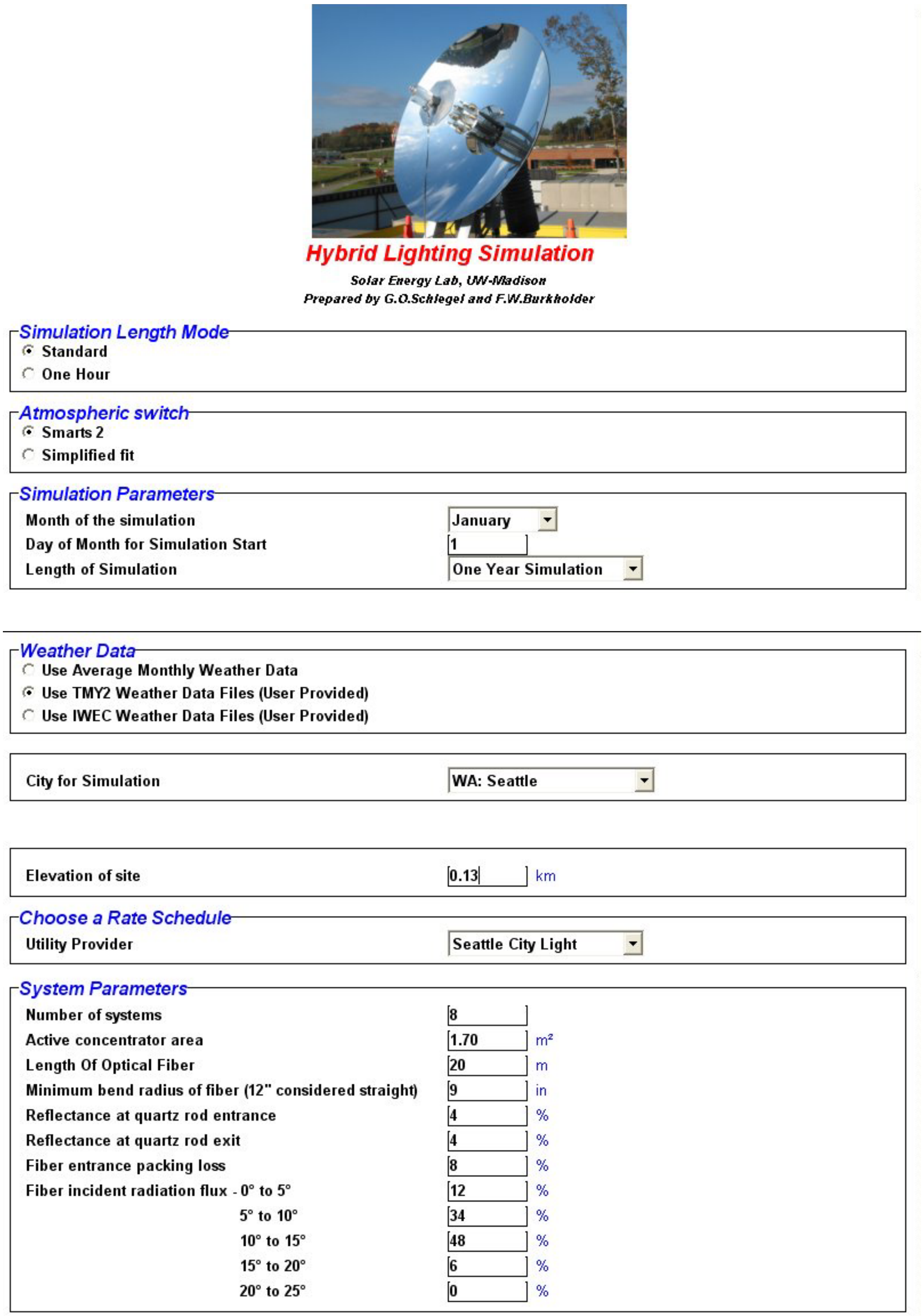


Figure 7.5a: TRNSYS model inputs, page 1

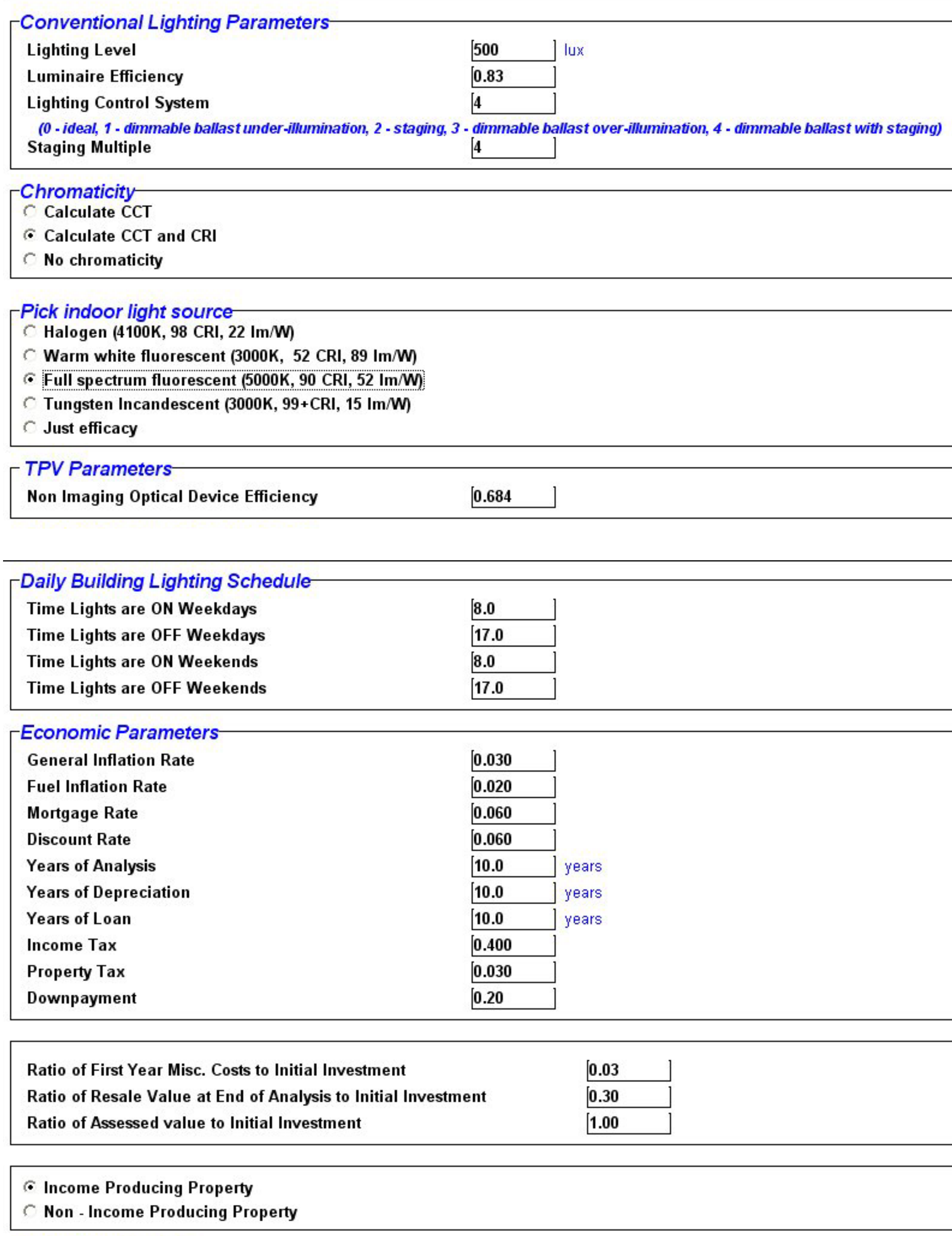


Figure 7.5b: TRNSYS model inputs, page 2

The model parameters above can be varied to generate numerous results. The challenge is to select the parameters that have the largest effect on the energy savings and

CCT and CRI of the delivered light, and then vary those parameters to determine their effect. The lamps included in this model were selected for their wide range of efficacy values, which will have a strong effect on energy savings, and their vastly different spectrums, which will affect CCT and CRI values of the delivered illumination. The other parameters that have the largest energy savings and chromaticity effects are the number of modules and collector area, which quantify the ratio of roof collector area to indoor illuminated area ($A_{coll.}/A_{illum.}$), and the length of optical fiber.

Important $A_{coll.}/A_{illum.}$ ratios can be determined from straightforward calculations. Beam normal radiation has luminous flux of about 100,000 lux (lumens/$m^2$). IESNA (2000) recommends illuminance levels of 500 lux for office environments. Therefore, 1 $m^2$ of collector area could service 200 $m^2$ building area ($A_{coll.}/A_{illum} = 1/200$) if the light could be collected and distributed without any losses. This quick calculation also assumes that it is desirable for the HLS to supply 100% of the required illumination when the sun is shining. If the HLS was required to provide only 50% of the desired illumination level (250 lux), 1 $m^2$ could provide light to 400 $m^2$ of building area ($A_{coll.}/A_{illum} = 1/400$), assuming perfect collection and distribution.

Realistically the light cannot be collected and distributed without loss. The reflection of the mirrors is not perfect, the fiber entrance region absorbs and reflects some of the visible light, the fiber further attenuates the light (as shown previously), and the luminaire absorbs some light as well. Figure 7.6 graphically illustrates the losses due to these components, and Table 7.1 shows the luminous efficiency of the entire system based on varying fiber lengths and whether the first prototype system (benchmark system) incidence angles or the newer alpha system incidence angles are used.

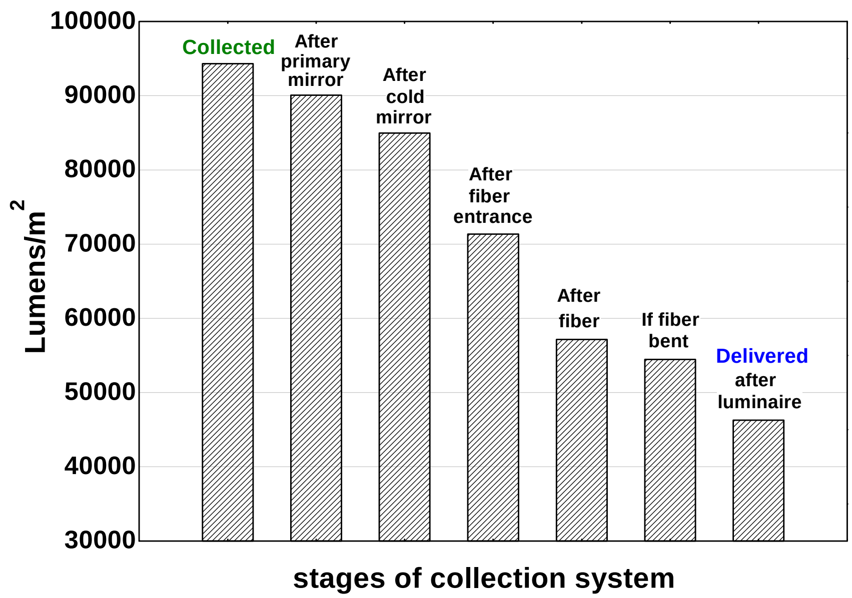


Figure 7.6: Lumens collected and lumens delivered based on 7 m fiber length and alpha system fluxes[B]. Luminous efficiency, η = Delivered/Collected, is approximately 0.5.

Table 7.1: Comparison of ORNL and TRNSYS Luminous Efficiencies

| **Fiber Length (m)** | **ORNL System Measured Efficiency (%)** benchmark flux[A] | **TRNSYS Predicted Efficiency (%)** benchmark flux[A] | **TRNSYS Predicted Efficiency (%)** alpha system flux[B] |
|---|---|---|---|
| 4.5 | 53.5 | 52.8 | 53.0 |
| 5.5 | 51.7 | 50.7 | 51.4 |
| 6.5 | 49.9 | 48.7 | 49.8 |
| **7.0** | not measured | 47.8 | **49.0** |
| 7.5 | 48.1 | 46.8 | 48.3 |
| 8.5 | 45.8 | 44.9 | 46.8 |
| 9.5 | 44.9 | 43.2 | 45.4 |
| **10.0** | not measured | 42.5 | **44.7** |
| 10.5 | 42.6 | 41.6 | 44.0 |
| **20.0** | not measured | 29.3 | **33.0** |

A: benchmark system flux 0˚-5˚: 10%, 5˚-10˚: 20%, 10˚-15˚: 30%, 15˚-20˚: 30%, and 20˚-25˚: 10%.
B: alpha system flux 0˚-5˚: 12%, 5˚-10˚: 34%, 10˚-15˚: 48%, 15˚-20˚: 6%, and 20˚-25˚: 0%.

Table 7.1 is noteworthy for two reasons. The first is that TRNSYS modeled luminous efficiencies for the benchmark system agree well with ORNL measured luminous efficiencies, thus validating the TRNSYS transmission model. The second is that for the newer alpha system incident flux angles, a fiber length of 10 m gives a total luminous efficiency of 45% (that for simplicity's sake will be approximated as 50%), and a fiber length of 20 m gives a total luminous efficiency of about 33%. These efficiencies can be used in the simple analysis begun earlier to determine important $A_{coll.}/A_{illum}$ ratios.

If 10 m of fiber is used, the 100,000 lux collected is reduced to 50,000 lux delivered because of the approximate 50% luminous efficiency associated with the overall HLS system. If the HLS is to provide all of the 500 lux required in the building, the $A_{coll.}/A_{illum}$ ratio that will deliver this is 1/100. In other words, a 1 $m^2$ collector will deliver all the illumination required to a 100 $m^2$ area inside the building. Using a greater $A_{coll.}/A_{illum}$ ratio is counter-productive: more light is delivered to the space than required, increasing the cooling load of the building while not reducing the lighting load any further. For the 2500 $m^2$ building used in this analysis, the closest number of 1.7 $m^2$ modules that creates an $A_{coll.}/A_{illum} \approx 1/100$ is fifteen modules (though because efficiency is actually less than 50%, sixteen modules are used in this analysis).

By similar reasoning, a HLS with 10 m fiber that supplies 50% of the required indoor illumination level during sunny conditions can service 200 $m^2$ building area per $m^2$ collector area, corresponding to $A_{coll.}/A_{illum} = 1/200$. In this analysis, eight 1.7 $m^2$ modules best approximate this $A_{coll.}/A_{illum}$ ratio.

The point of the discussion above was to show that 10 m of fiber and eight and sixteen 1.7 $m^2$ modules are useful inputs to the HLS model. For a 10 m fiber length, eight modules corresponds to a 50% hybrid light fraction in the building during sunny conditions when beam normal radiation is available. Similarly, sixteen modules correspond to a 100% hybrid light fraction, meaning that all the indoor illumination is provided by the HLS - the electric lights could be turned off entirely.

Ten meters of fiber is sufficient to distribute light collected by the HLS to a single story directly below the collector. However, there is no guarantee that the collectors can be installed directly over the area they are meant to service and it may be desired to deliver the light to a second story beneath the first. For this reason, twenty meters of fiber were used in many of the simulations presented in the results section. The overall luminous efficiency of the HLS with 20 m fiber is 33% therefore different $A_{coll.}/A_{illum}$ ratios correspond to 50% and 100% hybrid light fractions within the building. All things being the same except for a change in fiber length from 10 m to 20 m, eleven modules correspond to 50% and twenty-two modules correspond to 100% HLS fraction. Some simulations were run with 20 m of fiber and twenty-four modules to quantify the results of this configuration.

In summary, simulations were run with two fiber lengths: 10 m and 20 m. Simulations were also run with eight, sixteen, twenty, and twenty-four 1.7 $m^2$ modules to capture 50% and 100% hybrid light fraction behavior for these two fiber lengths. Four different lamps with differing efficacies and colorimetric indices were run for the fiber length and collecting area ratios mentioned above.

## 7.4 Results

A potential investor or buyer of a HLS will want to know how much energy the HLS will save, and correspondingly how much money the HLS will save per year. The modeled building has three energy loads: the heating load, the cooling load, and the lighting load. The energy saved is quantified by how these loads are reduced. Of course the HLS will reduce the electrical lighting load anywhere it is deployed because the illumination it delivers replaces light generated by electricity. The HLS also decreases building cooling loads because the light it delivers has a larger luminous efficacy than the light delivered by conventional lamps. In other words, less thermal energy enters with the desired amount of illumination. Because less thermal energy enters the building, less needs to be removed by the cooling system, thereby reducing the cooling load. In hot, sunny environments this effect is very significant. What Schlegel (2004) showed is that heating load effects are minimal, i.e. places that have large heating loads tend to be places where the HLS does not provide much illumination anyway and so the HLS has a minimal impact on the heating load. For this reason, heating loads will not be presented.

### 7.4.1 Energy Savings in selected U.S. cities

Figures 7.6(a,b) and 7.7(a,b) summarize the electrical reductions expected in the lighting load and cooling load in buildings in six U.S. cities equipped with the specified number of HLS modules versus identical buildings without them. The only difference between Figures 7.6 and 7.7 is the length of optical fiber in the HLS: 10 m in Figures 7.6(a-d) and 20 m in Figures 7.7(a-d). Simulations were run using a lamp efficacy of 52 lm/W which is the average luminous efficacy in commercial buildings (Muhs, 2004).

These results revise work done by Schlegel performed with the original HLS model.

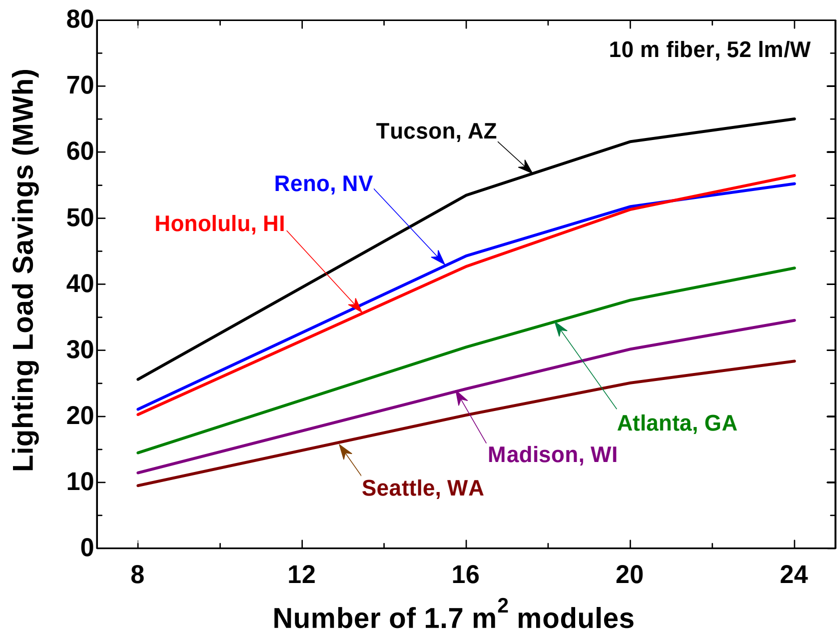


Figure 7.6a: Lighting Load Savings from HLS, 10 m fiber, 52 lm/W in six U.S. cities

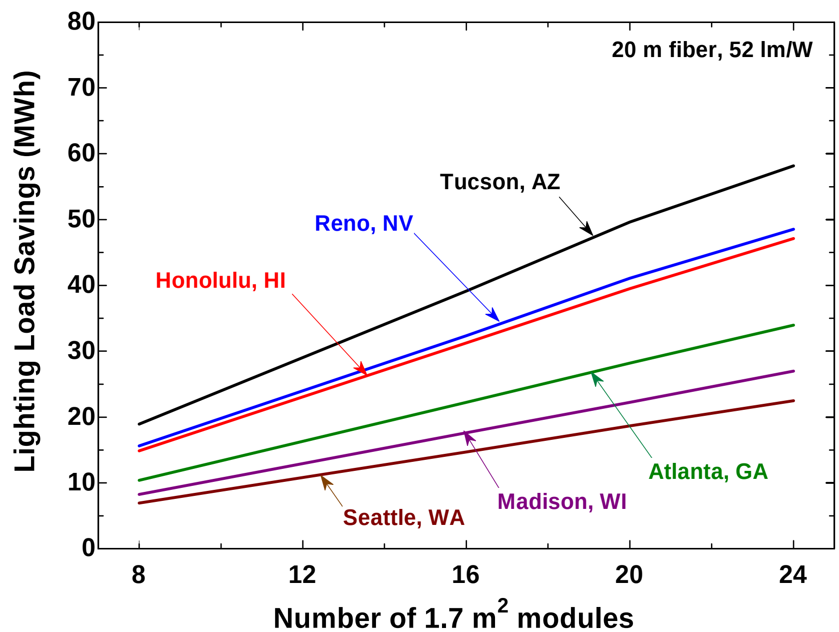


Figure 7.7a: Lighting Load Saving from HLS, 20 M fiber, 52 lm/W, in six U.S. cities

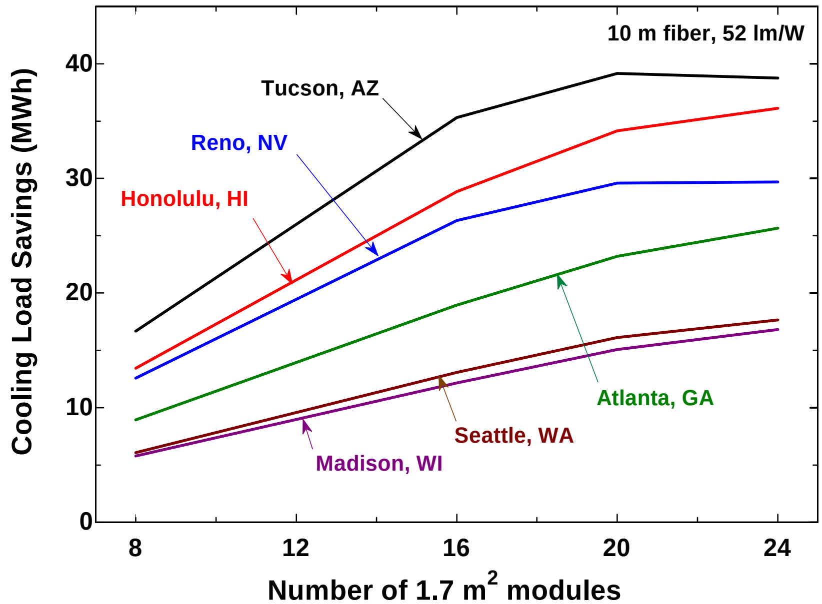


Figure 7.6b: Cooling Load Savings from HLS, 20 m fiber, 52 lm/W, in six U.S. cities

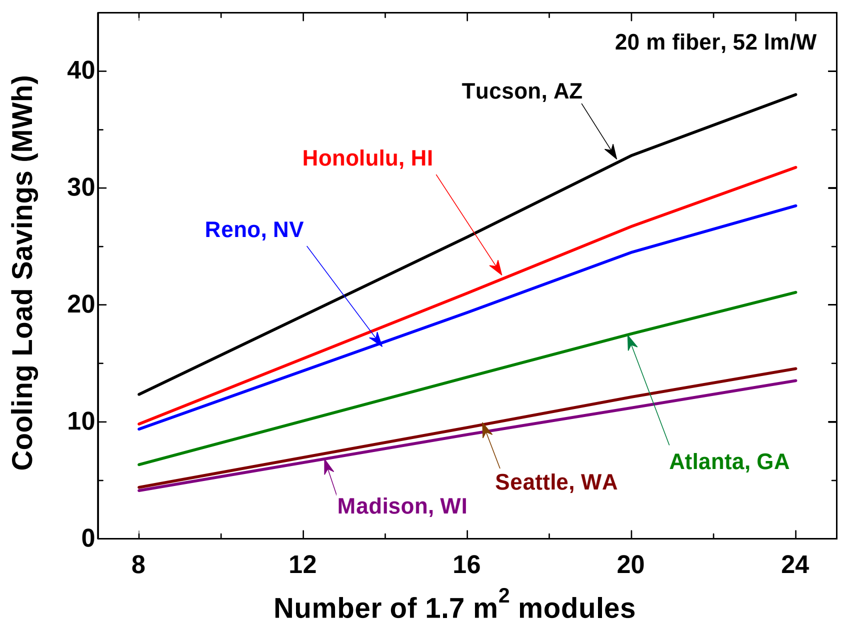


Figure 7.7b: Cooling Load Savings from HLS, 20 m fiber, 52 lm/W, in six U.S. cities

In Figure 7.6a, Tucson shows the largest annual lighting load reduction because of the abundance of its solar resource. Its curved nature is due to the saturation effect discussed earlier: adding increased collector area (measured by the number of modules) has diminishing returns because, at sixteen modules, under a sunny sky the HLS is providing about 100% of the light required in the building. The reason that the lighting load savings continue to increase, though at a slower rate, after sixteen modules is that the increased collector area is helping provide illumination during partly cloudy hours. The curve for Reno and Honolulu shows similar behavior, and the same saturation effect is present in Madison, Atlanta, and Seattle except that the larger ratio of cloudy hours to sunny hours shifts the saturation area to a larger number of modules, e.g. 20 in Atlanta. Honolulu's climate is cloudy at times, too, and for this reason its slope decreases slower than Reno's and therefore crosses the Reno curve.

Figure 7.7a shows reduction in lighting loads similar to Figure 7.6a, but with HLS equipped with 20 m of fiber instead of 10 m. More light is attenuated in the longer fiber and for this reason the saturation collector area is larger than it was in the 10 m case. Consequently, reductions in the lighting load continue to increase linearly as the number of modules increases, just as the curves increased linearly in Figure 7.6a until saturation points were reached. For 20 m fiber, the simple calculation performed earlier estimated 22 modules as the collector area after which diminishing lighting load reductions would be seen. For Tucson and Reno this estimate agrees will with the detailed simulation results.

Figures 7.6b and 7.7b show that for lamp efficacies of 52 lm/W, cooling load savings are significant: 50-100% of the lighting load savings, depending on the city. The behavior of the curves can be explained just as they were in Figures 7.6a and 7.7a, i.e. saturation areas. However, the Tucson curve in Figure 7.6b shows interesting behavior that all the curves would show if they were carried out to a large enough collecting area.

After a maximum cooling savings is reached, additional collection area causes a decrease in cooling savings. In other words, after a certain point adding more HLS modules can cause an increased cooling load that begins to reduce the cooling savings achieved from the larger efficacy HLS lighting. These additional modules are supplying more illumination than is required into the building, and the extra light becomes thermal energy that must be removed, thereby increasing the cooling load.

Figures 7.6c and 7.6d show the total electrical reduction, which is the sum of the lighting and cooling load reductions, and the annual energy saved per HLS module. Figures 7.7c and 7.7d show the same values but for an HLS with 20 m of optical fiber.

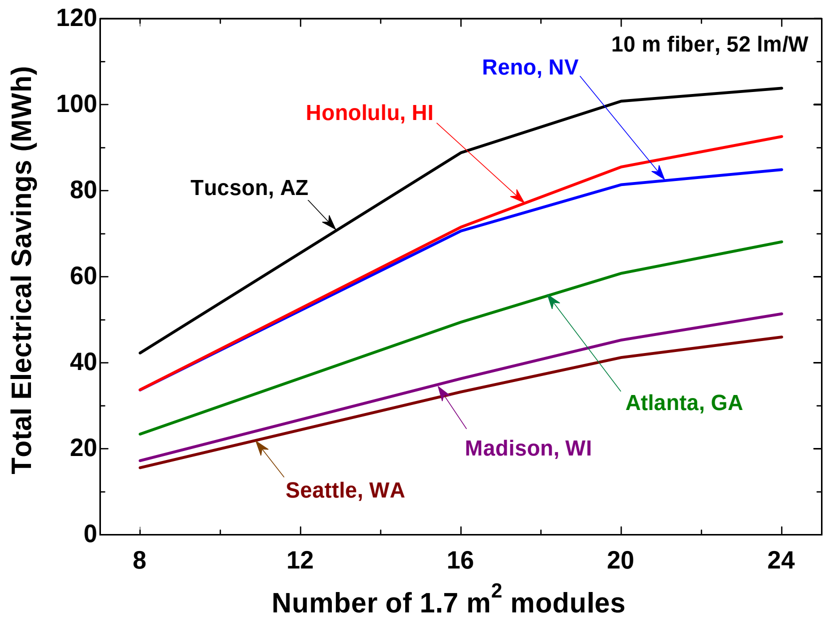


Figure 7.6c: Electrical Savings from HLS, 10 m fiber, 52 lm/W, in six U.S. cities

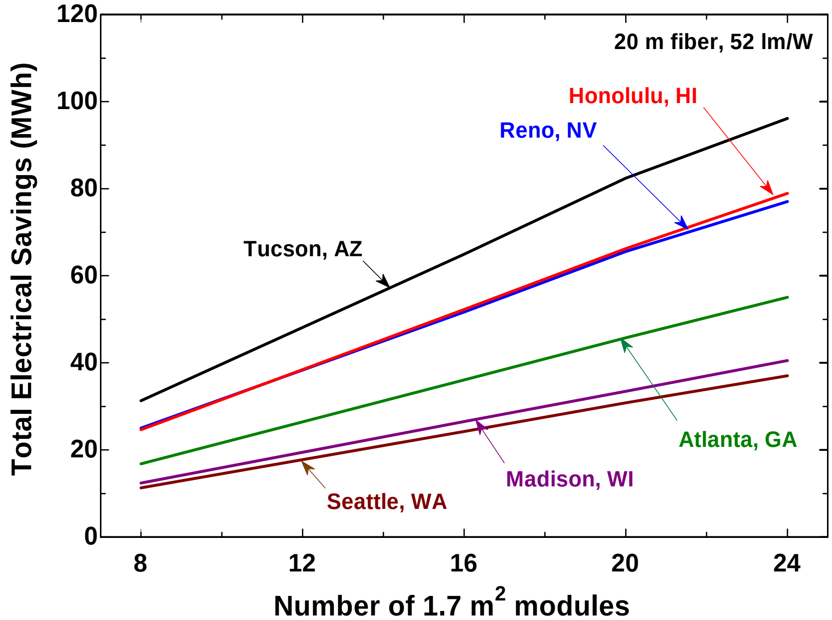


Figure 7.7c: Electrical Savings from HLS, 20 m fiber, 52 lm/W, in six U.S. cities

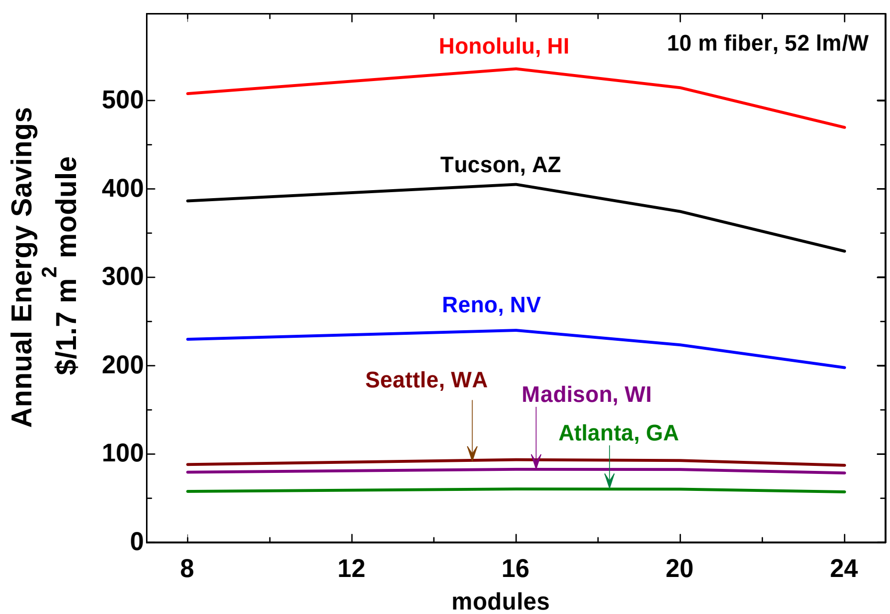


Figure 7.6d: Annual Energy Savings
from HLS, 10 m fiber, 52 lm/W, in six U.S. cities

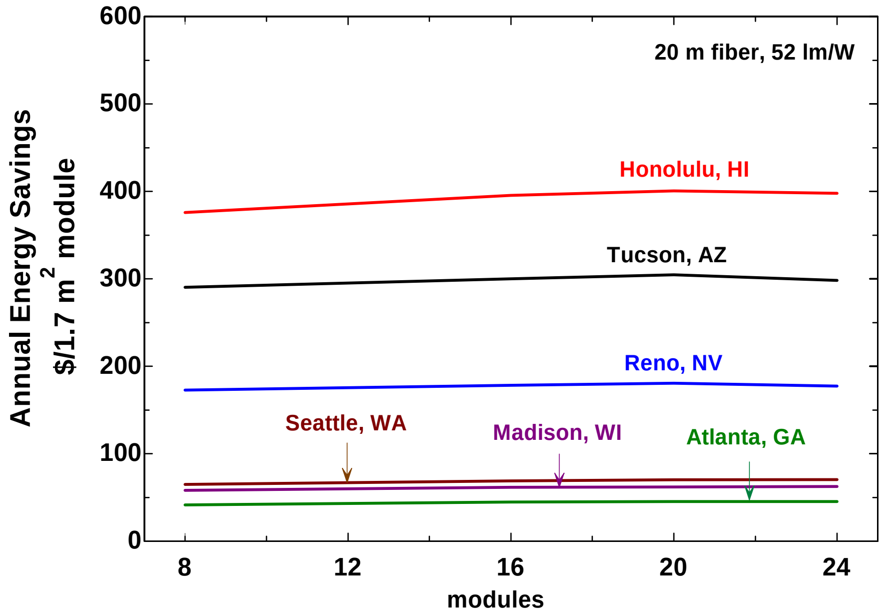


Figure 7.7d: Annual Energy Savings
from HLS, 20 m fiber, 52 lm/W, in six U.S. cities

For the 2500 $m^2$ building with 1.7 $m^2$ modules, Figures 7.6d and 7.7d show how much money is saved in a year per 1.7 $m^2$ module due to reductions in the total electrical load documented by Figures 7.6c and 7.7d. Though Honolulu's total electrical load reductions are less than Tucson (and Reno in some cases), its electricity rate is almost twice theirs so the money saved per module is correspondingly higher. Once again in Figure 7.6d, saturation effects are seen: annual energy savings per module decreases past 16 modules, corresponding to the collection area where the system first delivers 100% of the lighting load on sunny days. Any more collection area than this delivers more light (and thermal energy) than necessary which increases the cooling load, thereby decreasing the annual energy savings. Another interesting trend displayed by the annual energy savings graphs is the slight increase in AES until the saturation point is reached. This trend is due to the control system: if the control system were ideal, then the curves would travel horizontally from the left to the saturation point and then decrease off to the right.

As discussed in the Chapter 4, neither incandescents nor fluorescents dim perfectly. The control system used by this simulation uses staging that attempts to minimize dimming by turning off lamps in stages, but it still employs some dimming. This control system is described in further detail by Schlegel (2003).

Though the HLS simulations were run on a 2500 $m^2$ building with 1.7 $m^2$ modules, there is no reason that these results cannot be applied to a given illuminated space serviced by a specified collector area on the roof. Instead of defining the collector area by the number of modules, a more general and useful description is the ratio of the collector area to the area it's expected illuminated, defined previously by $A_{coll.}/A_{illum}$. Instead of using energy units (MWh) to define reductions in load, a percentage reduction can be defined by taking the difference between the total baseline (no hybrid) electrical load (lighting and cooling) and the total hybrid load and then dividing by the total baseline electrical load. Annual energy saving can be calculated per $m^2$ tracking area on the roof, as opposed to 1.7 $m^2$ modules. Figures 7.8(a,b) and 7.9(a,b) present the simulation results presented previously in Figures 7.6 and 7.7 but with these generalized parameters instead.

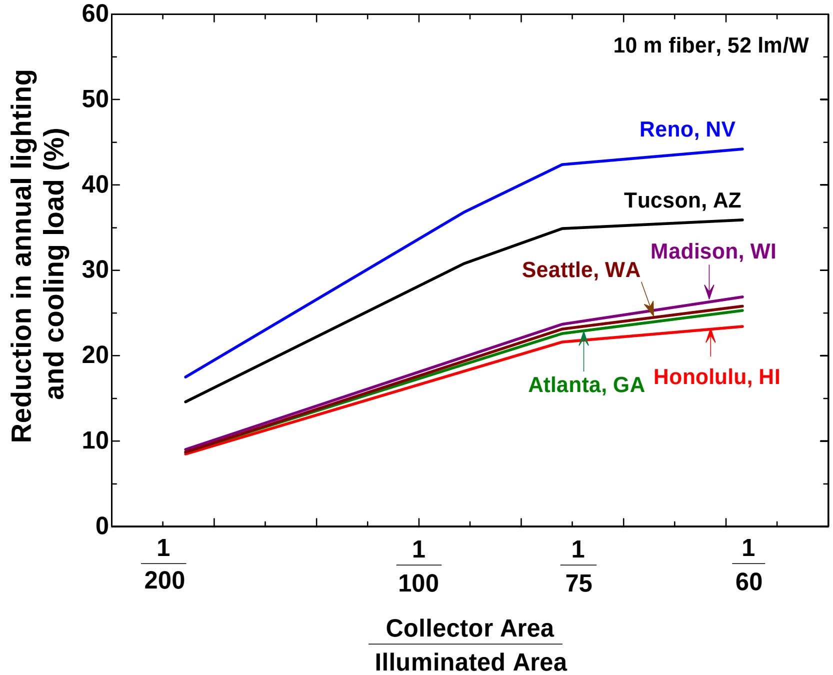


Figure 7.8a: Percentage reduction in electrical load from HLS, 10 m fiber

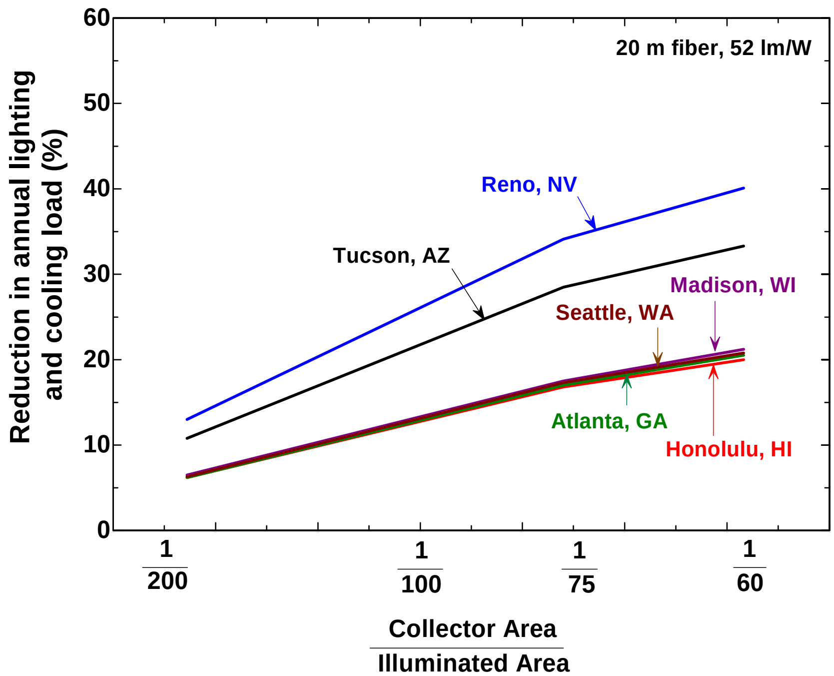


Figure 7.9a: Percentage reduction in electrical load from HLS, 20 m fiber

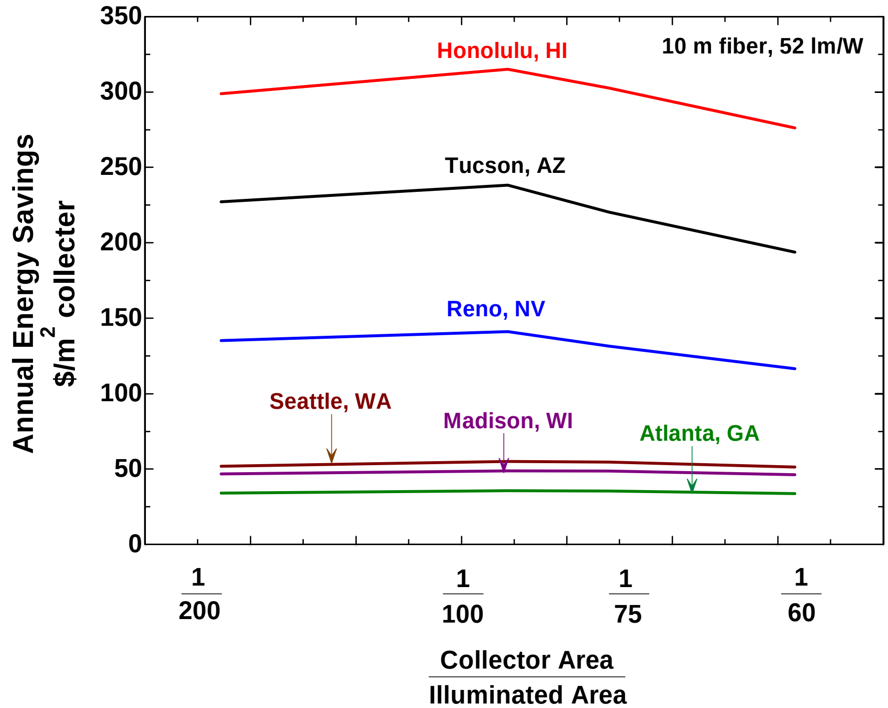


Figure 7.8b: Annual energy savings/m$^2$, 10 m fiber

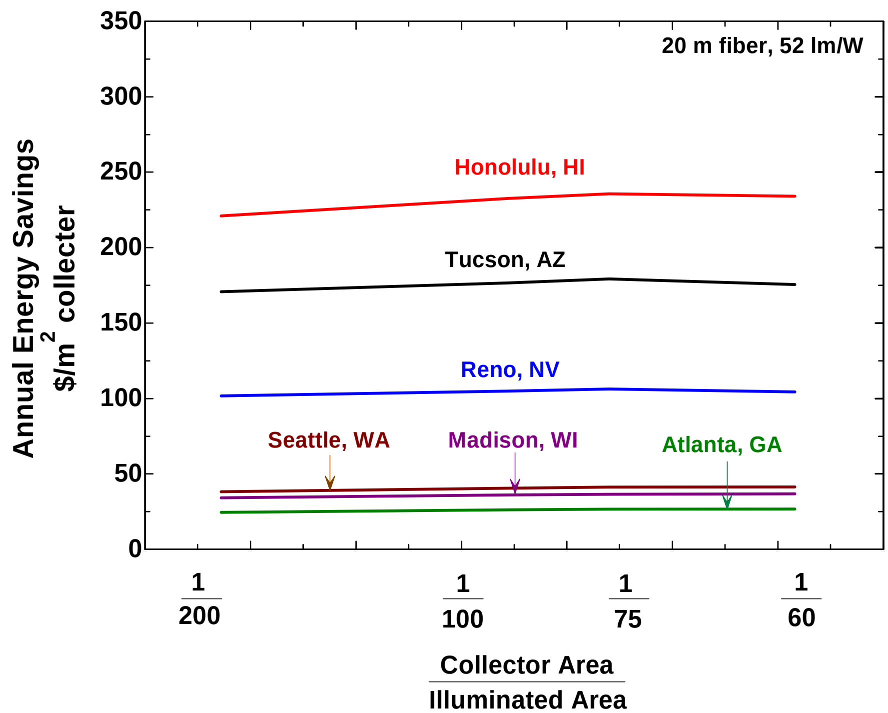


Figure 7.9b: Annual energy savings/m$^2$, 20 m fiber

The general trend of these graphs is the same as their earlier presented counterparts, with the clear exception the percentage reduction of Honolulu's electrical load. As seen in Figures 7.6c and 7.7c, the magnitude of this reduction in MWh is substantial, but when the percent reduction is calculated Honolulu's annual cooling load of 316 MWh in the denominator severely limits the magnitude of the percentage reduction. For comparison, Tucson's annual cooling load is 209 MWh, Reno is 113 MWh, Atlanta is 190 MWh, Madison is 112 MWh, and Seattle is 99 MWh. Though the HLS does help reduce the cooling load, a comparison of Figure 7.6a and 7.6b show that the lighting load reductions are about twice cooling load reductions for 52 lm/W.

### 7.4.2 Energy Savings - Efficacy Effects

All results presented above are for a lamp efficacy of 52 lm/W, the commercial building average. Lamps presented in Chapter 4 had a wide range of efficacies: 15 lm/W for the tungsten incandescent up to 90 lm/W for the energy efficient fluorescent. The purpose of this section is to explore how lamp efficacies affect reductions in electrical load and annual energy savings. To reduce the number of simulation runs necessary, just two cities were investigated: Tucson and Seattle. Additionally, an $A_{coll.}/A_{illum}$ ratio of 1/200 is the only ratio used because annual energy savings is only slightly affected by this ratio. Tucson and Seattle provide a kind of best-case, worst-case bracketing of results for the HLS. Tucson has consistent beam-normal radiation during the year, while Seattle has a lot of cloudy hours and days. In figures 7.8 and 7.9 Tucson performs very well with large annual energy savings, while Seattle's savings are small. Figures 7.10(a,b) and 7.11(a,b) show the effects lamp efficacy has on electric load reductions (lighting and cooling) and annual energy savings.

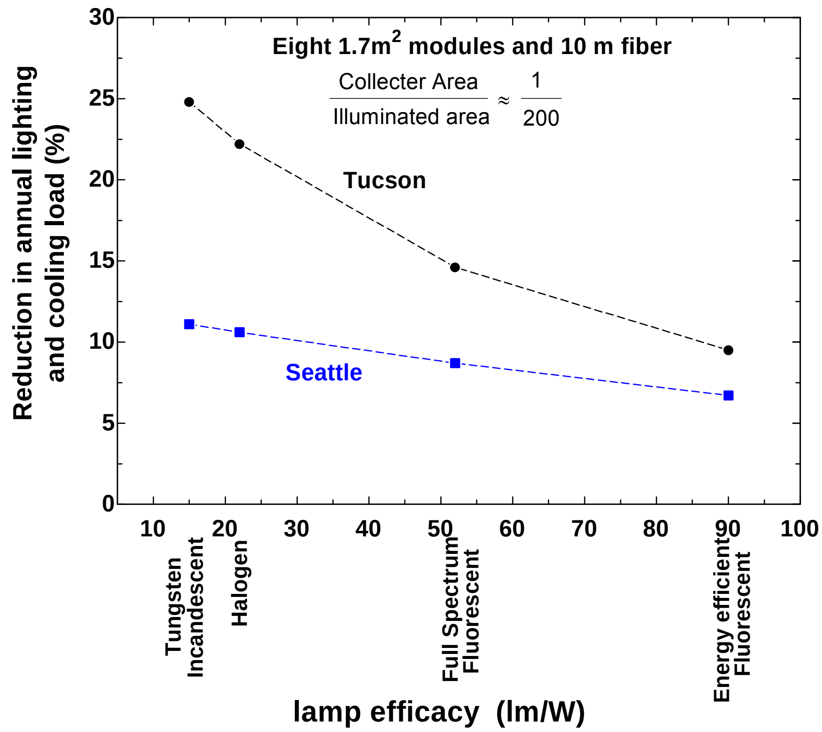


Figure 7.10a: Effect of efficacy on electrical load reduction, 10 m fiber

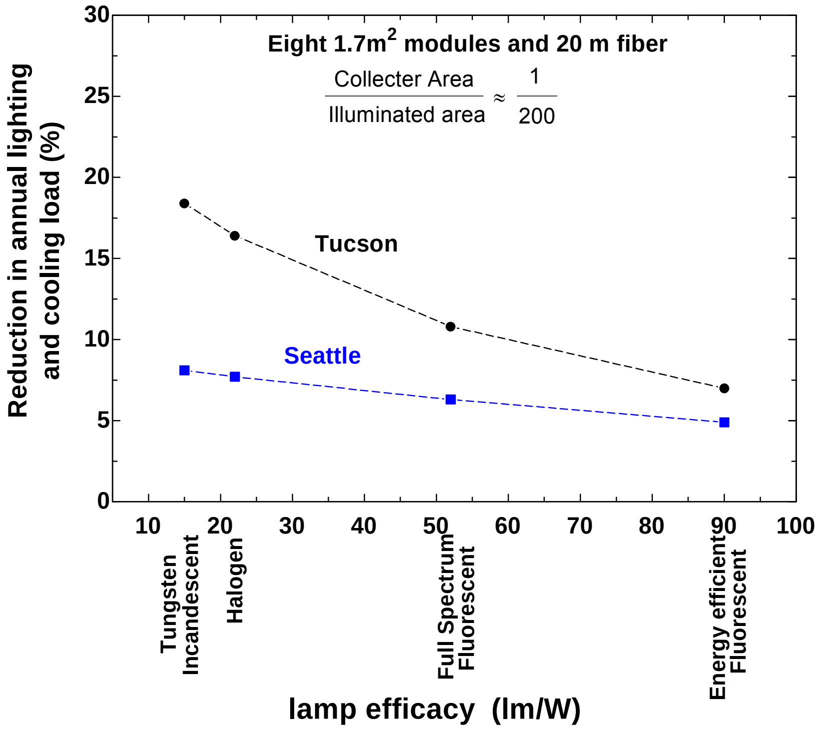


Figure 7.11a: Effect of efficacy on electric load reduction, 20 m fiber

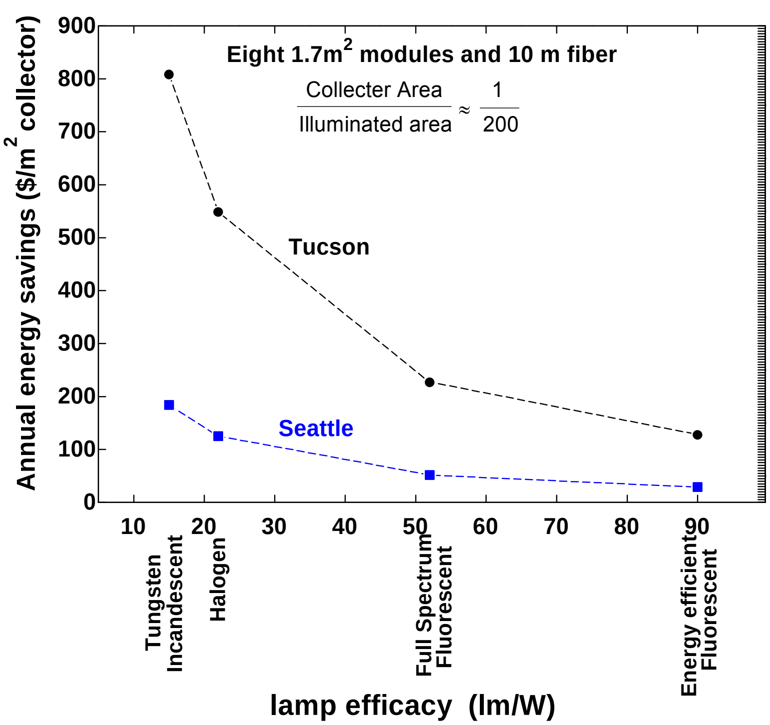


Figure 7.10b: Effect of efficacy on annual energy savings, 10 m fiber

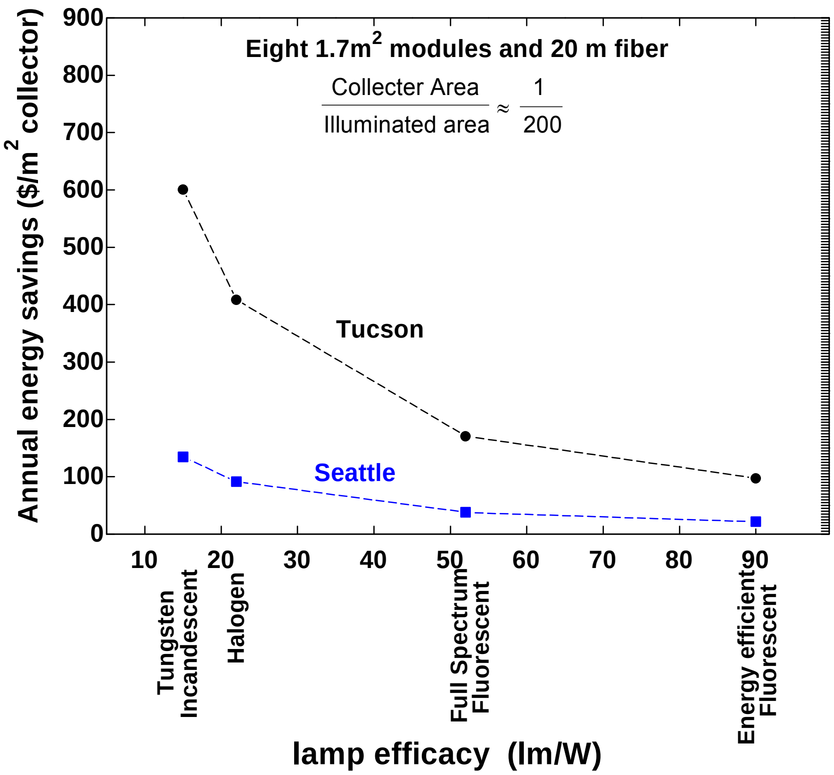


Figure 7.11b: Effect of efficacy on annual energy savings, 20 m fiber

What Figures 7.10a through 7.11b show is that the electric load reduction and the annual energy savings are very strong functions of lamp efficacy. The more inefficient the lamps inside are at making light (low efficacy), the more dramatic the reductions in electrical load and the greater the annual energy savings. However, these lower efficacies are often tolerated because of the better color rendering abilities of incandescent lamps.

### 7.4.3 Colorimetric Results

Colorimetric results are also highly dependent on the lamp used. When the sun is not shining the illumination indoors will have the CCT and the CRI of the installed lamps.

For the same reason, colorimetric results are very dependent on the $A_{coll.}/A_{illum}$ ratio. For 10 m fiber, an $A_{coll.}/A_{illum}$ ratio of 1/100 will result in the HLS providing 100% of the light fraction some of the time. At these times, the CCT and CRI of the light indoors will be that of the beam normal radiation filtered by the HLS, not the installed lamps. However, for $A_{coll.}/A_{illum}$ ratios closer to 1/200 the CCT and CRI values of the delivered light will be based on a combined SPD: the lamp SPD and the HLS SPD. For the 1/200 ratio, the maximum lighting fraction the HLS can supply is about 50% (for the 10 m fiber case). Figures 7.12 and 7.13 show the TRNSYS calculated HLS light fractions (the percentage amount of indoor illumination provided by the HLS) for Tucson and Seattle with collection ratios of 1/100 and 1/200. These simulations were run with 10 m of fiber. Note: these light fractions are completely independent of the lamp selected.

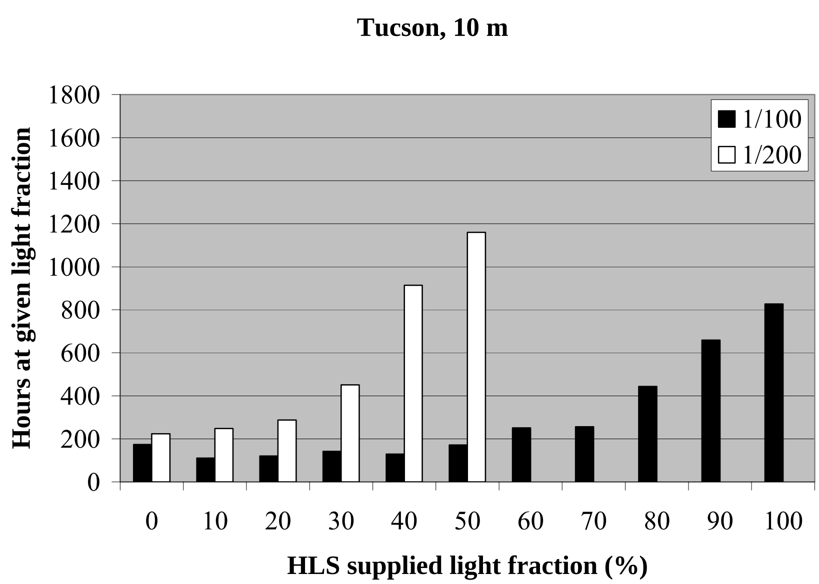


Figure 7.12: HLS light fraction in Tucson

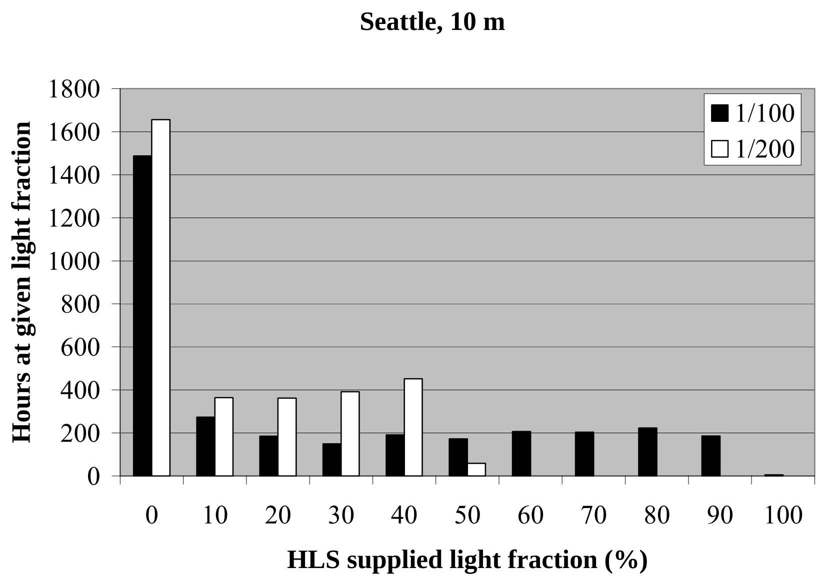


Figure 7.13: HLS light fraction in Seattle

Of the 3285 hours that the modeled office building is illuminated during the year, the figures above show how many hours that the HLS is providing a specified percentage of the indoor light in 10 % intervals. In Tucson the HLS provides more hours at 100% light fraction than Seattle because beam normal radiation in Tucson has slightly more lumens/$m^2$ than Seattle due to air mass and turbidity effects.

Figures 7.14 and 7.15 summarize correlated color temperature (CCT) results for the warm white fluorescent bulb (3000 K CCT, 52 CRI, 90 lm/W) used with HLS in Tucson and Seattle. During the TRNSYS runs, the CCT is calculated each hour and then sorted into the CCT ranges shown on the x-axis of these figures. A CCT of 4000 K on the figures actually corresponds to a range of CCT values from 3751 K to 4250 K. For an $A_{coll.}/A_{illum}$ ratio of 1/100 in Tucson, the CCT of the delivered illumination will often be larger than the 3000 K of the bulb alone. It could be a cause of concern that the CCT varies over such a wide range: some may find the changing color of the illumination disruptive. A lower range of CCT results in Tucson if the lower $A_{coll.}/A_{illum}$ ratio of 1/200 is used.

Seattle light fractions in Figure 7.13 show that as many as half of the 3285 hours the building is illuminated the HLS will be providing no light to supplement the electric light. For this reason, the CCT value of the warm white fluorescent lamp dominates the CCT values in Figure 7.15. This will be true of all CCT results for Seattle: most of the illuminated hours will have CCT values of the installed lamp.

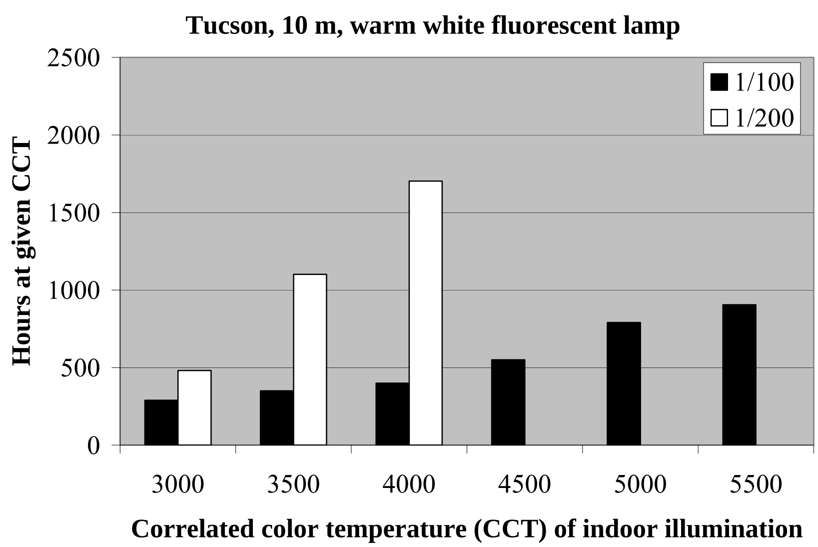


Figure 7.14: CCT results in Tucson, warm white fluorescent lamp

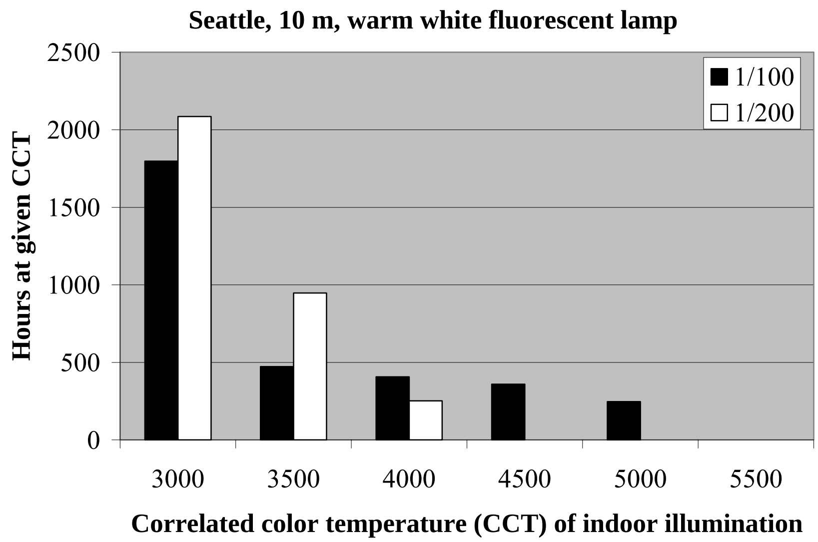


Figure 7.15: CCT results in Seattle, warm white fluorescent lamp

Figures 7.16 and 7.17 summarize color rendering index (CRI) results for the warm white fluorescent bulb used with HLS in Tucson and Seattle. In both Seattle and Tucson the addition of the HLS helps to increase the relatively low CRI of the warm white bulb. A CRI of 80 occurs when the HLS is providing most of the light.

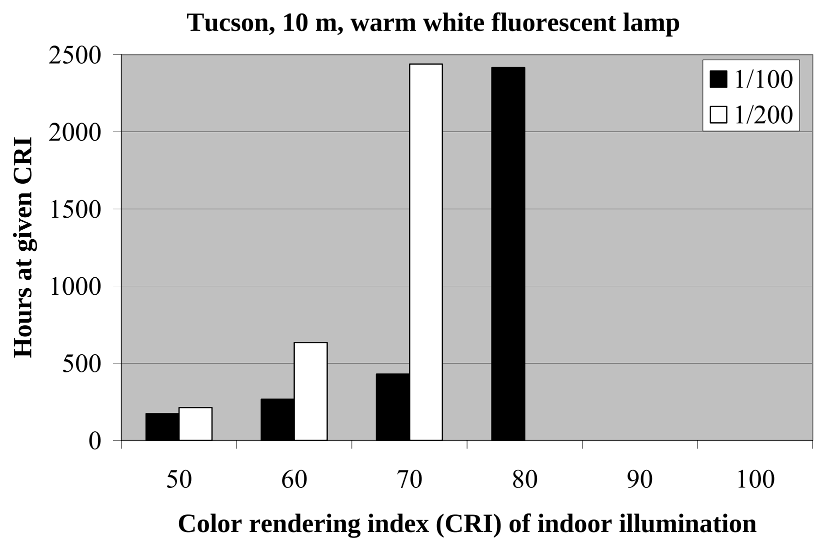


Figure 7.16 CRI results in Tucson, warm white fluorescent lamp

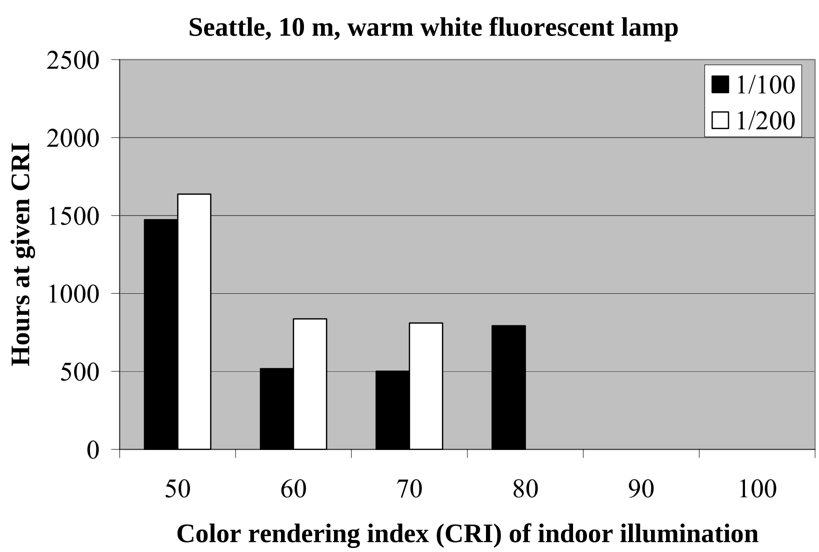


Figure 7.17 CRI results in Seattle, warm white fluorescent lamp

The reason that a CRI of 80 (i.e. in the range from 75-84) is the maximum for HLS light is shown in Figure 7.18. A noontime spectrum (AM 1.5) is attenuated by the HLS to deliver the spectrum shown on the figure. When the CRI is calculated, a reference SPD is created, and that reference SPD is also shown on Figure 7.18. The more similar the reference spectrum to the SPD delivered by the HLS, the higher the CRI. The two spectrums are similar except past 600 nm. Attenuation in the HLS, especially the optical fiber, is responsible for the lack of power at wavelengths higher than 600 nm. The difference in their SPDs causes a CRI less than 100.

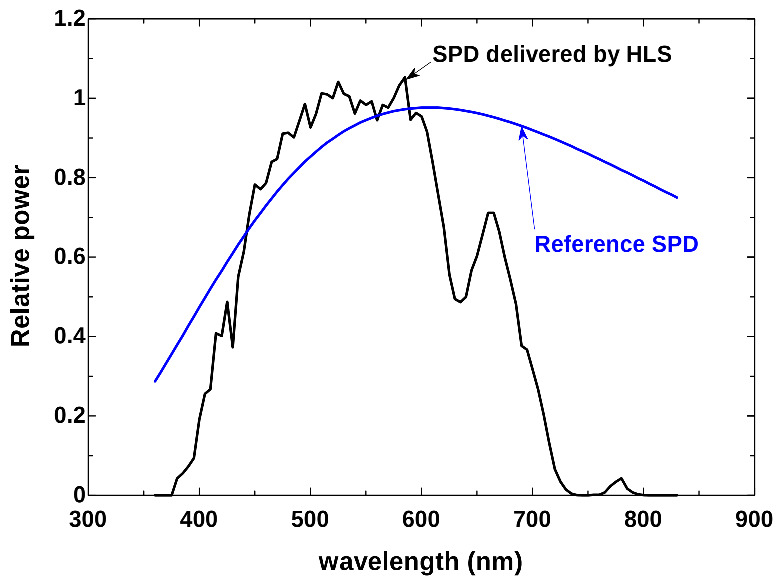


Figure 7.18: Comparison of HLS representative SPD and its reference SPD for CRI calculation

Figures 7.19 through 7.22 show CCT and CRI results for simulations in Tucson and Seattle with the full spectrum fluorescent lamp (5000 K CCT, 90 CRI, 52 lm/W). The CCT of solely HLS light tends to range from as low as 4500 K to as high as 5500 K, which the $A_{coll.}/A_{illum}$ = 1/100 ratio shows in both figures. The CRI is slightly affected by the HLS. Because the HLS light has a CRI of 80 and the CRI of the full spectrum bulb is 90, CRI values for a system combining the two are predictably in this relatively narrow range of values.

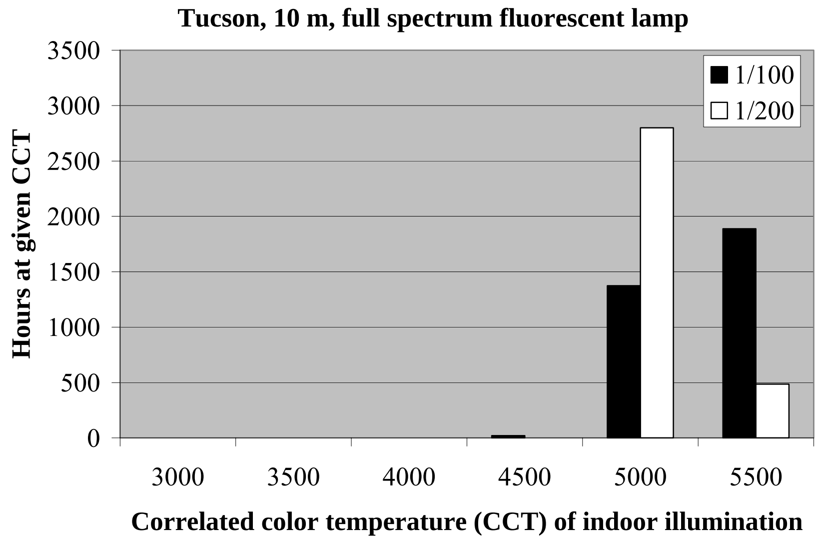


Figure 7.19: CCT results for Tucson, full spectrum fluorescent lamp

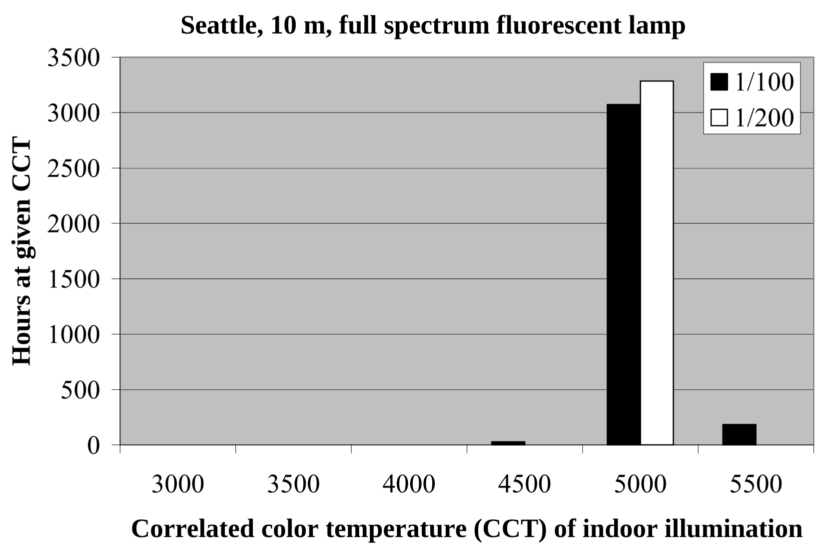


Figure 7.20: CCT results for Seattle, full spectrum fluorescent lamp

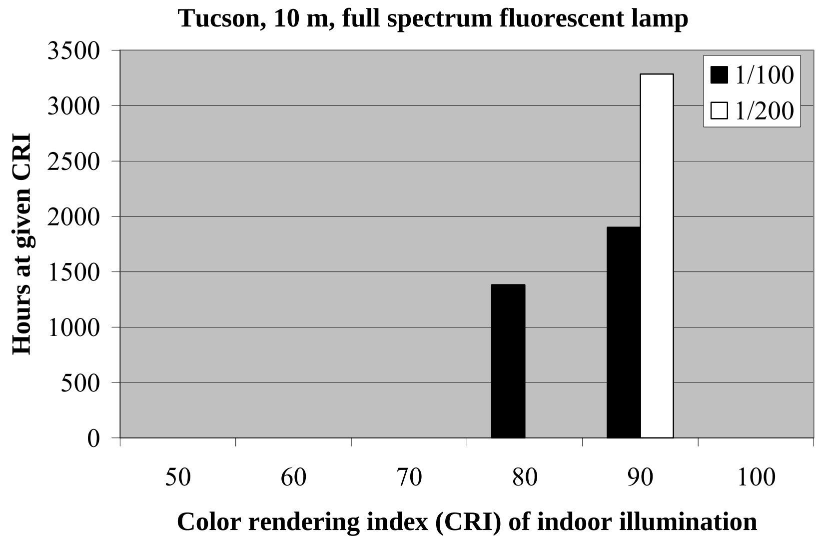


Figure 7.21: CRI results for Tucson, full spectrum fluorescent lamp

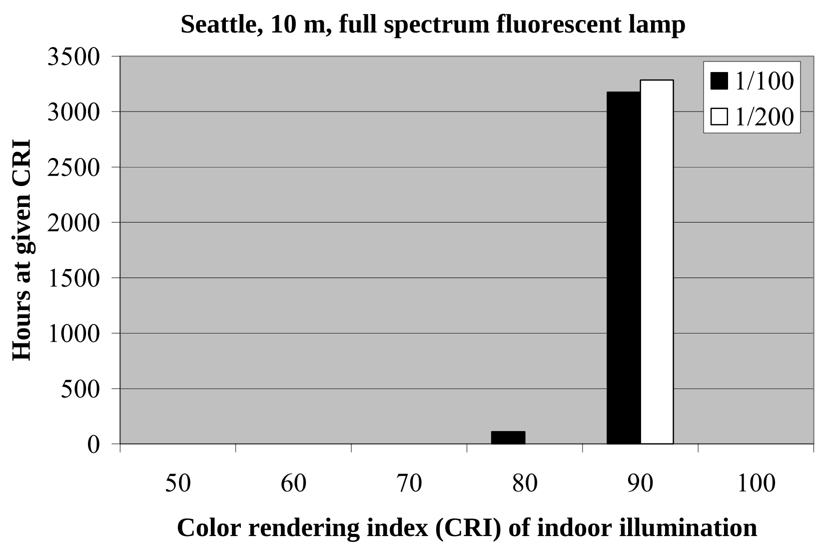


Figure 7.22: CRI results for Seattle, full spectrum fluorescent lamp

Figures 7.23 through 7.26 present CCT and CRI results for simulations in Tucson and Seattle with the tungsten incandescent lamp (3000 K CCT, 99+ CRI, 15 lm/W). As in the case of the warm white fluorescent lamp, CCT values range from 3000-5500 K for the $A_{coll.}/A_{illum}$ = 1/100 ratio, and a narrower range for $A_{coll.}/A_{illum}$ = 1/200. The reason that $A_{coll.}/A_{illum}$ = 1/200 does not yield higher CCT values is that the 5000 K HLS light is combining with 3000 K incandescent light yielding maximum CCTs around 4000 K. The tungsten incandescent bulb's CRI is 100, and CRI values in both cities are either at this value or slightly less due to the influence of the 80 CRI HLS light.

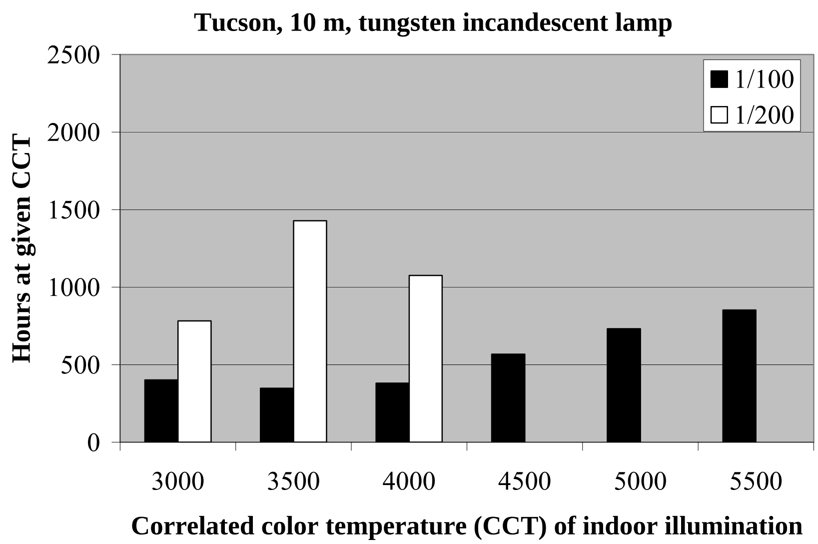


Figure 7.23: CCT results for Tucson, tungsten lamp

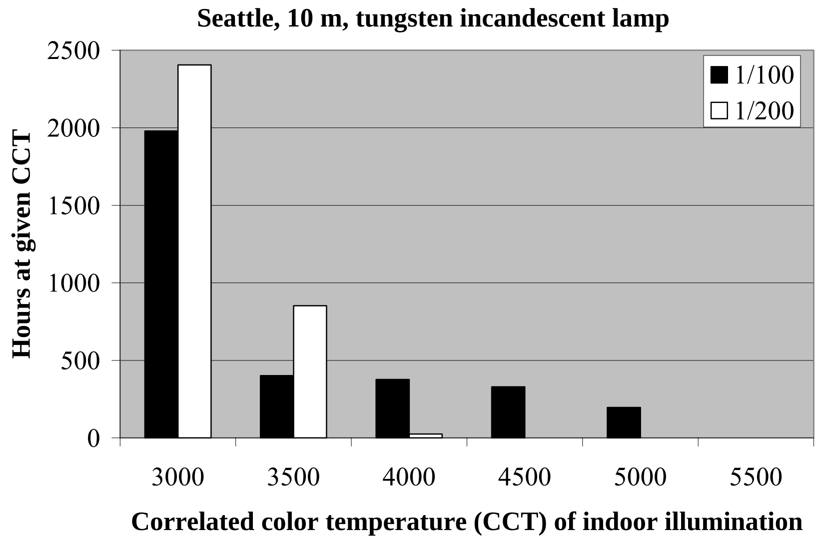


Figure 7.24: CCT results for Seattle, tungsten lamp

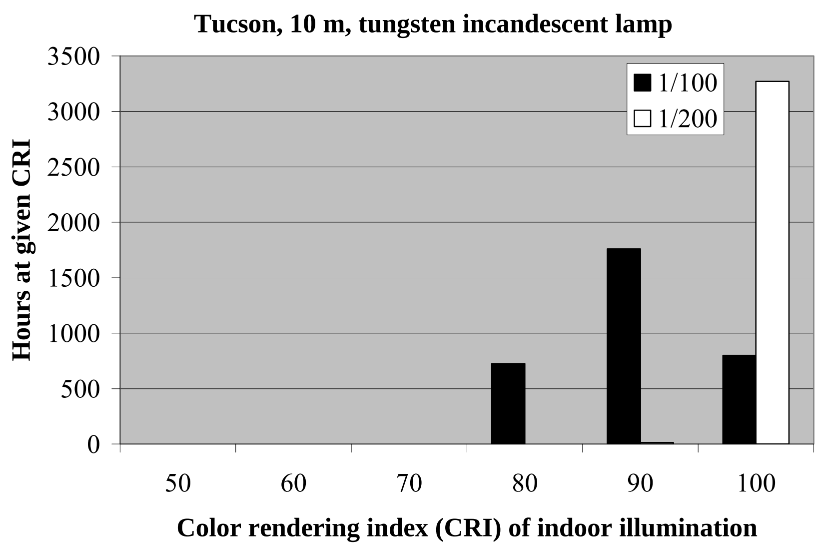


Figure 7.25: CRI results for Tucson, tungsten lamp

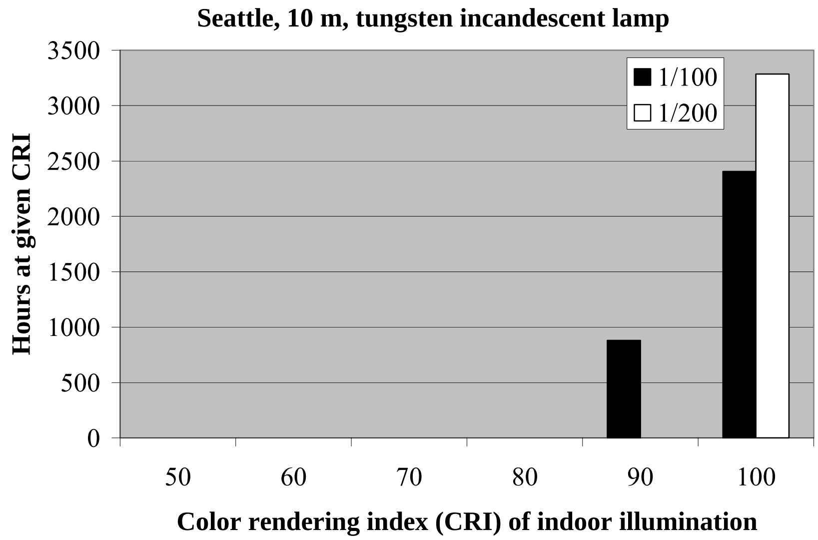


Figure 7.26: CRI results for Seattle, tungsten lamp

Figures 7.27 through 7.30 present CCT and CRI results for simulations in Tucson and Seattle with the halogen lamp (4100 K CCT, 98 CRI, 22 lm/W). CCT values increase from 4100 K up to 5500 K in the case of $A_{coll.}/A_{illum}$ = 1/100, with a more pronounced affect from the HLS light in Tucson than in Seattle. CRIs in Seattle are between 90 and 100, while CRIs in Tucson can be as low as 80 due to the affect of the HLS light mentioned previously.

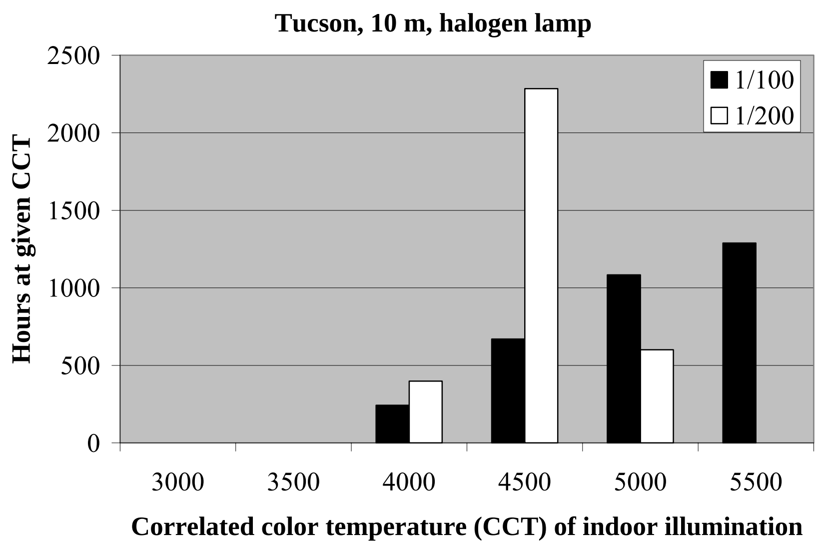


Figure 7.27: CCT results for Tucson, halogen lamp

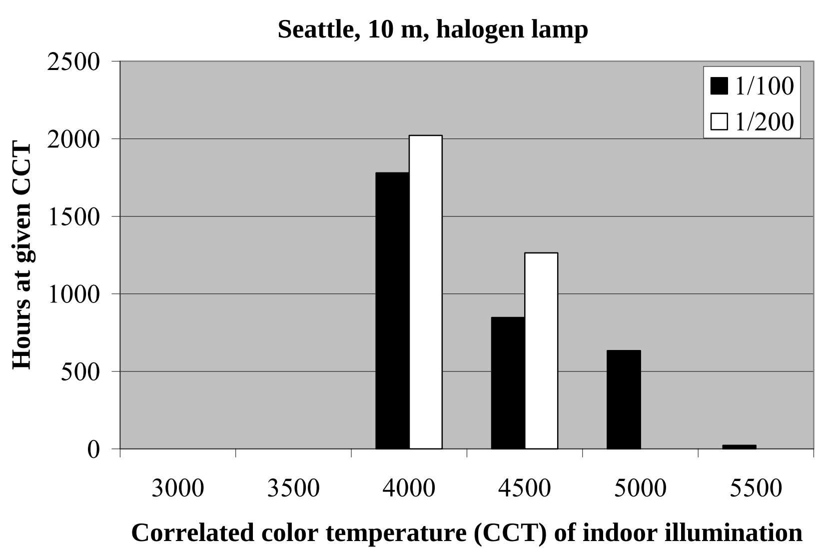


Figure 7.28: CCT results for Seattle, halogen lamp

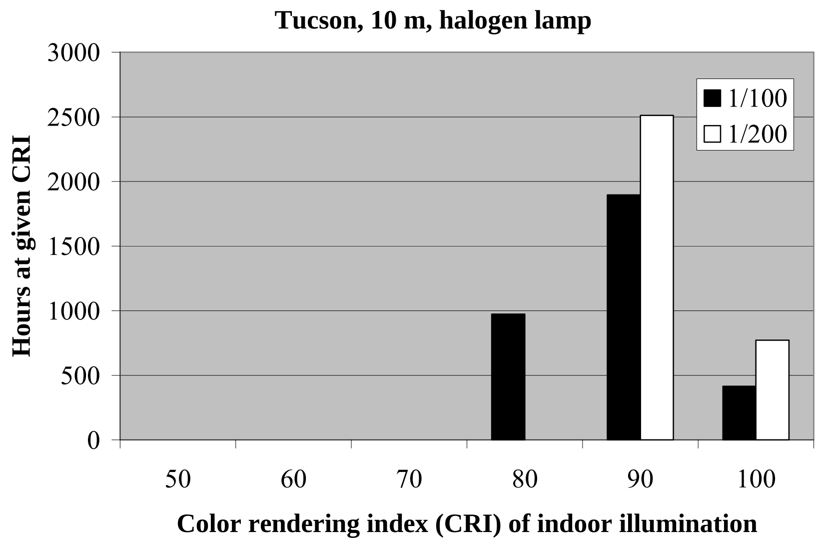


Figure 7.29: CRI results for Tucson, halogen lamp

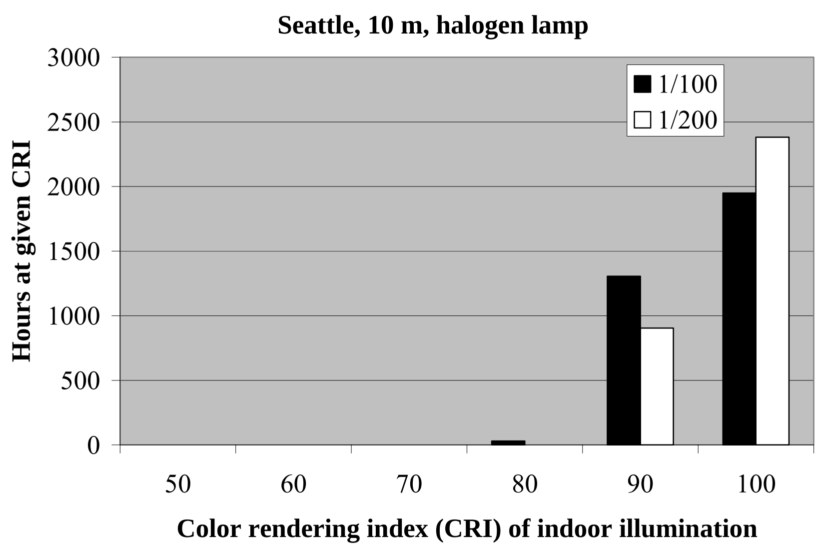


Figure 7.30: CRI results for Seattle, tungsten lamp

# Chapter 8

# Conclusion

## 8.1 Conclusion

To a potential investor, the annual energy savings values (\$/$m^2$ collector) presented in Figures 7.8b and 7.9b can be used to determine how long a HLS will take to pay itself off from energy savings alone. For instance, in Tucson the annual energy savings per $m^2$ collector is about \$225/year assuming that the efficacy of the lamps in the building is the commercial average of 52 lm/W. After a five year period, the investor could have afforded to spend 5×\$225 = \$1125 for a one square meter system neglecting interest. Tucson is admittedly one of the best places for the HLS; in Madison the investor could only afford to spend 5×\$50 = \$250 on the same system.

However, these energy savings values increase dramatically if the lighting application, such as museum displays, requires better color rendering ability and consequently lower luminous efficacy. Halogen lamps (22 lm/W) are commonly used in these applications, and the annual energy savings (\$/$m^2$ collector) from Figure 7.10b for Tucson is about \$550/$m^2$ for these lower efficacy lamps. The five year simple payback in this case is $2750/m$^2$. Madison's energy saving values are similar to Seattle, so using 7.10b to approximate the annual energy savings for Madison for halogen lamps yields an energy savings of $150/m$^2$ with a five year simple payback of $750/m$^2$.

The color and color rendering ability of the indoor illumination with a HLS is primarily affected by three factors: 1) the CCT and CRI of the installed lamp 2) the ratio of the collector area to illuminated area (if $A_{coll}/A_{illum} \approx 1/100$, then some hours the illumination will have a CCT between 4500 and 5500 K and a CRI of 80 regardless of the lamps the system is paired with, assuming 10 m fiber is used) and 3) the number of hours in the year the location of interest has full beam normal radiation. If the location is cloudy, then the ability of the HLS to affect the CCT or CRI is limited. However, buildings that use lighting that is energy efficient but has poor color rendering ability should consider a HLS because even at smaller $A_{coll}/A_{illum}$ ratios of 1/200 the HLS can dramatically increase the CRI of the indoor light. There are numerous industries (e.g. retail, manufacturing, art) where improvements in color rendering are valued.

## 8.2 Cost comparison with electrically generated light

The annual energy savings value is one way for investors to estimate how much they can afford to spend for a HLS. What this value neglects is the manufacturing and installation cost of the system and how expensive, at this time, HLS light is compared to electrically generated light. The parameter that best allows comparison of HLS and electric light is the cost per kilolumen-hour delivered ($/klmh). The sections that follow describe how this parameter is calculated for electrically generated and HLS delivered light.

Oak Ridge National Lab has compiled and extrapolated the part costs associated with building the first prototype - the benchmark system - and second and third prototypes, the alpha and beta prototypes, respectively. Figure 8.1 summarizes the part costs associated with each prototype and breaks down how much the mirrors, the tracking mechanism, the optical fibers, and the light distribution system contribute to system cost. The costs associated with the mirrors, tracking mechanism, and fiber optics holder have decreased dramatically. In the beta prototype, costs associated with distributing the light are more than 2/3 the system cost. Unfortunately, these costs are largely outside of ORNL control.

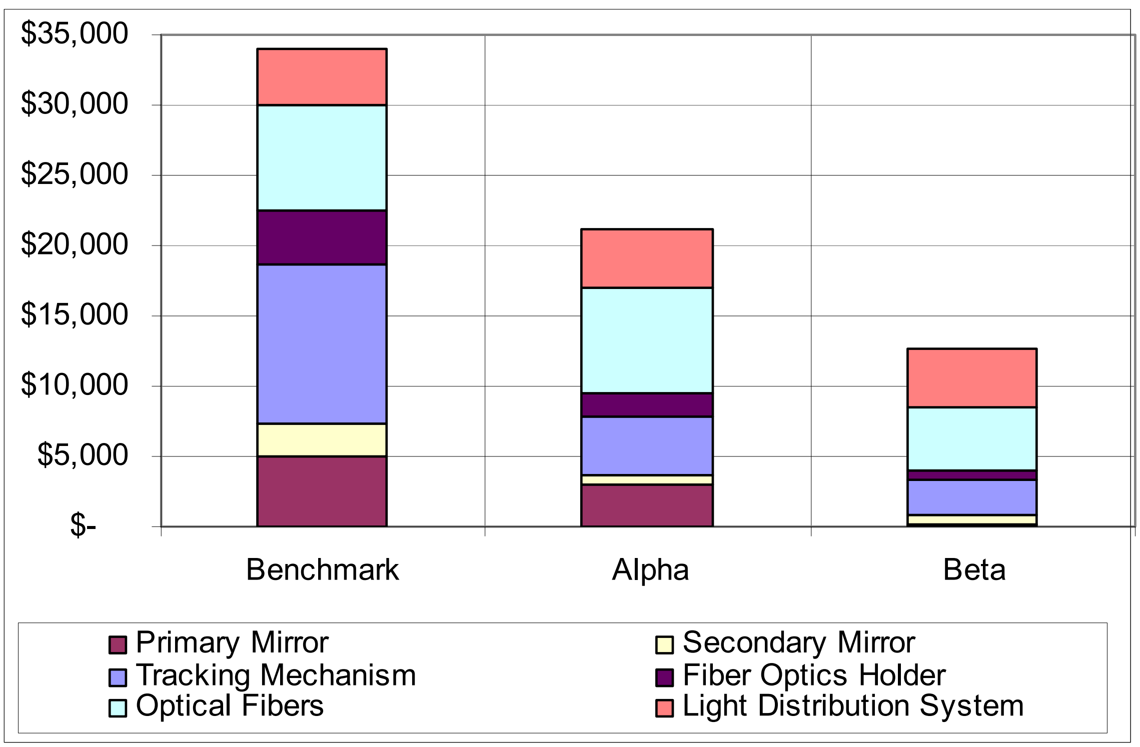


Figure 8.1: HLS part costs in the benchmark (first prototype), alpha (second prototype under construction), and beta (third prototype, projected costs) HLS systems (Muhs, 2004)

Figure 8.1 neglects installation costs. For the analysis that follows, the total assumed part, assembly, and installation cost is \$20,000 per $m^2$ collector area. Maintenance per $m^2$ collector area is assumed to be \$200 per year.

To calculate the cost per kilolumen-hour delivered by the HLS, the HLS cost and the number of lumens it delivers for a specified time period must be determined. The cost per kilolumen-hour is the HLS cost divided by the number of lumen-hours it delivers in that time period. A suitably short analysis period, such as five years, decreases the effect of interest and time value of money on the results. In this case, the cost of the HLS for the five year period is approximated by equation 8.1.

$$5\text{yr Cost}\left(\frac{\$}{\text{m}^2}\right) = \text{Initial Cost}\left(\frac{\$}{\text{m}^2}\right) + \left(\text{Maint.}\left(\frac{\$}{\text{m}^2-\text{yr}}\right) - \text{Savings}\left(\frac{\$}{\text{m}^2-\text{yr}}\right)\right) \times \text{yrs} \quad (8.1)$$

where

| | |
|---|---|
| 5yrCost | is the total cost over the five year period used to estimated the \$/klmh |
| Initial cost | is part, assembly, and installation costs: \$20,000/$m^2$ collector area |
| Maint. | is the yearly maintenance cost: \$200/$m^2$ collector area |
| Savings | is the annual energy saving (AES) value defined by different locations, utility rates, and lamp efficacies. The AES values were calculated by TRNSYS and summarized in Chapter 7. |
| yrs | is the length of the analysis period: five years |

Using annual energy savings of \$1344/$m^2$ (Honolulu using incandescents) and \$225/$m^2$ (Tucson using commercial average lamp efficacy) result in five year costs of \$14,280/$m^2$ in Honolulu and \$19,875/$m^2$ in Tucson. From TRNSYS modeling, the number of lumen-hours collected per $m^2$ collector per year is $9.41\times10^4$ klmh/$m^2$-yr in Honolulu and $1.17\times10^5$ klmh/$m^2$-yr in Tucson. The five year cost per kilolumen-hour delivered in each of these locations is therefore \$14,280/$m^2$/( $9.41\times10^4$ klmh/$m^2$-yr $\times5$ yrs.) = **\$0.030/klmh** for Honolulu (using energy savings from incandescents) and

$19,875/m^2/(1.17 \times 10^5$ klmh/m$^2 \times 5$ yrs.) = **$0.034/klmh** for Tucson (using energy savings from average lamp efficacy, 52 lm/W).

The average cost of electricity in the U.S. is $0.072/kWh, but in Hawaii the cost is the substantially larger value of $0.184/kWh. The ability of a lamp to turn this electricity into light is governed by its efficacy; the commercial average efficacy is 52 lm/W (52 klmh/kWh), while the efficacy of incandescent lamps is 15 lm/W (15 klmh/kWh). By dividing the cost of electricity by the efficacy of the lamps, the cost per kilolumen-hour can be calculated as **$0.0014/klmh** (U.S. average cost of electricity with average efficacy) and **$0.012/klmh** (cost of electricity in Honolulu with incandescent efficacy).

In a best case comparison of HLS light to electrically delivered light, the cost per lumen delivered by the HLS is twice as expensive as that delivered by the utility in Honolulu. The HLS fares worse when compared to the U.S. average cost of electricity per kilolumen-hour of $0.0014/klmh: it is almost 25 times more expensive. However, if the cost of the HLS can be cut in half ($10,000 instead of $20,000) and a ten year instead of five year analysis is used, then the HLS value is reduced to 10 times that of electrically supplied light. Clearly, a significant task is ahead of the HLS development team if the HLS is to be marketed as an economic addition to conventional lighting.

## 8.3 Future Work

Solar systems have often found niche markets where they are successful. The color rendering ability of HLS light and its higher color temperature are potential incentives that justify the increased cost relative to a solely electric alternative. Additionally, lamps that provide good color rendering abilities tend to be energy inefficient. Though electricity is cheap, the savings provided by displacing some of these lamps is substantial and will help justify the expense HLS.

Future work should focus on commercializing this technology in markets where it can succeed. The HLS is presently too expensive to present as an "economic" alternative to conventional fluorescent lighting. The design team should talk to lighting designers, museum and jewelry store owners, clothing retailers, and electrical component manufacturers to gather input and design a system for them. Once this design is relatively set, components need to be outsourced to vendors to provide price quotes based on realistic sale volumes. Finally, commercial investors need to be found and the system marketed.

Regarding system modeling, some work remains in quantifying how tracking errors affect performance. Presently very little error is allowed in the tracking mechanism, and consequently custom designed trackers and very precise optics are needed to get the light into the fiber; this translates into a large monetary expense. Some way to ease this precise tracking requirement would reduce costs.

Additionally, the attenuation and colorimetric effects of other types of fiber optic cables should be explored. Perhaps the optical fiber used presently is not the best economic or colorimetric fit for potential applications.

## Appendix A: EES Code to Calculate Chromaticity Coordinates

```
"x_bar_lambda, y_bar_lambda, and z_bar_lambda are the color matching
functions"

"find tristimulus values at each lambda"
X_lambda=P_lambda*x_bar_lambda*lambda_interval
Y_lambda=P_lambda*y_bar_lambda*lambda_interval
Z_lambda=P_lambda*z_bar_lambda*lambda_interval

u_bar_lambda = 2/3*x_bar_lambda
v_bar_lambda = y_bar_lambda
w_bar_lambda = -.5*x_bar_lambda+1.5*y_bar_lambda+0.5*z_bar_lambda
U_lambda=P_lambda*u_bar_lambda*lambda_interval
V_lambda=P_lambda*v_bar_lambda*lambda_interval
W_lambda=P_lambda*w_bar_lambda*lambda_interval

"total tristimulus values"
X_sum = k*sumparametric(tabl$,'X_lambda')
Y_sum = k*sumparametric(tabl$,'Y_lambda')
Z_sum = k*sumparametric(tabl$,'Z_lambda')

U_sum = k*sumparametric(tabl$,'U_lambda')
V_sum = k*sumparametric(tabl$,'V_lambda')
W_sum = k*sumparametric(tabl$,'W_lambda')

k=1

"chromaticity coordinates"
x = X_sum/(X_sum+Y_sum+Z_sum+noerror_div0)
y = Y_sum/(X_sum+Y_sum+Z_sum+noerror_div0)

u = U_sum/(U_sum+V_sum+W_sum+noerror_div0)
v = V_sum/(U_sum+V_sum+W_sum+noerror_div0)
```

Appendix B: EES code to determine Correlated Color Temperature

```
Function CCT_(u_s,v_s,u_T[1..31],v_T[1..31],t_T[1..31],T[1..31])
     i := 0
     REPEAT
          i:=i+1
          d[i] = ((v_s-v_T[i])-t_T[i]*(u_s-u_T[i]))/(1+t_T[i]^2)^(1/2)
     UNTIL (d[i]<0)
     CCT_:=1/(1/T[i-1]+d[i-1]/(d[i-1]-d[i])*(1/T[i]-1/T[i-1]))
end


"take chromaticity coordinates of source"
u_s = .19337
v_s = .33039


"read isotempline data into array"
duplicate i=1,31
     T[i] = LOOKUP('isotemplines',i,'T_bb')
     u_T[i] = LOOKUP('isotemplines',i,'u_T')
     v_T[i] = LOOKUP('isotemplines',i,'v_T')
     t_T[i] = LOOKUP('isotemplines',i,'t_T')
end


"find CCT using function"
CCT = CCT_(u_s,v_s,u_T[1..31],v_T[1..31],t_T[1..31],T[1..31])
```

Appendix C: EES code to determine the Color Rendering Index

```
"STEPS TO CALCULATING CRI"

"I. Find CCT of light source to be tested, k.  This will define the
reference illuminant,r.
If CCT_k < 5000 K, use planckian distribution for that CCT.  If CCT_k >
5000, use a daylight spectrum"

"II. Generate (or insert) reference (r) spd, and light source to be
tested (k) spd."

"III. Use y_bar_lambda color matching function to calculate total Y for
r and k spectrums.
     Calculate a scale factor for each that will bring the new Y for r
and k to be 100 each"

"IV.  Find the X,Y,Z and u,v of r and k.  _noB means coordinates of
light sources before reflection
     from samples."

"V.  Calculate values that will transform u_k_noB and v_k_noB into
u_r_noB and v_k_noB.
     This is the first part in accounting for the chromatic adaption of
the eye."

"VI.  Determine color sample reflectances (already in table)."

"VII.  Calculate the tristimulus values (X,Y,Z) and chromaticity
coordinates (x,y and u,v) for each of
the 8 color samples illuminated first by r and then k"

"VIII.  Modify (u,v) coordinates of the 8 samples illuminated by k to
account for chromatic adaption"

"IX.  Transform coordinates into 1964 Uniform Space Coordinates"

"X. Calculate the resultant shift for each color sample"

"XI. Calculate the Color Rendering Index of each color sample"

"XII. Calculate general color rendering Index"


lambda_interval = 5

"I. CCT calculated outside of this code"

"II.  Reference and Tested are lookup tables where spectrums must be
placed.
     Many sample spectrums in lookup tables."
```

```
"III"
"XYZ and uv - reference source and tested source, unscaled"
Duplicate l = 1,95
      Yr_us[l]=LOOKUP('Reference',l,2)*LOOKUP('CMFunctions',l,3)*lambda_
interval
      Yk_us[l]=LOOKUP('Tested',l,2)*LOOKUP('CMFunctions',l,3)*lambda_int
erval
end
Yr_us = SUM(Yr_us[z], z=1,95)
Yk_us = SUM(Yk_us[z], z=1,95)


"Find Y scaling factor for both reference and tested spectrums"
SF_r = 100/Yr_us
SF_k = 100/Yk_us

"Create scaled spectrums for reference and tested spectrums"
Duplicate m = 1,95
      lambda[m]=355+m*5
      P_r[m] = LOOKUP('Reference',m,2)*SF_r
      P_k[m] = LOOKUP('Tested',m,2)*SF_k
end

"IV"
"Find XYZ and uv of scaled source spectrums"
Duplicate l = 1,95
      Xr_noB[l]=P_r[l]*LOOKUP('CMFunctions',l,2)
      Yr_noB[l]=P_r[l]*LOOKUP('CMFunctions',l,3)
      Zr_noB[l]=P_r[l]*LOOKUP('CMFunctions',l,4)

      Xk_noB[l]=P_k[l]*LOOKUP('CMFunctions',l,2)
      Yk_noB[l]=P_k[l]*LOOKUP('CMFunctions',l,3)
      Zk_noB[l]=P_k[l]*LOOKUP('CMFunctions',l,4)
end
Xr_noB = SUM(Xr_noB[z], z=1,95)*lambda_interval
Yr_noB = SUM(Yr_noB[z], z=1,95)*lambda_interval
Zr_noB = SUM(Zr_noB[z], z=1,95)*lambda_interval
u_r_noB = 4*Xr_noB/(Xr_noB+15*Yr_noB+3*Zr_noB)
v_r_noB = 6*Yr_noB/(Xr_noB+15*Yr_noB+3*Zr_noB)

Xk_noB = SUM(Xk_noB[z], z=1,95)*lambda_interval
Yk_noB = SUM(Yk_noB[z], z=1,95)*lambda_interval
Zk_noB = SUM(Zk_noB[z], z=1,95)*lambda_interval
x_knoB = Xk_noB/(Xk_noB+Yk_noB+Zk_noB)
y_knoB = Yk_noB/(Xk_noB+Yk_noB+Zk_noB)
u_k_noB = 4*Xk_noB/(Xk_noB+15*Yk_noB+3*Zk_noB)
v_k_noB = 6*Yk_noB/(Xk_noB+15*Yk_noB+3*Zk_noB)

"V"
"values below to help account for adaptive color shift"
c_r = (4-u_r_noB-10*v_r_noB)/v_r_noB
c_k = (4-u_k_noB-10*v_k_noB)/v_k_noB
d_r = (1.708*v_r_noB+0.404-1.481*u_r_noB)/v_r_noB
d_k = (1.708*v_k_noB+0.404-1.481*u_k_noB)/v_k_noB
```

```
u`_k_noB = (10.872+0.404*(c_r/c_k)*c_k-
4*(d_r/d_k)*d_k)/(16.518+1.481*(c_r/c_k)*c_k-(d_r/d_k)*d_k)

v`_k_noB = 5.520/(16.518+1.481*(c_r/c_k)*c_k-(d_r/d_k)*d_k)

"VI and VII - Reflectances already in lookup table"
"XYZ and uv - color samples illuminated by reference and tested source"
Duplicate i = 1,8
     Duplicate j = 1,95

     Xr[i,j]=P_r[j]*LOOKUP('Reflectances',j,(i+1))*LOOKUP('CMFunctions'
,j,2)

     Yr[i,j]=P_r[j]*LOOKUP('Reflectances',j,(i+1))*LOOKUP('CMFunctions'
,j,3)

     Zr[i,j]=P_r[j]*LOOKUP('Reflectances',j,(i+1))*LOOKUP('CMFunctions'
,j,4)


     Xk[i,j]=P_k[j]*LOOKUP('Reflectances',j,(i+1))*LOOKUP('CMFunctions'
,j,2)

     Yk[i,j]=P_k[j]*LOOKUP('Reflectances',j,(i+1))*LOOKUP('CMFunctions'
,j,3)

     Zk[i,j]=P_k[j]*LOOKUP('Reflectances',j,(i+1))*LOOKUP('CMFunctions'
,j,4)
     end
     Xr[i] = SUM(Xr[i,z], z=1,95)*lambda_interval
     Yr[i] = SUM(Yr[i,z], z=1,95)*lambda_interval
     Zr[i] = SUM(Zr[i,z], z=1,95)*lambda_interval
     u_r[i] = 4*Xr[i]/(Xr[i]+15*Yr[i]+3*Zr[i])
     v_r[i] = 6*Yr[i]/(Xr[i]+15*Yr[i]+3*Zr[i])

     Xk[i] = SUM(Xk[i,z], z=1,95)*lambda_interval
     Yk[i] = SUM(Yk[i,z], z=1,95)*lambda_interval
     Zk[i] = SUM(Zk[i,z], z=1,95)*lambda_interval
     x_k[i] = Xk[i]/(Xk[i]+Yk[i]+Zk[i])
     y_k[i] = Yk[i]/(Xk[i]+Yk[i]+Zk[i])
     u_k[i] = 4*Xk[i]/(Xk[i]+15*Yk[i]+3*Zk[i])
     v_k[i] = 6*Yk[i]/(Xk[i]+15*Yk[i]+3*Zk[i])

     "VIII"
     "find new u`_k and v`_k to account for adaptive color shift"
     c_k[i] = (4-u_k[i]-10*v_k[i])/v_k[i]
     d_k[i] = (1.708*v_k[i]+0.404-1.481*u_k[i])/v_k[i]

     u`_k[i] = (10.872+0.404*(c_r/c_k)*c_k[i]-
4*(d_r/d_k)*d_k[i])/(16.518+1.481*(c_r/c_k)*c_k[i]-(d_r/d_k)*d_k[i])

     v`_k[i] = 5.520/(16.518+1.481*(c_r/c_k)*c_k[i]-(d_r/d_k)*d_k[i])

     "IX"
     W|star_r[i] = 25*(Yr[i])^(1/3)-17
```

```
      U|star_r[i] = 13*W|star_r[i]*(u_r[i]-u_r_noB)
      V|star_r[i] = 13*W|star_r[i]*(v_r[i]-v_r_noB)

      W|star_k[i] = 25*(Yk[i])^(1/3)-17
      U|star_k[i] = 13*W|star_k[i]*(u`_k[i]-u`_k_noB)
      V|star_k[i] = 13*W|star_k[i]*(v`_k[i]-v`_k_noB)

      "X"
      DELTAE[i]=((U|star_r[i]-U|star_k[i])^2+(V|star_r[i]-
V|star_k[i])^2+(W|star_r[i]-W|star_k[i])^2)^.5

      "XI"
      R[i]=100-4.6*DELTAE[i]
end

"XII"
CRI=1/8*SUM(R[y], y=1,8)
```

## Appendix D: TRNSED Interface

```
*|<Background> WHITE
*|<COLOR1> RED
*|<SIZE1> 14
*|<ALIGN1> CENTER
*|<STYLE1> BOLD ITALIC
*|<STYLE2> BOLD
*|<SIZE2> 10
*|<ALIGN2> LEFT
*|<SIZE3> 10
*|<TAB2> 4 IN
*|<PICTURE> COLLECTOR.BMP  RIGHT
*|*Hybrid Lighting Simulation
*|<COLOR1> BLACK
*|<SIZE1> 8
*|*Solar Energy Lab, UW-Madison
*|*Prepared by G.O.Schlegel and F.W.Burkholder
*|<COLOR1> red
*|<SIZE1> 9
*|<COLOR1> BLUE
*|<SIZE1> 12

ASSIGN ***.LST   6
ASSIGN W4-LIB.DAT   128
ASSIGN SIMWITHCCTIII.OUT   117
ASSIGN SIMWITHCCTIII_INT.OUT   118
ASSIGN SIMSPDIII.OUT       119
ASSIGN SOLAR4.DAT   132
ASSIGN CONCENTRATOR.DAT   133
ASSIGN COLDMIRROR.DAT   134
ASSIGN VLAMBDA.DAT   129
ASSIGN ATTENRPI.DAT   130
ASSIGN GASB.DAT   131
ASSIGN WDATA.DAT   125
*ASSIGN TYPE56.OUT   135
ASSIGN 31XYZ5NM.DAT  136
ASSIGN ISOTEMPLINES.DAT  137
ASSIGN HALOGENSPD.DAT  138
ASSIGN WWFLUORSPD.DAT  139
ASSIGN MUNSELL8B.DAT 140
ASSIGN FSFLUORSPD.DAT 141
ASSIGN TUNGSTSPD.DAT 142


***********************************************************************
********
*** Control cards
***********************************************************************
********

*|(SimLengthMode|Simulation Length Mode
```

```
*|Standard|SIMPAR|_OneHour//checked
*|One Hour|_SIMPAR|OneHour
*|)

*|(ATMS|Atmospheric switch
*|Smarts 2|SMARTS2ATM|_SIMPLEATM//checked
*|Simplified fit|_SMARTS2ATM|SIMPLEATM
*|)

*|[SMARTS2ATM
equations 1
ATMSwitch = 1
*|]

*|#*|[SIMPLEATM
*|#equations 1
*|#ATMSwitch = 0
*|#*|]

*|[SIMPAR|Simulation Parameters
EQUATIONS 7
I_MONTH= 0
*|<Month of the simulation|Month1.dat|1|2|19
I_DAY1= 1.0000000000000E+00
*|Day of Month for Simulation Start           |||0|1|1|31|20
I_DAY=I_MONTH/24+I_DAY1
I_LENGTH= 365
*|<Length of Simulation|Length.dat|2|1|21
WEEKS=I_LENGTH/7
START=24*(I_DAY-1)+1
STOP=START+I_LENGTH*24-1
*|]

*|#*|[OneHour|One Hour Simulation
*|#Equations 3
*|#START1 = 1.9330000000000E+03
*|#*|Start Hour|h|h|0.0|1.0|0|8760|999
*|#Start=Start1-1
*|#Stop=Start1
*|#*|]



EQUATIONS 2
STEP=1.0
StartDay=INT(START/24)+1
SIMULATION  START  STOP  STEP


*|(WEATHER|Weather Data
*|Use Average Monthly Weather
Data|MONTHLY|MONTHLY_2|MONTHLY_3|_TMY2|_TMY2_2|_TMY2_3|_IWEC|_IWEC_2|_I
WEC_3
```

```
*|Use TMY2 Weather Data Files (User
Provided)|_MONTHLY|_MONTHLY_2|_MONTHLY_3|TMY2|TMY2_2|TMY2_3|_IWEC|_IWEC
_2|_IWEC_3//checked
*|Use IWEC Weather Data Files (User
Provided)|_MONTHLY|_MONTHLY_2|_MONTHLY_3|_TMY2|_TMY2_2|_TMY2_3|IWEC|IWE
C_2|IWEC_3
*|)

*|[TMY2|
EQUATIONS 3
CITY= 7
*|<City for Simulation|CitiesK1.dat |2|1|22
LAT= 47.45
*|<Latitude of City|CitiesK1.dat |0|3|1000
TIMESHIFT= -2.30
*|<Adjustment to solar time|CitiesK1.dat |0|5|1000
ASSIGN weather\seattle.tm2 113
*|<City Path|CitiesK1.dat |0|6|1000
EQUATIONS 3
TURB=[18,22]
W = [18,21] /10
PMBAR = [18,18]*1000
*|]

*|#*|[MONTHLY|
*|#EQUATIONS 6
*|#CITY= 127
*|#*|<City for Simulation|Cities1.dat |2|1|22
*|#LAT= 43.13
*|#*|<Latitude of City|Cities1.dat |0|3|1000
*|#TIMESHIFT= 0.0
*|#TURB= 1.0000000000000E-01
*|#*|Average Annual Turbidity Level|||0.0|1.0|0|0.20|23
*|#W=1.42
*|#PMBAR=1013.25
*|#*|]

*|#*|[IWEC|
*|#EQUATIONS 3
*|#CITY= 2
*|#*|<City for Simulation|CitiesIwec.dat |2|1|22
*|#LAT= 43.65
*|#*|<Latitude of City|CitiesIwec.dat |0|3|1000
*|#TIMESHIFT= -7.80
*|#*|<Adjustment to solar time|CitiesIwec.dat |0|5|1000
*|#ASSIGN Weather\076900.iwc 113
*|#*|<City Path|CitiesIwec.dat |0|9|1000
*|#EQUATIONS 3
*|#TURB=[18,22]
*|#W=[18,21]/10
*|#PMBAR = [18,18]*1000
*|#*|]

*|[ELEVATION
equations 1
```

```
elev = 1.3000000000000E-01
*|Elevation of site|km||0.00|5.00|0.00|5.00|3
*|]

*|[EXISTING|Choose a Rate Schedule
EQUATIONS 16
SHHRON= 10.00
*|<Utility Provider|Rates.dat |2|3|43
SHON= 0.0586
*|<
|Rates.dat |0|4|17
SUMHRON = 12.0
*|<
|Rates.dat |0|5|17
SUMON= 0.0586
*|<                               |Rates.dat |0|6|17
SUMHROFF= 21.0
*|<                               |Rates.dat |0|7|17
SUMOFF= 0.0586
*|<                               |Rates.dat |0|8|17
SHHROFF= 21.0
*|<
|Rates.dat |0|9|17
WINHRON= 10.0
*|<                               |Rates.dat |0|10|17
WINON= 0.0586
*|<                               |Rates.dat |0|11|17
WINHROFF= 21.0
*|<                               |Rates.dat |0|12|17
WINOFF= 0.0586
*|<                               |Rates.dat |0|13|17
edaily= 0
*|<                               |Rates.dat |0|14|17
emonthly= 103.0
*|<                               |Rates.dat |0|15|17
STARTSUM= 3625
*|<                               |Rates.dat |0|16|17
STARTWIN= 6553
*|<                               |Rates.dat |0|17|17
NGPRICE= 0.02798
*|<                               |Rates.dat |0|18|18
*|]



*|[SYSPAR|System Parameters
CONSTANTS  12
NUMBEROF= 8.0000000000000E+00
*|Number of systems|||0|1|0|1000|1
CONCENT1= 1.7000000000000E+00
*|Active concentrator area|m²|ft²|0|10.76|0.0|100.00|4
TLENGTH= 2.0000000000000E+01
*|Length Of Optical Fiber|m|ft|0|3.28084|0.0|1000000.00|6
BNDRAD = 9.0000000000000E+00
```

```
*|Minimum bend radius of fiber (12" considered
straight)|in||0|1|3.5|12|1
RHOQENT= 4.0000000000000E+00
*|Reflectance at quartz rod entrance|%||0|1|0|100|1
RHOQEX= 4.0000000000000E+00
*|Reflectance at quartz rod exit|%||0|1|0|100|1
LPACK= 8.0000000000000E+00
*|Fiber entrance packing loss|%||0|1|0|100|1
FLX05= 1.2000000000000E+01
*|Fiber incident radiation flux - 0° to 5°|%||0|1|0|100|1
FLX510= 3.4000000000000E+01
*|                                                 5° to
10°|%||0|1|0|100|1
FLX1015= 4.8000000000000E+01
*|                                                 10° to
15°|%||0|1|0|100|1
FLX1520= 6.0000000000000E+00
*|                                                 15° to
20°|%||0|1|0|100|1
FLX2025= 0.0000000000000E+00
*|                                                 20° to
25°|%||0|1|0|100|1
*|]

*|[SMARTS2|Narrow Band Model Parameters
CONSTANTS 9
CONCTYPE= 1.0000000000000E+00
*|Concentrator material|||0|1|0|1000|24
RHO1= 9.7000000000000E-01
RHO2= 9.3000000000000E-01
FILTERIR= 7.3000000000000E-01
ATTEN= 1.3000000000000E+00
TPVEFFIC= 1.6000000000000E-01
IRSPECTR= 5.1000000000000E-01
VISIBLES= 4.7000000000000E-01
TUBEREFL= 9.5000000000000E-01
*|<COLOR1> BLACK
*|<SIZE1> 10
*|*(1=ECP-305, 2=FLABEG, 3=REFLECTECH)
*|<COLOR1> BLUE
*|<SIZE1> 12
*|]


*|[BLDGPAR|Conventional Lighting Parameters
CONSTANTS 4
LIGHTLEV= 5.0000000000000E+02
*|Lighting Level|lux|lux|0|1|0|1000|13
LUMEFF= 8.3000000000000E-01
*|Luminaire Efficiency|||0|1|0|1.00|15
CONTROL= 4.0000000000000E+00
*|Lighting Control System|||0|1|0|4|25
*|<SIZE1> 9
*|*(0 - ideal, 1 - dimmable ballast under-illumination, 2 - staging, 3
- dimmable ballast over-illumination, 4 - dimmable ballast with staging)
```

```
*|<SIZE1> 12
MULT= 4.0000000000000E+00
*|Staging Multiple|||0|1|0|100|26
*|]


*|(CHROMATICITY|Chromaticity
*|Calculate CCT|CORCOLT|_CCTCRI|_NOCHROM
*|Calculate CCT and CRI|_CORCOLT|CCTCRI|_NOCHROM//checked
*|No chromaticity|_CORCOLT|_CCTCRI|NOCHROM
*|)

*|#*|[CORCOLT|
*|#EQUATIONS 2
*|#CALCCT = 1
*|#CALCRI = -1
*|#*|]

*|[CCTCRI|
EQUATIONS 2
CALCCT = 1
CALCRI = 1
*|]

*|#*|[NOCHROM|
*|#EQUATIONS 2
*|#CALCCT = -1
*|#CALCRI = -1
*|#CONSTANTS 1
*|#LAMPEFFI= 5.2000000000000E+01
*|#*|Lamp Efficacy|lm/w|lm/w|0|1|0|683|14
*|#*|]


*|(convSPD|Pick indoor light source
*|Halogen (4100K, 98 CRI, 22
lm/W)|HALOGEN|_WWFLUOR|_FSFLUOR|_TUNGINC|_JEFFIC
*|Warm white fluorescent (3000K,  52 CRI, 89
lm/W)|_HALOGEN|WWFLUOR|_FSFLUOR|_TUNGINC|_JEFFIC
*|Full spectrum fluorescent (5000K, 90 CRI, 52
lm/W)|_HALOGEN|_WWFLUOR|FSFLUOR|_TUNGINC|_JEFFIC//checked
*|Tungsten Incandescent (3000K, 99+CRI, 15
lm/W)|_HALOGEN|_WWFLUOR|_FSFLUOR|TUNGINC|_JEFFIC
*|Just efficacy|_HALOGEN|_WWFLUOR|_FSFLUOR|_TUNGINC|JEFFIC
*|)

*|#*|[HALOGEN|
*|#EQUATIONS 2
*|#WHICHB = 138
*|#LAMPEFFI=22.0
*|#*|]

*|#*|[WWFLUOR|
*|#EQUATIONS 2
*|#WHICHB = 139
```

```
*|#LAMPEFFI = 89.0
*|#*|]

*|[FSFLUOR|
EQUATIONS 2
WHICHB = 141
LAMPEFFI= 52.0
*|]

*|#*|[TUNGINC|
*|#EQUATIONS 2
*|#WHICHB = 142
*|#LAMPEFFI = 15.0
*|#*|]


*|#*|[JEFFIC|
*|#EQUATIONS 1
*|#WHICHB = 141
*|#*|]




*|[TPVPAR| TPV Parameters
CONSTANTS 1
OPTEFF= 6.8400000000000E-01
*|Non Imaging Optical Device Efficiency|||0|1|0.000|1.000|12
*|]

*|[LIGHTSCH|Daily Building Lighting Schedule
CONSTANTS 4
WDLON= 8.0000000000000E+00
*|Time Lights are ON Weekdays|||0|1|0|24.0|16
WDLOFF= 1.7000000000000E+01
*|Time Lights are OFF Weekdays|||0|1|0|24.0|17
WELON= 8.0000000000000E+00
*|Time Lights are ON Weekends|||0|1|0|24.0|57
WELOFF= 1.7000000000000E+01
*|Time Lights are OFF Weekends|||0|1|0|24.0|58
*|]

*|[ECON1|Economic Parameters
EQUATIONS 13
INF= 3.0000000000000E-02
*|General Inflation Rate|||0|1|0|1.000|44
FUELINF= 2.0000000000000E-02
*|Fuel Inflation Rate|||0|1|0|1.000|45
M= 6.0000000000000E-02
*|Mortgage Rate|||0|1|0|1.000|46
DIS= 6.0000000000000E-02
*|Discount Rate|||0|1|0|1.000|47
N_E= 1.0000000000000E+01
```

```
*|Years of Analysis|years|years|0|1|0|100.0|48
N_D= 1.0000000000000E+01
*|Years of Depreciation|years|years|0|1|0|100.0|49
N_L= 1.0000000000000E+01
*|Years of Loan|years|years|0|1|0|100.0|50
TBAR= 4.0000000000000E-01
*|Income Tax|||0|1|0|1.000|51
PRTAX= 3.0000000000000E-02
*|Property Tax|||0|1|0|1.000|52
DOWN= 2.0000000000000E-01
*|Downpayment|||0|1|0|1.00|53
*|]
*|[ECON2|
*|<TAB2>5 IN
M_S= 3.0000000000000E-02
*|Ratio of First Year Misc. Costs to Initial Investment|||0|1|0|1.00|54
R_V= 3.0000000000000E-01
*|Ratio of Resale Value at End of Analysis to Initial
Investment|||0|1|0|1.00|55
VAL= 1.0000000000000E+00
*|Ratio of Assessed value to Initial Investment|||0|1|0|1.00|56
*|]

*|(INCOME|
*|Income Producing Property|INCF|_NINCF//checked
*|Non - Income Producing Property|_INCF|NINCF
*|)

*|{OUT|Output Parameters
*|Generate Online Plot|ONLINE
*|}
*<><><><><><><><><><><><><><><><><><><><><><><><><><><><><><><><><><><><>
VERSION 15
TOLERANCES 0.00001 0.00001
LIMITS 30 30 30
DFQ 1
WIDTH 80
LIST
MAP
SOLVER 0
*<><><><><><><><><><><><><><><><><><><><><><><><><><><><><><><><><><><><>

*----------------------------------------------------------------------
--------
* EQUATIONS "Electric Eqn"
EQUATIONS 9
rate = [17,9]*([10,1]*[13,1]+([11,1]*(1-[13,1])))+(1-[17,9])*(((1-
[17,8])*[9,1]+[17,8]*[10,1])*[13,1]+(((1-
[17,8])*[12,1]+[17,8]*[11,1])*(1-[13,1])))
base = [31,3]*rate+0.5*((edaily/24)+(emonthly/720))
hybrid=[31,2]*rate+0.5*((edaily/24)+(emonthly/720))
*|#*|[NINCF|
*|#IFLAG=0
*|#*|]
*|[INCF|
```

```
IFLAG=1
*|]
TPVR =([31,12]/1000)*rate
COP = 3
HCCost = ([31,4]/COP)*rate+0.5*((edaily/24)+(emonthly/720))
BCCOST = ([31,5]/COP)*rate+0.5*((edaily/24) +(emonthly/720))
MODELFLAG=-1
ASSIGN LIGHTHUM.BLD   126
ASSIGN LIGHTHUM.TRN   127

*-------------------------------------------------------------------------
--------
*In-House Skylighting Comparison, Use Daylight group
CONSTANTS 2
SLAREA=1.7
SLTAU=0.53
*-------------------------------------------------------------------------
--------
* EQUATIONS "Gas Prices"
CONSTANTS 5
NGSUM= NGPRICE
NGWIN= NGPRICE
NGDAILY= 0
NGON= 2.8810000000000E+03
NGoff= 7.2970000000000E+03
EQUATIONS 3
Eta = .80
HHCOST = ([31,6]/Eta)*[14,1]+NGDAILY/24
BHCOST = ([31,7]/Eta)*[14,1]+NGDAILY/24
*-------------------------------------------------------------------------
--------
* EQUATIONS "Light"
EQUATIONS 4
SchLight = [17,9]*[16,1]+(1-[17,9])*((1-[17,8])*[15,1]+([17,8]*[16,1]))
SchHLight = SchLight
Light = [31,8]
Hlight = [31,1]
*-------------------------------------------------------------------------
--------
*****Schedules*****
*-------------------------------------------------------------------------
--------
UNIT 9 TYPE 14     $/kwh, WD, SUM Schedule T14h
PARAMETERS 20
0 SUMOFF SHHRON  SUMOFF SHHRON SHON SUMHRON SHON SUMHRON SUMON SUMHROFF
SUMON SUMHROFF SHON SHHROFF SHON SHHROFF SUMOFF 24 SUMOFF
*-------------------------------------------------------------------------
--------
UNIT 10 TYPE 14    $/kwh, WE,SUM Schedule, T14h
PARAMETERS 4
0 SUMOFF 24 SUMOFF
*-------------------------------------------------------------------------
--------
UNIT 11 TYPE 14    $/kwh, WE,WIN Schedule, T14h-2
PARAMETERS 4
```

```
0 WINOFF 24 WINOFF
*----------------------------------------------------------------------
--------
UNIT 12 TYPE 14    $/kwh, WD, WIN Schedule, T14h-3
PARAMETERS 12
0 WINOFF WINHRON WINOFF WINHRON WINON WINHROFF WINON WINHROFF WINOFF 24
WINOFF
*----------------------------------------------------------------------
--------
UNIT 13 TYPE 14    SEASON
PARAMETERS 12
0 0 STARTSUM 0 STARTSUM 1 STARTWIN 1 STARTWIN 0 8760 0
*----------------------------------------------------------------------
--------
* Model "Natural Gas Schedule T14h" (Type 14)
UNIT 14 TYPE 14    Natural Gas Schedule T14h
PARAMETERS 12
0 NGWIN NGON NGWIN NGON NGSUM NGOFF NGSUM NGOFF NGWIN 8760 NGWIN
*----------------------------------------------------------------------
--------
*Weekday Lighting Schedule
UNIT 15 TYPE 14    Light Wday
PARAMETERS 12
1 0 WDLON 0 WDLON 1 WDLOFF 1 WDLOFF 0 24 0
*----------------------------------------------------------------------
--------
*Weekend Lighting Schedule
UNIT 16 TYPE 14    Light Sched T14h
PARAMETERS 12
1 0 WELON 0 WELON 1 WELOFF 1 WELOFF 0 24 0
*----------------------------------------------------------------------
--------
UNIT 17 TYPE 95    holidays_T95a
PARAMETERS 4
0 1998 0 1
*----------------------------------------------------------------------
--------
****TRNSYS TYPES****
*----------------------------------------------------------------------
--------
*|#*|[MONTHLY_2|
*|#UNIT 18 TYPE 54       TYPE54a
*|#PARAMETERS 19
*|#1 125 CITY 2 1 1 4.0 4.0 4.0 4.0 4.0 4.0 4.0 4.0 4.0 4.0 4.0 4.0 0.0
*|#
*|#Equations 1
*|#Tamb = [18,4]
*|#
*|#*-------------------------------------------------------------------
-----------
*|#UNIT 19 TYPE 16       TYPE16g
*|#PARAMETERS 9
*|#4 1 3 StartDay LAT 4871.0 0.0 2 -1
*|#INPUTS 13
*|#18,7 18,8 18,99 18,100 0,0 0,0 0,0 0,0 0,0 0,0 0,0 0,0 0,0
```

```
*|#0.0 0.0 0.0 1.0 0.2 90 0.0 90 90 90 180 90 270
*|#*-----------------------------------------------------------------
-----------
*|#UNIT 20 TYPE 16       TYPE16g-2
*|#PARAMETERS 9
*|#4 4 3 StartDay LAT 4871.0 0.0 2 -1
*|#INPUTS 7
*|#18,7 18,8 18,99 18,100 0,0 0,0 0,0
*|#0.0 0.0 0.0 1.0 0.2 90 0.0
*|#*-----------------------------------------------------------------
-----------
*|#UNIT 21 TYPE 69       TYPE69b
*|#PARAMETERS 2
*|#0 0
*|#INPUTS 5
*|#18,4 18,5 18,8 0,0 0,0
*|#0 20 0 0 0
*|#*|]
*--------------------------------------------------------------------
--------
*|[TMY2_2|
UNIT 18 TYPE 89    TYPE89b-2
PARAMETERS 2
-2 113

Equations 1
Tamb = [18,5]

*--------------------------------------------------------------------
--------
UNIT 19 TYPE 16    TYPE16g
PARAMETERS 9
*HorMode  TrackMode TiltMode  StartDay  Latitude  SolConst  Shift
NotUsed   SolarTime
4 1 3 StartDay LAT 4871.0 TIMESHIFT 2 1
INPUTS 13
18,4 18,3 18,99 18,100 0,0 0,0 0,0 0,0 0,0 0,0 0,0 0,0 0,0
*** INITIAL INPUT VALUES
0.0 0 0.0 1.0 0.2 90 0.0 90 90 90 180 90 270
*--------------------------------------------------------------------
--------
UNIT 20 TYPE 16    TYPE16g-2
PARAMETERS 9
4 4 3 StartDay LAT 4871.0 TIMESHIFT 2 1
INPUTS 7
18,4 18,3 18,99 18,100 0,0 0,0 0,0
0.0 0.0 0.0 1.0 0.2 90 0.0
*--------------------------------------------------------------------
--------
UNIT 21 TYPE 69    TYPE69b
PARAMETERS 2
0 0
INPUTS 5
18,5 18,9 18,3 0,0 0,0
0 20 0 0 0
```

```
*|]

*|#*|[IWEC_2|
*|#UNIT 18 TYPE 89       TYPE89b-2
*|#PARAMETERS 2
*|#-4 113
*|#
*|#Equations 1
*|#Tamb = [18,5]
*|#
*|#*-----------------------------------------------------------------
-----------
*|#UNIT 19 TYPE 16       TYPE16g
*|#PARAMETERS 9
*|#*HorMode  TrackMode TiltMode  StartDay  Latitude  SolConst  Shift
NotUsed   SolarTime
*|#4 1 3 StartDay LAT 4871.0 TIMESHIFT 2 1
*|#INPUTS 13
*|#18,4 18,3 18,99 18,100 0,0 0,0 0,0 0,0 0,0 0,0 0,0 0,0 0,0
*|#*** INITIAL INPUT VALUES
*|#0.0 0 0.0 1.0 0.2 90 0.0 90 90 90 180 90 270
*|#*-----------------------------------------------------------------
-----------
*|#UNIT 20 TYPE 16       TYPE16g-2
*|#PARAMETERS 9
*|#4 4 3 StartDay LAT 4871.0 TIMESHIFT 2 1
*|#INPUTS 7
*|#18,4 18,3 18,99 18,100 0,0 0,0 0,0
*|#0.0 0.0 0.0 1.0 0.2 90 0.0
*|#*-----------------------------------------------------------------
-----------
*|#UNIT 21 TYPE 69       TYPE69b
*|#PARAMETERS 2
*|#0 0
*|#INPUTS 5
*|#18,5 18,9 18,3 0,0 0,0
*|#0 20 0 0 0
*|#*|]


*--------------------------------------------------------------------
--------
***TYPE 56***
*--------------------------------------------------------------------
--------
UNIT 22 TYPE 56    type56
PARAMETERS 5
126 127 128 0 0.50
INPUTS 24
*|[TMY2_3|
18,5 18,10
*|]
*|#*|[MONTHLY_3|
*|#18,4 18,6
*|#*|]
```

```
*|#*|[IWEC_3|
*|#18,5 18,10
*|#*|]
21,1 19,17 19,7 19,22 19,12 19,4 19,18 19,8 19,23 19,13 19,5 19,20
19,10 19,25 19,15 19,2
Light
HLIGHT
SCHlight
SCHHLIGHT
31,9
31,10
*** INITIAL INPUT VALUES
0 0 0 0 0 0 0 0 0 0 0 0 0 0 0 0 0 0 0 0 0 0 0 0 
*-----------------------------------------------------------------------
--------
UNIT 23 TYPE 24    TYPE24
PARAMETERS 1
* 1 Reset time
stop
INPUTS 30
*                                                          P       LF0
10      20        30      40      50       60        70       80    90
LF100
31,2 31,3 31,4 31,5 31,6 31,7 31,12 31,35 31,36 31,37 31,38 31,39 31,40
31,41 31,42 31,43 31,44 31,45
*CCT5500 ------------------->CCT3000 CRI100----------------------------
->CRI50
31,49 31,50 31,51 31,52 31,53 31,54 31,55 31,56 31,57 31,58 31,59 31,60
*** INITIAL INPUT VALUES
0.0 0.0 0.0 0.0 0.0 0.0 0.0 0.0 0.0 0.0 0.0 0.0 0.0 0.0 0.0 0.0 0.0 0.0
0.0 0.0 0.0 0.0 0.0 0.0 0.0 0.0 0.0 0.0 0.0 0.0
*-----------------------------------------------------------------------
--------
UNIT 24 TYPE 24    TYPE24-2
PARAMETERS 1
* 1 Reset time
stop
INPUTS 12
HCCost HHCOST BCCOST BHCOST 31,3 31,6 31,4 base hybrid TPVR
31,12
20,8
*** INITIAL INPUT VALUES
0.0 0.0 0.0 0.0 0.0 0.0 0.0 0.0 0.0 0.0 0.0 0
*-----------------------------------------------------------------------
--------
*|#*|[ONLINE|
*|#EQUATIONS 3
*|#HLIGHTOUT=[23,1]/1000
*|#LIGHTOUT=[23,2]/1000
*|#TPVOUT=[23,7]/1000000
*|#
*|#UNIT 25 TYPE 65       Lighting-Int
*|#PARAMETERS 10
*|#2 1 0.0 50 0.0 10 1 14 0 -1
*|#INPUTS 3
```

```
*|#Lightout hlightout TPVOUT
*|#Baseline w/Hybrid TPV
*|#LABELS  5
*|#MWh MWh MWh
*|#Lighting Energy (MWh)
*|#TPV Energy (MWh)
*|#Lighting Energy
*|#*|]

*-----------------------------------------------------------------------
--------
UNIT 28 TYPE 25    TYPE25b
PARAMETERS 6
STEP START STOP 117 1 1
INPUTS 24
Tamb 22,7 22,8 31,7 31,6 31,5 31,4 31,3 31,2 31,11 31,12 31,27 31,28
31,30 31,31 31,22 31,47 31,25 31,26 31,48 31,46 31,62 31,61 31,34
TAMB TZONE1 TZONE2 BHeat HHeat BCool HCool BLight HLight Lumens TPVOUT
Zenith HExtra
TBEAM BEAMA CCT1 CRI CCT2 AMASS W TURB P Elev SF
C C C kj/hr kj/hr kj/hr kj/hr kWh kWh lumens Wh deg kj/hr-m2
kj/hr-m2 kj/hr-m2 K dim K dim in dim mbar km dim
*-----------------------------------------------------------------------
--------
UNIT 29 TYPE 25
PARAMETERS 6
STEP STOP STOP 118 1 1
INPUTS 23
*CCT5500 ------------------->CCT3000 CRI100----------------------------
->CRI50
23,19 23,20 23,21 23,22 23,23 23,24 23,25 23,26 23,27 23,28 23,29 23,30
23,8 23,9 23,10 23,11 23,12 23,13 23,14 23,15 23,16 23,17 23,18
CCT5500 CCT5000 CCT4500 CCT4000 CCT3500 CCT3000
CRI100 CRI90 CRI80 CRI70 CRI60 CRI50
LF0 LF10 LF20 LF30 LF40 LF50 LF60 LF70 LF80 LF90 LF100
dim dim dim dim dim dim dim dim dim dim dim dim
dim dim dim dim dim dim dim dim dim dim dim
*-----------------------------------------------------------------------
--------
UNIT 31 TYPE 296   Type296
PARAMETERS 63
LAT 132 133 CONCTYPE 134 129 130 TLENGTH 131 CONCENT1 RHO1 RHO2
TUBEREFL VISIBLES
IRSPECTR FILTERIR NUMBEROF ATTEN LUMEFF TPVEFFIC LIGHTLEV 2500 LAMPEFFI
MODELFLAG
TBAR IFLAG N_D DOWN M_S VAL PRTAX R_V N_E N_L INF FUELINF DIS M OPTEFF
CONTROL
MULT SLAREA SLTAU RHOQENT RHOQEX LPACK FLX05 FLX510 FLX1015 FLX1520
FLX2025 BNDRAD
CALCCT 136 137 119 WHICHB WHICHB WHICHB ATMSwitch elev CALCRI 140
INPUTS 23
20,2 20,1 20,4 TURB 20,6 20,5 20,8 SchLight
22,4 22,5 22,6 22,1 22,2 22,3
24,8 24,9 24,3 24,1 24,4 24,2 24,10 W PMBAR
*** INITIAL INPUT VALUES
```

```
0 0 0 0.1 0 0 0 0 0 0 0 0 0 0 0 0 0 0 0 0 0 0 1000

UNIT 32 TYPE 580 TYPE580
PARAMETERS 3
21 1 0

INPUTS 19
* NumMod      HL    BL  HC   BC    HH   BH $BL $HL $BC $HC $BH$HHTPVR
AES  BECC TPVP
NUMBEROF 23,1 23,2 23,3 23,4 23,5 23,6 24,8 24,9 24,3 24,1 24,4 24,2
24,10 31,13 31,14 31,15 31,16  23,7
0 0 0 0 0 0 0 0 0 0 0 0 0 0 0 0 0 0 0

*\*|<APPLINK1> TRNINFO1.bmp brochure.pdf
*\*|<APPLINK1> MANUAL.bmp  HLsim.pdf
*\*|*NOTE: User's manual will not run if Adobe Acrobat is not
installed...

! --- Online plot for debugging --------------------------------------
-------------------

ASSIGN ***.PLT  101

Unit 101 Type 65 Solar Radiation Plot
Parameters 10

*NbLeft   NbRight   LeftMin   LeftMax   RightMin  RightMax
4         1         2000       5500       45      100
*NbPlots  XGridPts  OFF       LU
1         10        0         101

Inputs 5

18,4 18,3 31,22 31,25 31,47
GHoz Gbn CCTamb CCTin CRI

Labels 5

Radiation [kJ/h-m^2]
Radiation [kJ/h-m^2] and CCT[K]
CRI [dim]
Radiation [kJ/h-m^2]

END
```

Appendix E: TYPE 296 that includes CCT and CRI revisions

```
   SUBROUTINE TYPE296(TIME,XIN,OUT,T,DTDT,PAR,INFO,ICNTRL,*)



C**********************************************************************
C     HYBRID LIGHTING - SOLAR IRRADIANCE MODEL
C                                                                 *
C     THIS COMPONENT GENERATES THE SPECTRAL SOLAR IRADIANCE DATA      *
C     BASED ON SMARTS2 OUTPUT FOR AIR MASS 2.25, BETA=.1, BETA=0.2    *
C     AND EXTRATERRESTRIAL SOLAR IRRADIANCE.  THE INTEGRATED
C     VALUE OF THE SMARTS2 DATA IS SCALED SO THE MAGNITUDE
C     OF THE BEAM COMPONENT MATCHES THE BEAM COMPONENT IN TRNSYS
C                                                       *
C     THE COMPONENT ALSO CALCULATES THE SPECTRAL LOSSES ASSOCIATED
C     WITH THE HYBRID LIGHTING SYSTEM INCLUDING REFLECATNCE LOSSES
C     FROM THE PRIMARY MIRROR, REFLECTANCE AND TRANSMITTANCE LOSSES
C     FROM THE COLD MIRROR, TPV EFFICIENCY LOSSES, AND LIGHT FIBER
C     ATTENUATION LOSSES.  LUMINAIRE LOSSES ARE NOT MODELED AS
C     SPECTRALLY DEPENDENT.  LOSSES DUE TO SUPPLEMENTAL FILTERS WILL
C     BE INLCUDED AS THE INFORMATION IS OBTAINED
C
C     ALL SPECTRAL DATA IS PREPROCESSED AND READ INTO FORTRAN IN 5
C     NANOMETER INCREMENTS FROM 280-2500 NM.  THE VISIBLE SPECTRUM
C     IS ASSUMED TO BE 380-780 NM, THE IR SPECTRUM IS 780-2500 NM,
C     AND THE UV SPECTRUM IS 280-380 NM.
C**********************************************************************

C     DECLARATION OF VARIABLES
      IMPLICIT NONE
      REAL PAR,TIME,T,DTDT,IUNIT,ET,AMONE,ZETA,ZENARAD,PI,RHOECP,
     &ZETAB,AMONEB,RHORFT,RHOFBG,RHO,RHOCM,GRTWO,GTTWO,GTPV,G,GRONE,
     &GVIS,ETA_QE,PHOTOPIC,LIGHT,ELEC,CAREA,ALAMBDA,GBEAM,THETA,
     &RB,BEAMRATIO,IDI,HEXTRA,E,PHOTONI,GBEAMA,F,GEFF,GRTHREE,GRFOUR,
     &GRFIVE,ETSum,GHLS,AMR16,AT841,GINSIDE,GCONV

      DOUBLE PRECISION XIN,OUT,ETA,LAT,AIRMASS,NTOTAL,LENGTH,KAPPA,
     &KAPPAB,ZENA,TURB,KAPPA2,TFD,TURBRATIO,FIBERLENGTH,KT,HHOR,HBEAM,
     &TPVAREA,VMAX,HOZ,SCALEFAC,HDIFF,TBEAM,IDICH,RBCH,SYSEFF,LIGHTEFF
     &,BEAMA,KAPPATAU,TAULAMBDA,RHO1,RHO2,TUBEREFL,VISPECTR,IRSPECTR,
     &FILTERIR,NUMBEROF,ATTENAVG,LUMEFFIC,TPVEFFIC,LIGHTLEV,BLDGAREA,
     &LAMPEFF,MODELFLAG,TBAR,IFLAG,N_D,DOWN,M_S,VAL,PRTAX,R_V,N_E,N_L,

&INF,FUELINF,DIS,M,SEAREA,LFLGIN,SHEAT,SCOOL,LATENT,BHEAT,BCOOL,NLF
     &,BLATENT,CBLIGHT,CHLIGHT,BCCOST,HCCOST,BHCOST,HHCOST,TPVREV,VOC,
     &ISC,IMAX,VMAXARRAY,MUISC,MUVOC,TCREF,TC,EPSILON,NS,GT,GTREF,V,LF,
     &A,IL,IO,I,RS,P,ILREF,AREF,IOREF,RSREF,TAU,KAPPATAUAVG,LOADLNH,NAP,
     &LOADLH,XTRALGHT,LSCALE,LFLGOUT,SUNLIGHT,XTRAHEAT,LLNH,LLH,OPTEFF,
     &LATENTCOOL,BLATENTHEAT,BLATENTCOOL,LATENTHEAT,HEAT,COOL,BASECOOL,
     &BASEHEAT,AES,BECC,P1,PWF,NMIN,NMIN1,A1,A2,A3,A4,A5,A6,P2,ZERO,
```

```
&NEWEFF,MULT,Z,SLAREA,SLTAU,NLEFF,ETAPV,PVAREA,RHOQENT,RHOQEX,LPACK
     &,FLX05,FLX510,FLX1015,FLX1520,FLX2025,T05,T510,T1015,T1520,T2025,
     &TAU05,TAU510,TAU1015,TAU1520,TAU2025,BNDRAD,TAUBEND,U1,V1,CCT1,
     &U2,V2,CCT2,XBAR,YBAR,ZBAR,U1lam,V1lam,W1lam,U2lam,V2lam,W2lam,
     &Ubar,Vbar,Wbar,U1sum,V1sum,W1sum,U2sum,V2sum,W2sum,Tbb,uT,vT,tT,
     &Diso1,Diso2,DCOMB,LUMENSCONV,LFract,elevation,smartsOutput,CRI,W,
     &wvlng,C1,C2,BB, deltawv,wvlng2,Yr_T,Yk_T,Yr_,Yk_,SF_r,SF_k,Pr,Pk,
     &Xr_noB,Yr_noB,Zr_noB,Xk_noB,Yk_noB,Zk_noB,ur_noB,uk_noB,vr_noB,
     &vk_noB,cr,ck,cks,dr,dk,dks,uk_noB_t,vk_noB_t,B,Xr,Yr,Zr,Xk,Yk,Zk,
     &ur,vr,uk,vk,uk_t,vk_t,WSr,USr,VSr,WSk,USk,VSk,DELE,R,RT,PMBAR

      INTEGER :: INFO,CMODE,NP,NI,NO,ND,JJ,NRS,JH,JI,LUD,LUW,LUK,ICNTRL
     &,IFORM,LUR,REF,JK,RTOTAL,MIRROR,CLDMIR,CMTOTAL,LAMBDA
     &,VLAMBDA,FIBATT,ATTENTOTAL,VLTOTAL,TPV,TPVTOTAL,CONTROL,CALCCT
     &,XYZ,CHROMTOT,ISOL,ITOT,SPD,MR16,T841,LAMBDAC,WHICHB,HALTOT,
     &MR16TOT,CCTOUTSIDE,CCTINSIDE,LF0,LF10,LF20,LF30,LF40,LF50,LF60,
     &LF70,LF80,LF90,LF100,ATMS,inpLU=996,extLU=997,CALCRI,MUNSELL8B,

&CT5500,CT5000,CT4500,CT4000,CT3500,CT3000,CRI100,CRI90,CRI80,CRI70
     &,CRI60,CRI50

      character(len=2000) dumString

      LOGICAL FLAG
      PARAMETER (NI=23,NP=63,NO=62,ND=0)
      CHARACTER*3 YCHECK(NI),OCHECK(NO),CARD
      CHARACTER FILNAM*40,COMP*4
      DIMENSION PAR(NP),XIN(NI),OUT(NO),INFO(15),ET(445),KAPPAB(445),
     &G(445),KAPPA(445),AMONE(445),RHOECP(445),GRONE(445),AMONEB(445),
     &KAPPA2(445),RHORFT(445),RHOFBG(445),RHO(445),RHOCM(445),GRTWO(445)
     &,GTTWO(445),GRTHREE(445),GRFOUR(445),GRFIVE(445),LAMBDA(445),
     &GTPV(445),GVIS(445),ETA_QE(445),
     &PHOTOPIC(445),ALAMBDA(445),GBEAM(445),E(445),PHOTONI(445),
     &GBEAMA(445),KAPPATAU(445),TAULAMBDA(445),F(445),GEFF(445),
     &T05(445),T510(445),T1015(445),T1520(445),T2025(445),XBAR(445),
     &YBAR(445),ZBAR(445),U1lam(445),V1lam(445),W1lam(445),
     &U2lam(445),V2lam(445),W2lam(445),Tbb(31),uT(31),vT(31),tT(31),
     &Diso1(31),Diso2(31),GHLS(445),AMR16(445),AT841(81),GINSIDE(445),
     &GCONV(445),smartsOutput(2,445),wvlng(95),BB(95),Yr_(95),
     &Yk_(95),Pr(95),Pk(95),B(8,95),Xr(8),Yr(8),Zr(8),Xk(8),Yk(8),Zk(8),
     &ur(8),vr(8),uk(8),vk(8),ck(8),dk(8),uk_t(8),vk_t(8),WSr(8),USr(8),
     &VSr(8),WSk(8),USk(8),VSk(8),DELE(8),R(8)

      COMMON /LUNITS/ LUR,LUW,IFORM,LUK
      COMMON /SYSTMX/ COMP
      DATA IUNIT/0/PI/3.1415926/
C-----------------------------------------------------------------------

C           IF ITS THE FIRST CALL TO THIS UNIT, DO SOME BOOKKEEPING
                  IF (INFO(7).GE.0) GO TO 100

C           FIRST CALL OF SIMULATION, CALL THE TYPECK SUBROUTINE TO
CHECK THAT THE
```

```
C            USER HAS PROVIDED THE CORRECT NUMBER OF INPUTS,PARAMETERS,
AND DERIVS
                   INFO(6)=NO
                   INFO(9)=1
                   CALL TYPECK(1,INFO,NI,NP,ND)

C            GET THE VALUES OF THE PARAMETERS FOR THIS COMPONENT
                   LAT=PAR(1)
                   LUD=PAR(2)
                   REF=PAR(3)
                   MIRROR=PAR(4)
                   CLDMIR=PAR(5)
                   VLAMBDA=PAR(6)
                   FIBATT=PAR(7)
                   FIBERLENGTH=PAR(8)
                   TPV=PAR(9)
               CAREA=PAR(10)
                   RHO1=PAR(11)
                   RHO2=PAR(12)
                   TUBEREFL=PAR(13)
                   VISPECTR=PAR(14)
                   IRSPECTR=PAR(15)
                   FILTERIR=PAR(16)
                   NUMBEROF=PAR(17)
                   ATTENAVG=PAR(18)
                   LUMEFFIC=PAR(19)
                   TPVEFFIC=PAR(20)
                   LIGHTLEV=PAR(21)
                   BLDGAREA=PAR(22)
                   LAMPEFF=PAR(23)
                   MODELFLAG=PAR(24)
                   TBAR=PAR(25)
                   IFLAG=PAR(26)
                   N_D=PAR(27)
                   DOWN=PAR(28)
                   M_S=PAR(29)
                   VAL=PAR(30)
                   PRTAX=PAR(31)
                   R_V=PAR(32)
                   N_E=PAR(33)
                   N_L=PAR(34)
                   INF=PAR(35)
                   FUELINF=PAR(36)
                   DIS=PAR(37)
                   M=PAR(38)
                   OPTEFF=PAR(39)
                   CONTROL=PAR(40)
                   MULT=PAR(41)
                   SLAREA=PAR(42)
                   SLTAU=PAR(43)
               RHOQENT=PAR(44)
               RHOQEX=PAR(45)
               LPACK=PAR(46)
               FLX05=PAR(47)
               FLX510=PAR(48)
```

```
              FLX1015=PAR(49)
              FLX1520=PAR(50)
              FLX2025=PAR(51)
              BNDRAD=PAR(52)
              CALCCT=PAR(53)
              XYZ=PAR(54)
              ISOL=PAR(55)
              SPD=PAR(56)                  !output file used to print
stuff from 296
              MR16=PAR(57)
              T841=PAR(58)
              WHICHB=PAR(59)
              ATMS = int(PAR(60)+0.001)  ! Switch between smarts2 and
fit (smarts2 if 1)
              elevation = par(61)        ! weather station elevation
                CALCRI = PAR(62)            !whether to calculate CRI
or not
              MUNSELL8B = PAR(63)          !color sample data

C     SET DUMMY ECONOMIC PARAMETER OUTPUTS
      P1=0
      P2=0
      AES=0
      BECC=0


C     PROTECT AGAINST WEIRD TYPE 56 EFFECTS IF NUMBEROF=0
      IF (NUMBEROF.EQ.0.00) THEN
            NUMBEROF=0.0001
      ENDIF




C     CHECK TO SEE WHICH MODEL IS BEING RUN AND DIRECT TRAFFIC
ACCORDINGLY
      IF (MODELFLAG.GT.0)THEN
            GOTO 100
            ELSE
            GOTO 50
      ENDIF


C***********************************************************************
C    OPEN DATA FILE
                        *
C***********************************************************************


50    IF (COMP .EQ. 'MICR') THEN
C       CHECK TO SEE IF FILE IS ALREADY OPENED.  IF NOT, GET NAME AND
OPEN
         INQUIRE(UNIT=LUD,OPENED=FLAG)
         IF (.NOT. FLAG) THEN
           WRITE(LUW,221) INFO(1), INFO(2)
```

```
221         FORMAT(//2X,'**** UNIT ',I3,' TYPE ',I3,' SOLAR IRRADIANCE
MO
     &        DEL'/4X,'ENTER FILE NAME FOR SOLAR IRRADIANCE DATA.')
            READ(LUK,222,ERR=223) FILNAM
222         FORMAT(A40)
            OPEN(LUD,FILE=FILNAM,STATUS='OLD',ERR=223)
            GO TO 25
223         WRITE(LUW,224) 143,INFO(1),INFO(2)
224          FORMAT(//,1X,'***** ERROR *****',8X,'TRNSYS ERROR # ',I3,/1X,
     .      'UNIT ',I3,' TYPE ',I3,' WEATHER GENERATOR',/1X,
     .      'ERROR READING INPUT WEATHER FILE FOR TYPE 54 SUBROUTINE')
            CALL MYSTOP(143)
            RETURN
25          CONTINUE
          ENDIF
        ELSE
          INQUIRE(UNIT=LUD,EXIST=FLAG)
          IF (.NOT. FLAG) THEN
            OPEN(LUD,STATUS='OLD')
          ENDIF
        END IF
      REWIND LUD

C     READ IRRADIANCE DATA
      READ(LUD,*) NTOTAL
      DO 70 JJ=1,NTOTAL
      READ(LUD,*) LAMBDA(JJ),ET(JJ),AMONE(JJ),AMONEB(JJ)
C     CALCULATE ARRAYS OF DECAY COEFFICIENTS
C     AMONEB IS THE TOTAL HORIZONTAL IRRADIANCE AT AM=2.25, BETA=0.2
C     AMONE IS THE TOTAL HORIZONTAL IRRADIANCE AT AM=2.25, BETA=0.1
      LENGTH=2.25
      ZETA=AMONE(JJ)/ET(JJ)
      ZETAB=AMONEB(JJ)/ET(JJ)
      IF (ZETA.GT.0) THEN
            KAPPA(JJ)=(-1/LENGTH)*LOG(ZETA)
      ELSE
            KAPPA(JJ)=5
      ENDIF

      IF (ZETAB.GT.0) THEN
            KAPPAB(JJ)=(-1/LENGTH)*LOG(ZETAB)
            KAPPA2(JJ)=KAPPAB(JJ)-KAPPA(JJ)
      ELSE
            KAPPA2(JJ)=0
      ENDIF

70    CONTINUE
      CLOSE(UNIT=LUD)

C     READ PRIMARY MIRROR REFLECTANCE DATA
      READ(REF,*) RTOTAL
      DO 80 JK=1,RTOTAL
            READ(REF,*) RHOECP(JK),RHORFT(JK), RHOFBG(JK)

      IF (MIRROR.NE.1) THEN
```

```
            IF (MIRROR.NE.2) THEN
                  RHO(JK)=RHOFBG(JK)
            ELSE
                  RHO(JK)=RHORFT(JK)
            ENDIF
      ELSE
            RHO(JK)=RHOECP(JK)
      ENDIF

80    CONTINUE

C     READ COLDMIRROR REFLECTANCE DATA (0-100 %)
      READ(CLDMIR,*) CMTOTAL
      DO 85 JK=1,CMTOTAL
            READ(CLDMIR,*) RHOCM(JK)
85    CONTINUE

C     READ VISIBILITY CURVE DATA, V-LAMBDA (0-1)
      READ(VLAMBDA,*) VLTOTAL
      DO 86 JK=1,VLTOTAL
            READ(VLAMBDA,*) PHOTOPIC(JK)
86    CONTINUE

C     READ FIBER TRANSMITTANCE DATA, (0-1/m)
C     First calculate transmissivity due to bend in fiber
C     Curve fit assumes BNDRAD = 12" is no attenuation
C     fit based on data from 3.5" to 9" radii
      TAUBEND = 0.0995*(LOG(BNDRAD)/LOG(2.718282))+0.7505
      READ(FIBATT,*) ATTENTOTAL
      DO 87 JK=1,ATTENTOTAL
            READ(FIBATT,*)
T05(JK),T510(JK),T1015(JK),T1520(JK),T2025(JK)
          TAU05=FLX05/100*T05(JK)**FIBERLENGTH
          TAU510=FLX510/100*T510(JK)**FIBERLENGTH
          TAU1015=FLX1015/100*T1015(JK)**FIBERLENGTH
          TAU1520=FLX1520/100*T1520(JK)**FIBERLENGTH
          TAU2025=FLX2025/100*T2025(JK)**FIBERLENGTH
          TAULAMBDA(JK)= (TAU05+TAU510+TAU1015+TAU1520+TAU2025)*TAUBEND

87    CONTINUE

C     READ THERMAL PHOTOVOLAIC CELL QUANTUM EFFICIENCY DATA, (0-1)
      READ(TPV,*) TPVTOTAL
      DO 88 JK=1,TPVTOTAL
            READ(TPV,*) ETA_QE(JK)
88    CONTINUE

C     READ COLOR MATCHING FUNCTIONS
C     reads in xbar,ybar, and zbar in 5 nm increments
C     used to find x,y and u,v chromaticity coordinates

      READ(XYZ,*) CHROMTOT
      DO 89 JK=1,CHROMTOT
            READ(XYZ,*) XBAR(JK),YBAR(JK),ZBAR(JK)
89    CONTINUE
```

```
C     READ ISOTEMPLINES
C     used to calculate CCT
      READ(ISOL,*) ITOT
      DO 90, JK=1,ITOT
          READ(ISOL,*) Tbb(JK),uT(JK),vT(JK),tT(JK)
90    CONTINUE

C     READ Halogen Spectrum Data - Solalux MR16 CCT 4200
      READ(MR16,*) HALTOT
      DO 91 JK=1,HALTOT
         READ(MR16,*) LAMBDAC,AMR16(JK)
91    CONTINUE

C     READ T841 Spectrum Data - Solalux MR16 CCT 4200
c      READ(T841,*) MR16TOT
c     DO 92 JK=1,MR16TOT
c        READ(T841,*) LAMBDAC,AT841(JK)
c92   CONTINUE

C     Read Color sample reflectance data
      Do 93 JK = 1,95
         READ(MUNSELL8B,*) LAMBDAC,B(1,JK),B(2,JK),B(3,JK),B(4,JK),
     &B(5,JK),B(6,JK),B(7,JK),B(8,JK)
93    CONTINUE
      RETURN 1



C           END OF THE FIRST ITERATION BOOKKEEPING

C     *****************************************************************
C     *
C     *                                    MAIN PROGRAM
C     *
C     *****************************************************************

100    CONTINUE



C     GET THE VALUES OF THE INPUTS TO THIS COMPONENT
                  ZENA=XIN(1)
                  HEXTRA=XIN(2)
                  HHOR=XIN(3)
                  TURB=XIN(4)

C     CHEATER INPUTS
                  HDIFF=XIN(5)
                  HBEAM=XIN(6)
                  TBEAM=XIN(7)
```

```
C     INPUTS FROM THE TYPE FORMERLY KNOWN AS 291
                  LFLGIN=XIN(8)
                  SHEAT=XIN(9)
                  SCOOL=XIN(10)
                  LATENT=XIN(11)
                  BHEAT=XIN(12)
                  BCOOL=XIN(13)
                  BLATENT=XIN(14)

C     COSTING INPUTS - SHOULD ONLY BE READ IN ONCE AT END OF SIMULATION
                  CBLIGHT=XIN(15)
                  CHLIGHT=XIN(16)
                  BCCOST=XIN(17)
                  HCCOST=XIN(18)
                  BHCOST=XIN(19)
                  HHCOST=XIN(20)
                  TPVREV=XIN(21)
              W=XIN(22)
              PMBAR = XIN(23)

C     IF ITS THE LAST CALL CALCULATE THE ECONOMIC PARAMETERS
      IF (INFO(8).EQ.-1) THEN
            GOTO 700
      ENDIF
C     CHECK TO SEE WHICH MODEL IS BEING RUN AND DIRECT TRAFFIC
ACCORDINGLY
      IF (MODELFLAG.EQ.1)THEN
            NLEFF=200
            GOTO 500
      ENDIF
      IF (MODELFLAG.EQ.2) THEN
            NLEFF=100
            GOTO 550
      ENDIF
      NLEFF=200


C
      *****************************************************************
*
C     *
                         *
C     *                                    NARROW BAND MODEL
                   *
C     *
                         *
C
      *****************************************************************
*


C     RESET THE INTEGRATION VARIABLES
      LIGHT=0
      LIGHTEFF=0
      SYSEFF=0
```

```
      ELEC=0
      BEAMA=0
      HOZ=0
      ETSum = 0
      LF0 = 0
      LF10 = 0
      LF20 = 0
      LF30 = 0
      LF40 = 0
      LF50 = 0
      LF60 = 0
      LF70 = 0
      LF80 = 0
      LF90 = 0
      LF100 = 0
      RT = 0.0
      CT5500 = 0
      CT5000 = 0
      CT4500 = 0
      CT4000 = 0
      CT3500 = 0
      CT3000 = 0
      CRI100 = 0
      CRI90 = 0
      CRI80 = 0
      CRI70 = 0
      CRI60 = 0
      CRI50 = 0

C     TURBIDITY RATIO DEFINED AS
C     (ACTUAL TURBIDTY-TURBIDITY FIT DIFF)/TURB FIT DIFF
      TFD=0.1
      TURBRATIO=(TURB-TFD)/TFD
C     CALCULATE VALUE OF AIR MASS
      IF (ZENA.GT.80.0) THEN !80 limits analysis to AM less than equal
to 5.76
            AIRMASS = 0
          SCALEFAC = 0
C     IRRADIANCE CALCULATION, INITIALIZE ARRAYS
          DO 110 JI=1,NTOTAL
                G(JI)=0
                GEFF(JI)=0
                GBEAM(JI)=0
                GBEAMA(JI)=0
                GRONE(JI)=0
                GRTWO(JI)=0
              GRTHREE(JI)=0
              GRFOUR(JI)=0
              GRFIVE(JI)=0
                GTTWO(JI)=0
                GVIS(JI)=0
110       CONTINUE

      ELSE
            ZENARAD=ZENA*(PI/180)
```

```
            AIRMASS=1/COS(ZENARAD)
C     Using Erbs et al, from Solar Eng of Thermal Processes (2.10.1)
            KT=HHOR/HEXTRA
            IF    (KT.GT.0.80) THEN
                  IDI=0.165
            ELSE
                        IF (KT.GT.0.39) THEN
                        IDI=0.9511-(0.1604*KT)+(4.388*(KT**2))-
(16.638*(KT**3)
     &                  )+(12.336*(KT**4))
                        ELSE
                              IDI=1.0-(0.09*KT)
                        ENDIF
            ENDIF
C     RATIO OF BEAM RADIATION ON A TILTED SURFACE TO A HORIZONTAL
SURFACE
C     ASSUME THE CONCENTRATING COLLECTOR TRACKS PERFECTLY (THETA=0).
C     EQUATION 1.8.1 SOLAR ENGINEERING OF THERMAL PROCESSES
C     TOTAL HORIZONTAL IRRADIANCE CALCULATION, G IS W/M2-NM,
C     GBEAM IS IN W/M2-NM

          if (ATMS .eq. 0) then

          ! --- Fit to airmass 2.25 --- GOS

                DO 112 JI=1,NTOTAL
                  G(JI)=ET(JI)*EXP(-1*(KAPPA(JI)+(KAPPA2(JI)*TURBRATIO))
     1                  *AIRMASS)

112             CONTINUE

          else

          ! --- Use Smarts2 ---

              ! --- write data to smarts2.inp ---
             open(inpLU,file='Smarts2Data\smarts2.inp',status='unknown')
              write(inpLU,'(a)') "'Smarts2_input_(Type296)'"
              write(inpLU,'(a)')   "1"
C             write(inpLU,'(a,f5.3)') "1013.25 ",elevation
              write(inpLU,'(f7.2,a,f5.3)') PMBAR," ",elevation
              write(inpLU,'(a)') "1"
              write(inpLU,'(a)') "'USSA'"
              write(inpLU,'(a)') "0"
C             write(inpLU,'(a)') "1.42"
              write(inpLU,'(f5.2)') W
              write(inpLU,'(a)') "0"
              write(inpLU,'(a)') "0 0.34"
              write(inpLU,'(a)') "1"
              write(inpLU,'(a)') "370.0"
              write(inpLU,'(a)') "1"
              write(inpLU,'(a)') "'S&F_RURAL'"
              write(inpLU,'(a)') "1" !TMY2 doesn't specify, but values
look like Beta
```

```
              write(inpLU,'(f5.3)') TURB !Though TMY2 manual says data
between 0 and 270, actual data between 0 and 0.270
              write(inpLU,'(a)') "-1"
              write(inpLU,'(a)') "0.2"
              write(inpLU,'(a)') "0"
              write(inpLU,'(a)') "280 2500 1.0 1367.0"
              write(inpLU,'(a)') "2"
              write(inpLU,'(a)') "280 2500 5"
              write(inpLU,'(a)') "1"
              write(inpLU,'(a)') "2"
              write(inpLU,'(a)') "0"
              write(inpLU,'(a)') "0"
              write(inpLU,'(a)') "1"
              write(inpLU,'(a)') "0"
              write(inpLU,'(a)') "2"
              if(airmass .ge. 38.19) then
                  airmass = 38.19
              endif
              write(inpLU,'(f7.3)') airmass
              close(inpLU)

              ! --- Call smarts2 ---

              call smarts(1.0,2.0)

              ! --- Read data from smarts2.ext ---

             open(extLU,file='Smarts2Data\smarts2.ext',status='old')
             read(extLU,'(a2000)') dumString
             read(extLU,*) smartsOutput
             G=smartsOutput(2,:)
             close(extLU)

          endif

          ! Set GBeam = G

          GBEAM = G

          ! Hoz is the total beam radiation in kJ/h/m2

          HOZ=sum(G)*5*3.6

C     WHEN THE INTEGRATED RADIATION BOTH BEAM AND TOTAL HORIZONTAL
C     IS DIFFERENT THAN THE RESULTS FROM THE RADIATION PROCESSOR
C     SCALEFAC SCALES THE SMARTS2 INTEGRATED BEAM RESULTS TO MATCH
C     THE LEVELS OF THE RADIATION PROCESSOR.
            SCALEFAC=TBEAM/(HOZ*1.01) ! 1.01 to account for power >
2500 nm
            DO 114 JK=1,NTOTAL
C     SCALE BEAM RADIATION, AND INTEGRATE TO COMPARE WITH TRNSYS OUTPUT
                  GBEAMA(JK)=GBEAM(JK)*SCALEFAC
                  BEAMA=BEAMA+GBEAMA(JK)*5 !Beam A in W/m2
C     PRIMARY MIRROR REFLECTANCE LOSSES
                  GRONE(JK)=GBEAMA(JK)*RHO(JK)*.01
```

```
C     COLD MIRROR LOSSES R - REFLECTANCE, T - TRANSMITTANCE,IGNORING
ABSORPTION
                  GRTWO(JK)=GRONE(JK)*RHOCM(JK)*.01
                  GTTWO(JK)=GRONE(JK)*(1-(RHOCM(JK)*.01))
C     LOSS DUE TO REFLECTION AT QUARTZ ROD ENTRANCE
              GRTHREE(JK)=GRTWO(JK)*(1.0-(RHOQENT*.01))
C     LOSS DUE TO REFLECTION AT QUARTZ ROD EXIT
              GRFOUR(JK)=GRTHREE(JK)*(1.0-(RHOQEX*.01))
C     LOSS DUE TO FIBER PACKING
              GRFIVE(JK)=GRFOUR(JK)*(1.0-(LPACK*.01))
C     EFFICACY CALCULATION
                  IF (LAMBDA(JK).LT.360) THEN
                        GVIS(JK)=0
                        GEFF(JK)=0
                  ELSE
                        IF (LAMBDA(JK).GT.830) THEN
                              GVIS(JK)=0
                              GEFF(JK)=0
                        ELSE
                              GEFF(JK)=GRFIVE(JK)*TAULAMBDA(JK)

      GVIS(JK)=GRFIVE(JK)*TAULAMBDA(JK)*PHOTOPIC(JK)*683
                        ENDIF
                  ENDIF
114         CONTINUE
      ENDIF




C     INTEGRATE RESULTS OF VISIBLE ENERGY
C     LIGHT IS IN LUMENS/M2
      DO 130 JK=1,NTOTAL
      LIGHT=LIGHT+GVIS(JK)*5
      LIGHTEFF=LIGHTEFF+GEFF(JK)*5
130   CONTINUE
      LIGHT=LIGHT*NUMBEROF*CAREA*LUMEFFIC
      SYSEFF=(LIGHTEFF)/((TBEAM/3.6))
C     ENDIF

C     Calculate the Chromaticity if CALCCT = 1

      IF (CALCCT.EQ.1) THEN
C     will calculate the CCT of incident beam radiation if sun above
horizon
C     finds the inside spectrum of the sunlight GHLS() for chromaticity
calculations
          if (ZENA.LE.89) then
              CCTOUTSIDE = 1
              DO 140 JK=1,NTOTAL
                  IF (LAMBDA(JK).LT.360) THEN
                                GHLS(JK)= 0.0
```

```
                    ELSE
                      IF (LAMBDA(JK).GT.830) THEN
                            GHLS(JK)=0.0
                        ELSE
                            GHLS(JK)=GEFF(JK)*CAREA*NUMBEROF*LUMEFFIC
                        ENDIF
                    ENDIF
C               WRITE(SPD,*) JK,LAMBDA(JK),GEFF(JK),GHLS(JK)
140         CONTINUE
        else
            CCTOUTSIDE = 0
            DO 142 JK=1,NTOTAL
                GHLS(JK)=0
142         CONTINUE
        endif



C     will calculate inside CCT if the conventional lights aren't on
but there is sun
C     sets GINSIDE() to the spectrum of light delivered by HLS

        if (LFLGIN.LT.1.0) then
                CCTINSIDE = 0
                DO 146 JK=1,NTOTAL
                    GINSIDE(JK) = 0.0
146             CONTINUE
C            endif
C     calculation of CCT with conventional lights on
        else
            CCTINSIDE = 1
            LOADLNH=((BLDGAREA)*LIGHTLEV)
            if (ZENA.LE.89) then
                if (LOADLNH.GT.LIGHT) then
                    LUMENSCONV = LOADLNH-LIGHT
                    LFract = LIGHT/LOADLNH
                    if (LFract.GE.0.95) then
                        LF100 = 1
                    else if (LFract.GE.0.85) then
                        LF90 = 1
                    else if (LFract.GE.0.75) then
                        LF80 = 1
                    else if (LFract.GE.0.65) then
                        LF70 = 1
                    else if (LFract.GE.0.55) then
                        LF60 = 1
                    else if (LFract.GE.0.45) then
                        LF50 = 1
                    else if (LFract.GE.0.35) then
                        LF40 = 1
                    else if (LFract.GE.0.25) then
                        LF30 = 1
                    else if (LFract.GE.0.15) then
                        LF20 = 1
                    else if (LFract.GE.0.05) then
```

```
                        LF10 = 1
                    else
                        LF0 = 1
                    endif
                else
                    LF100 = 1
                    LUMENSCONV = 0
                endif

                DO 148 JK=1,NTOTAL
                    GCONV(JK)=LUMENSCONV*AMR16(JK)
                    GINSIDE(JK)=GCONV(JK)+GHLS(JK)
148             CONTINUE
            else
                LF0 = LF0+1
                LUMENSCONV=LOADLNH
                DO 150 JK=1,NTOTAL
                    GCONV(JK)=LUMENSCONV*AMR16(JK)
                    GINSIDE(JK)=GCONV(JK)
150             CONTINUE
            endif

        endif



C       calculates outside CCT
        IF(CCTOUTSIDE.EQ.1) then
            U1sum = 0.0
            V1sum = 0.0
            W1sum = 0.0
            DO 160 JK = 1,NTOTAL
                Ubar = XBAR(JK)*2/3
                Vbar = YBAR(JK)
                Wbar = -0.5*XBAR(JK)+1.5*YBAR(JK)+0.5*ZBAR(JK)
                U1lam(JK) = GBEAMA(JK)*Ubar*5
                V1lam(JK) = GBEAMA(JK)*Vbar*5
                W1lam(JK) = GBEAMA(JK)*Wbar*5
                U1sum = U1sum+U1lam(JK)
                V1sum = V1sum+V1lam(JK)
                W1sum = W1sum+W1lam(JK)
160         CONTINUE
            U1 = U1sum/(U1sum+V1sum+W1sum)
            V1 = V1sum/(U1sum+V1sum+W1sum)
            DO 170 JK = 1,ITOT
          Diso1(JK) = (V1-vT(JK)-tT(JK)*(U1-
uT(JK)))/(1+tT(JK)**2)**.5
            IF (Diso1(JK)<0) THEN
                DCOMB = Diso1(JK-1)/(Diso1(JK-1)-Diso1(JK))
                CCT1 = 1/(1/Tbb(JK-1)+DCOMB*(1/Tbb(JK)-1/Tbb(JK-1)))
                EXIT
                IF (ITOT.EQ.31) then
                    CCT1 = 0.0
                ENDIF
            ENDIF
```

```
170           CONTINUE
          ELSE
              CCT1=0.0
          ENDIF
C         calculates inside CCT
          IF(CCTINSIDE.EQ.1) then
              U2sum = 0.0
              V2sum = 0.0
              W2sum = 0.0
              DO 180 JK = 1,NTOTAL
                  Ubar = XBAR(JK)*2/3
                  Vbar = YBAR(JK)
                  Wbar = -0.5*XBAR(JK)+1.5*YBAR(JK)+0.5*ZBAR(JK)
                  U2lam(JK) = GINSIDE(JK)*Ubar*5
                  V2lam(JK) = GINSIDE(JK)*Vbar*5
                  W2lam(JK) = GINSIDE(JK)*Wbar*5
                  U2sum = U2sum+U2lam(JK)
                  V2sum = V2sum+V2lam(JK)
                  W2sum = W2sum+W2lam(JK)
C                 WRITE(SPD,*) ET(JK),GBEAM(JK),GBEAMA(JK)
180           CONTINUE
              U2 = U2sum/(U2sum+V2sum+W2sum)
              V2 = V2sum/(U2sum+V2sum+W2sum)
              DO 190 JK = 1,ITOT
            Diso2(JK) = (V2-vT(JK)-tT(JK)*(U2-
uT(JK)))/(1+tT(JK)**2)**.5
                  IF (Diso2(JK)<0) THEN
                      DCOMB = Diso2(JK-1)/(Diso2(JK-1)-Diso2(JK))
                   CCT2  =  1/(1/Tbb(JK-1)+DCOMB*(1/Tbb(JK)-1/Tbb(JK-1)))
                      if (CCT2.GE.5250.0) then
                          CT5500 = 1
                      else if (CCT2.GE.4750.0) then
                          CT5000 = 1
                      else if (CCT2.GE.4250.0) then
                          CT4500 = 1
                      else if (CCT2.GE.3750) then
                          CT4000 = 1
                      else if (CCT2.GE.3250) then
                          CT3500 = 1
                      else
                          CT3000 = 1
                      endif
                      EXIT
                  ENDIF
                  IF (ITOT.EQ.31) then
                      CCT2 = 0.0
                  ENDIF
190           CONTINUE
C             Calculates CRI of indoor light
              IF(CALCRI.GT.0.AND.CCT2.GT.1.0) THEN
                  ! calculate BB spectrum based on CCT2, use as
reference for all right now
                  C1 = 3.7418*10**8 !W-µm^4/m^2
                  C2 = 14388 !µm-K
                  deltawv = .005 !µm
```

```
                DO 191 JK = 1,95
                    wvlng(JK) = 355+JK*5 !nm
                    wvlng2 = wvlng(JK)/1000.0 !μm
                   BB(JK) = (C1*(wvlng2**(-5))*(EXP(C2/(wvlng2*CCT2))
     &-1)**(-1))*deltawv
C               WRITE(SPD,*) wvlng(JK),BB(JK)
191             CONTINUE
                ! calculate Y for reference (r) and indoor (k)
spectrums
C     Add 16 to JK indices below because want them to start at 360nm,
not 280 nm
C     go to 95 in loop because want to go to 830 nm
                Yr_T = 0.0
                Yk_T = 0.0
                DO 192 JK=1,95
                    Yr_(JK)=BB(JK)*YBAR(JK+16)
                    Yk_(JK)=GINSIDE(JK+16)*YBAR(JK+16)
                    Yr_T = Yr_T+Yr_(JK)
                    Yk_T = Yk_T+Yk_(JK)
192             CONTINUE
                !find scale factors
                SF_r = 100.0/Yr_T
                SF_k = 100.0/Yk_T
                !generate scaled reference and indoor spectrums
                DO 193 JK=1,95
                    Pr(JK)=SF_r*BB(JK)
                    Pk(JK)=SF_k*GINSIDE(JK+16)
C                     WRITE(SPD,*) wvlng(JK),Pr(JK),Pk(JK)
193             CONTINUE
                !find X,Y,Z and uv of scaled spectrums, noB refers to
source, not reflected
                Xr_noB = 0.0
                Yr_noB = 0.0
                Zr_noB = 0.0
                Xk_noB = 0.0
                Yk_noB = 0.0
                Zk_noB = 0.0
                Do 194 JK=1,95
                    Xr_noB = Xr_noB+Pr(JK)*XBAR(JK+16)
                    Yr_noB = Yr_noB+Pr(JK)*YBAR(JK+16)
                    Zr_noB = Zr_noB+Pr(JK)*ZBAR(JK+16)
                    Xk_noB = Xk_noB+Pk(JK)*XBAR(JK+16)
                    Yk_noB = Yk_noB+Pk(JK)*YBAR(JK+16)
                    Zk_noB = Zk_noB+Pk(JK)*ZBAR(JK+16)
194             CONTINUE
                !calculate chromaticity coordinate of r and k
spectrums
                ur_noB = 4*Xr_noB/(Xr_noB+15*Yr_noB+3*Zr_noB)
                vr_noB = 6*Yr_noB/(Xr_noB+15*Yr_noB+3*Zr_noB)
                uk_noB = 4*Xk_noB/(Xk_noB+15*Yk_noB+3*Zk_noB)
                vk_noB = 6*Yk_noB/(Xk_noB+15*Yk_noB+3*Zk_noB)
                !calculate variables that will help account for
chromatic shift
                cr = (4-ur_noB-10*vr_noB)/vr_noB
                cks = (4-uk_noB-10*vk_noB)/vk_noB
```

```
                  dr = (1.708*vr_noB+0.404-1.481*ur_noB)/vr_noB
                  dks = (1.708*vk_noB+0.404-1.481*uk_noB)/vk_noB
                  !transformed k chromaticity coordinates
                  uk_noB_t = (10.872+0.404*(cr/cks)*cks-
4*(dr/dks)*dks)/
     &(16.518+1.481*(cr/cks)*cks-(dr/dks)*dks)
                  vk_noB_t = 5.520/(16.518+1.481*(cr/cks)*cks-(dr/dks)*
     &dks)
                  !find the XYZ an uv coordinates of each of the 8
color samples
                  !illuminated by Pr then by Pk
                  RT = 0.0
                  DO 196 i = 1,8
                      Xr(i)=0.0
                      Yr(i)=0.0
                      Zr(i)=0.0
                      Xk(i)=0.0
                      Yk(i)=0.0
                      Zk(i)=0.0
                      DO 195 JK=1,95
                          Xr(i)=Xr(i)+Pr(JK)*B(i,JK)*XBAR(JK+16)
                          Yr(i)=Yr(i)+Pr(JK)*B(i,JK)*YBAR(JK+16)
                          Zr(i)=Zr(i)+Pr(JK)*B(i,JK)*ZBAR(JK+16)

                          Xk(i)=Xk(i)+Pk(JK)*B(i,JK)*XBAR(JK+16)
                          Yk(i)=Yk(i)+Pk(JK)*B(i,JK)*YBAR(JK+16)
                          Zk(i)=Zk(i)+Pk(JK)*B(i,JK)*ZBAR(JK+16)
195                   CONTINUE
                  ur(i) = 4*Xr(i)/(Xr(i)+15*Yr(i)+3*Zr(i))
                  vr(i) = 6*Yr(i)/(Xr(i)+15*Yr(i)+3*Zr(i))
                  uk(i) = 4*Xk(i)/(Xk(i)+15*Yk(i)+3*Zk(i))
                  vk(i) = 6*Yk(i)/(Xk(i)+15*Yk(i)+3*Zk(i))
                  !now uk and vk must be changed to account for
chromatic adaption
                  ck(i) = (4-uk(i)-10*vk(i))/vk(i)
                  dk(i) = (1.708*vk(i)+0.404-1.481*uk(i))/vk(i)
                  uk_t(i) =(10.872+0.404*(cr/cks)*ck(i)-4*(dr/dks)*
     &dk(i))/(16.518+1.481*(cr/cks)*ck(i)-(dr/dks)*dk(i))
                  vk_t(i) =5.520/(16.518+1.481*(cr/cks)*ck(i)-(dr/dks)*
     &dk(i))
                  !transform to 1964 uniform space coordinates
                  WSr(i)=(25*Yr(i)**0.333333333)-17
                  USr(i)=13*WSr(i)*(ur(i)-ur_noB)
                  VSr(i)=13*WSr(i)*(vr(i)-vr_noB)

                  WSk(i)=(25*Yk(i)**0.333333333)-17
                  USk(i)=13*WSk(i)*(uk_t(i)-uk_noB_t)
                  VSk(i)=13*WSk(i)*(vk_t(i)-vk_noB_t)

                  !resultant color shift of each sample
                  DELE(i)=((USr(i)-USk(i))**2+(VSr(i)-VSk(i))**2+
     &(WSr(i)-WSk(i))**2)**0.5

                  !Rendering index of each sample
                  R(i)=100-4.6*DELE(i)
```

```
                  RT=RT+R(i)
196               CONTINUE
                  !calculate CRI
                  CRI = RT/8.0
                  if (CRI.GE.95) then
                      CRI100 = 1
                  else if (CRI.GE.85) then
                      CRI90 = 1
                  else if (CRI.GE.75) then
                      CRI80 = 1
                  else if (CRI.GE.65) then
                      CRI70 = 1
                  else if (CRI.GE.55) then
                      CRI60 = 1
                  else
                      CRI50 = 1
                  endif
              ELSE
                  CRI = 0.0
              ENDIF
          ELSE
              CCT2 = 0.0
              CRI = 0.0
          ENDIF
          IF (ZENA.GT.89) then
              CCT1 = 0.0
              CCT2 = 0.0
              CRI = 0.0
          ENDIF
      ELSE
      U1=0.0
      V1=0.0
      CCT1 = 0.0
      U2 = 0.0
      V2 = 0.0
      CCT2 = 0.0
      CRI = 0.0
      ENDIF

C
C
      *****************************************************************
*
C     *
                                *
C     *           THERMAL PHOTOVOLTAIC LIGHT CURRENT CALCULATION
       *
C     *
                                *
C
      *****************************************************************
*
C
C     THE ARRAY USED IN THE HYBRID LIGHTING SYSTEM IS MADE OF GASB
CELLS.
```

```
C     THE FIRST STEP OF THE CALCULATION IS TO CONVERT THE INCCOMING
C     IRRADIANCE INTO PHOTONS, NEXT APPLY THE QE, CALCULATE THE AMOUNT
OF
C     RESULTING FREE ELECTRONS, AND CALCULATE THE ASSOCIATED CURRENT.
C     1240 IS A CONSTANT WHICH FACTORS INTO ACCOUNT PLANCK'S
CONSTANT(h),
C     THE CHARGE OF AN ELECTRON(e), AND THE SPEED OF LIGHT IN A
VACUUM(c).
C     0.01 IS INCLUDED TO REPRESENT ONE CELL OF THE 100 CELL ARRAY

      DO 200 JK=1,NTOTAL
      PHOTONI(JK)=(CAREA/1240)*(GTTWO(JK)*ETA_QE(JK)*LAMBDA(JK)*0.01)
      ELEC=ELEC+PHOTONI(JK)*5
200   CONTINUE

C
      *****************************************************************
*
C     *
                               *
C     *                                    I-V MODEL
                        *
C     *
                               *
C
      *****************************************************************
*
      VOC=47.72
      IMAX=5.13
      VMAXARRAY=34.52
      MUISC=0.00031
      MUVOC=-0.001205
      TCREF=298
      TC=273+25
      EPSILON=0.382
      NS=100

C     NO REFERENCE IRRADIANCE WAS AVAILABLE FOR THE ARRAY, GUESS VALUE
C     OF 850 W/M2 WORKS WELL, (SEE FRAAS,L. ET AL., PP.3, 2002.)
      GT=BEAMA
      GTREF=850

C     IRRADIANCE TO MATCH THE MEASURED SHORT CIRCUIT CURRENT.
      ISC=ELEC

C     RESET TPV ARRAY ELECTRICAL CURRENT GUESS VALUE
      I=5

C     PROTECTION AGAINST SMALL LIGHT CURRENT
      IF (ISC.LT.0.05) THEN
            P=0
            LIGHT=0
            GOTO 600
      ELSE
```

```
C     DUFFIE & BECKMAN, EQ 23.2.3.,23.2.11.,23.2.4.
C     "REFERENCE CONDITIONS"
      ILREF=ISC
      AREF=(MUVOC*TCREF-VOC+EPSILON*NS)/(((MUISC*TCREF)/ILREF)-3)
      IOREF=ILREF*exp(-VOC/AREF)

C     CELL TEMPERATURE CONDITIONS
C     DUFFIE & BECKMAN, EQ 23.2.6.,23.2.7.,23.2.8.,23.2.5
      A=(TC/TCREF)*AREF
      IL=(GT/GTREF)*(ILREF+MUISC*(TC-TCREF))
      IO=IOREF*((TC/TCREF)**3*exp(((EPSILON*NS)/AREF)*(1-(TCREF/TC))))
      RSREF=(AREF*LOG(1-MIN(0.9,IMAX/ILREF))-VMAXARRAY+VOC)/IMAX

C     ASSUME SERIES RESISTANCE TO BE INDEPENDENT OF TEMPERATURE
      RS=RSREF

C     ASSUME LOAD MATCHES MAX ARRAY VOLTAGE
      V=VMAXARRAY

C     DUFFIE & BECKMAN, EQ 23.2.1
C     NEGLECT LAST TERM OF EQUATION 23.2.1 DUE TO LARGE SHUNT
RESISTANCE
C     BOTH VERSIONS OF EQUATIONS ARE THE SAME
C     V=A*LOG(MAX(0.01,(IL+IO-I)/IO))-I*RS
      I=IL-IO*(exp((V+I*RS)/A)-1)
C     LIMIT CURRENT TO POSTIIVE VALUES
      I=MAX(0.0,I)
C     THE COOLING FAN CONSUMES 5 WATTS OF POWER, OPTEFF IS THE OPTICAL
C     LOSSES ASSOCIATED WITH THE NON-IMAGING OPTICAL DEVICE
      P=((I*V)-5)*NUMBEROF*OPTEFF
      ENDIF


      GOTO 600

C
      *****************************************************************
*
C     *
                                 *
C     *                                    WIDE BAND MODEL
                           *
C     *
                                 *
C
      *****************************************************************
*

500   KAPPATAUAVG=-1.0*LOG(1.0-(ATTENAVG/100))
      TAU=EXP(-1.0*KAPPATAUAVG*FIBERLENGTH)
C     200 IS THE APPROXIMATE EFFICACY OF FILTERED SOLAR RADIATION
      LIGHT=NUMBEROF*RHO1*RHO2*TUBEREFL*VISPECTR*(TBEAM/3.6)*CAREA*TAU*
     &LUMEFFIC*200
      P=NUMBEROF*RHO1*FILTERIR*(TBEAM/3.6)*IRSPECTR*CAREA*TPVEFFIC*
     &OPTEFF
```

```
      SYSEFF=RHO1*RHO2*TUBEREFL*TAU*LUMEFFIC
      GOTO 600

C     DAYLIGHTING COMPARISON; 100 IS APPROXIMATE EFFICACY OF UNFILTERED
C     SUNLIGHT, 0.65 IS THE WELL EFFICIENCY, 0.7 IS A FACTOR TO ACCOUNT
C     FOR DIRT ON THE SKYLIGHT.  SEE IESNA LIGHTING HANDBOOK, 2000.
550   LIGHT=NUMBEROF*(HHOR/3.6)*SLAREA*SLTAU*100*.65*.7
      GOTO 600

C
      ****************************************************************
*
C     *
                                 *
C     *                                   FORMERLY TYPE 291
                     *
C     *
                                 *
C
      ****************************************************************
*

C     CALCULATE LOADS ASSOC WITH LIGHTING - LOADLNH IN LUMENS
600   IF (LFLGIN .LT. 1.0) THEN
            LOADLNH=0
            ELSE
            LOADLNH=((BLDGAREA)*LIGHTLEV)
      ENDIF

C     WILL HAVE TO ADD SOMETHING HERE TO IF HLS CAN BE TURNED OFF
C     CHECK TO SEE IF VAR LIGHT IS LARGER THAN NORMAL LOAD
      IF(LIGHT .GT. LOADLNH) THEN
            LOADLH=0
            XTRALGHT=LIGHT-LOADLNH
      ELSE
            LOADLH=LOADLNH-LIGHT
            XTRALGHT=0
      ENDIF

C     SCALE OF THERMAL LOAD ASSOCIATED WITH LIGHTING LOAD, BASED ON
C     ILLUMINATION LEVEL IN LUX, EFFICACY OF LAMP USED IN BLDG, AND A
C     BUILDING LIGHTING GAIN OF 10 W/M2.
      LSCALE=(LIGHTLEV/LAMPEFF)/10

C     NORMALIZED OUTPUT FOR TYPE 56 RECALCULATION OF
HEATING/COOLINGLOADS
C     LFLGOUT IS SENT TO THE TYPE 56 BLDG MODEL WHICH HAS A THERMAL
GAIN
C     DUE TO LIGHTING OF 10 W/M2 WHICH CANCELS OUT THE SEEMINGLY RANDOM
C      10 W/M2 IN THE DENOMINATOR OF LSCALE.
      IF (LOADLNH .GT. 0) THEN
            LF=(LOADLH/LOADLNH)
C           LFLGOUT=LSCALE*LF
```

```
C     SUNLIGHT IS SENT TO TYPE 56 TO CALCULATE FRACTION OF HEAT OF
ORIGINAL
C     LIGHTING WHICH IS CONTAINED IN NATURAL LIGHT.  ASSUMED THE
EFFICACY OF
C     FILTERED SUNLIGHT TO BE 200 LM/W.
C     THE GAIN IN THE TYPE 56 BLDG MODEL SHOULD BE SET UP WITH A
C     SCHEDULE OF 1 (ALWAYS ON), AND A SCALE OF 1*SUNLIGHT.
            SUNLIGHT=((1-(LOADLH/LOADLNH))*(LOADLNH/NLEFF))*3.6
      ELSE
            LF=0
C           LFLGOUT=1*LSCALE
            SUNLIGHT=0
      ENDIF

C     ON DAYS WHEN THERE IS TOO MUCH LIGHT THE THERMAL ENERGY OF THE
C     ADDTIONAL LIGHT IS ADDED TO THE BUILDING LOAD, UNITS OF KJ/HR.
C     THE GAIN IN THE TYPE 56 BLDG MODEL SHOULD BE SET UP WITH A
C     SCHEDULE OF 1 (ALWAYS ON), AND A SCALE OF 1*XTRAHEAT.
      XTRAHEAT=(XTRALGHT/NLEFF)*3.6

C     CONVERT LIGHTING LOADS FROM LUMEN-HRS TO KWH
      LLNH=(LOADLNH/LAMPEFF)/1000

C     DETERMINE CONTROL STARTEGY AND DIRECT TRAFFIC
      IF (CONTROL.EQ.0) THEN
            GOTO 800
            ELSE
                  IF (CONTROL.EQ.1) THEN
                        GOTO 900
                        ELSE
                              IF (CONTROL.EQ.2) THEN
                                    GOTO 1000
                                    ELSE
                                          IF (CONTROL.EQ.3) THEN
                                                GOTO 950
                                                ELSE
                                                      GOTO 1100
                                          ENDIF
                              ENDIF
                  ENDIF
      ENDIF


C     HYBRID LIGHTING LOAD WITHOUT DIMMABLE BALLASTS
800   LLH=(LOADLH/LAMPEFF)/1000
      LFLGOUT=LSCALE*LF
      GOTO 1200

C     HYBRID LIGHTING LOAD WITH DIMMABLE BALLASTS
C     BASED ON ELECTRONIC BALLASTS AND F32T8 LAMPS
C     BASICALLY THE LIGHTING EFFICACY DECREASES WHEN THE BULBS
C     ARE DIMMED
C     IF THE LIGHT FRACTION IS LESS THAN 0.20 THE BUILDING WILL
C     BE UNDER-ILLUMINATED IN THE SPIRIT OF CONSERVATION.
900   IF(LF.EQ.0.00) THEN
```

```
      LLH=0
      LFLGOUT=0
            ELSE
            IF (LF.LT.0.20) THEN
            LLH=0
            LFLGOUT=0
            ELSE
                  NAP=(((LF*100)+29.701847)/(1.81576002*71.43))
                  NEWEFF=MIN(LAMPEFF,(LAMPEFF*(LF/NAP)))
                  LLH=LOADLH/(NEWEFF*1000)
                  LFLGOUT=(LIGHTLEV/(NEWEFF*10))*LF
            ENDIF
      ENDIF
      GOTO 1200

C     IF THE LIGHT FRACTION IS LESS THAN 0.20 THE BUILDING WILL
C     BE OVER-ILLUMINATED IN THE SPIRIT OF WASTE.
950   IF(LF.EQ.0.00) THEN
      LLH=0
      LFLGOUT=0
            ELSE
            IF (LF.LT.0.20) THEN
            LLH=(LOADLNH*.20)/(44*1000)
            LFLGOUT=(LIGHTLEV/(44*10))*.2
            ELSE
                  NAP=(((LF*100)+29.701847)/(1.81576002*71.43))
                  NEWEFF=MIN(LAMPEFF,(LAMPEFF*(LF/NAP)))
                  LLH=LOADLH/(NEWEFF*1000)
                  LFLGOUT=(LIGHTLEV/(NEWEFF*10))*LF
            ENDIF
      ENDIF
      GOTO 1200

C     STAGING CONTROLS
1000  IF (LF.EQ.0) THEN
            LLH=0
            LFLGOUT=0
            ELSE
                  IF (LF.GT.(1-(1/MULT))) THEN
                        LLH=LLNH
                        LFLGOUT=LSCALE
                        ELSE
                        DO 1001 Z=2,MULT
                              IF (LF.GT.(1-(Z*(1/MULT)))) THEN
                                    LLH=(1-((Z-1)*(1/MULT)))*LLNH
                                    LFLGOUT=(1-(Z*(1/MULT)))*LSCALE
                                    GOTO 1002
                              END IF
1001                    CONTINUE

1002              ENDIF
      ENDIF
      GOTO 1200

C     STAGING CONTROLS WITH DIMMABLE BALLASTS
```

```
1100  IF (LF.EQ.0) THEN
            LLH=0
            LFLGOUT=0
            ELSE
                  IF (LF.GT.(1-(1/MULT))) THEN
                        NAP=(((LF*100)+29.701847)/(1.81576002*71.43))
                        NEWEFF=MIN(LAMPEFF,(LAMPEFF*(LF/NAP)))
                        LLH=LOADLH/(NEWEFF*1000)
                        LFLGOUT=(LIGHTLEV/(NEWEFF*10))*LF
                        ELSE
                              DO 1101 Z=2,MULT
                              IF (LF.GT.(1-(Z*(1/MULT)))) THEN
                                    NLF=LF/(1-((Z-1)*(1/MULT)))

      NAP=(((NLF*100)+29.701847)/(1.81576002*71.43))

      NEWEFF=MIN(LAMPEFF,(LAMPEFF*(NLF/NAP)))
                                    LLH=LOADLH/(NEWEFF*1000)
                                    LFLGOUT=(LIGHTLEV/(NEWEFF*10))*LF
                                    GOTO 1102
                              ENDIF
1101                          CONTINUE
1102              ENDIF
      ENDIF

C     DETERMINE WHETHER THE LATENT LOAD IS ASSOCIATED WITH COOLING(+)
C     OR HEATING(-)
1200  IF (LATENT .GT. 0) THEN
            LATENTCOOL=LATENT
            LATENTHEAT=0
      ELSE
            LATENTHEAT=ABS(LATENT)
            LATENTCOOL=0
      ENDIF

      IF (BLATENT .GT. 0) THEN
            BLATENTCOOL=BLATENT
            BLATENTHEAT=0
      ELSE
            BLATENTHEAT=ABS(BLATENT)
            BLATENTCOOL=0
      ENDIF

C     CALCULATION OF THE TOTAL HEATING & COOLING LOADS
C     CONVERSION FROM KJ TO KWH
      HEAT=((SHEAT+LATENTHEAT)/3600.00)
      COOL=((SCOOL+LATENTCOOL)/3600.00)
      BASEHEAT=(BHEAT+BLATENTHEAT)/3600.0
      BASECOOL=(BCOOL+BLATENTCOOL)/3600.0
      GOTO 300

C
      *****************************************************************
*
```

```
C     *
                                *
C     *                                    P1,P2 ANALYSIS
                         *
C     *
                                *
C
      ****************************************************************
*

C     DUFFIE & BECKMAN,EQ.11.8.2
700   ZERO=0
      P1=(1-(IFLAG*TBAR))*PWF(N_E,INF,DIS)

C     DUFFIE & BECKMAN,EQ.11.8.3
      NMIN=MIN(N_E,N_L)
      NMIN1=MIN(N_E,N_D)
      A1=DOWN+(1-DOWN)*PWF(NMIN,ZERO,DIS)/PWF(N_L,ZERO,M)
      A2=TBAR*(1-DOWN)*(PWF(NMIN,M,DIS)*(M-1/PWF(N_L,ZERO,M))+PWF(NMIN,
     &ZERO,DIS)/PWF(N_L,ZERO,M))
      A3=M_S*(1-IFLAG*TBAR)*PWF(N_E,INF,DIS)
      A4=PRTAX*VAL*(1-TBAR)*PWF(N_E,INF,DIS)
      A5=IFLAG*TBAR*PWF(NMIN1,ZERO,DIS)/MAX(N_D,1.0)
      A6=R_V*(1-IFLAG*TBAR)/(1+DIS)**N_E
      P2=A1-A2+A3+A4-A5-A6

C     AES IS THE ANNUAL ENERGY SAVINGS PER SYSTEM
C     BECC IS THE BREAK EVEN CAPITAL COST OF ONE SYSTEM
      AES=((CBLIGHT-CHLIGHT)+(BCCOST-HCCOST)+(BHCOST-HHCOST)+TPVREV)
     &/NUMBEROF
      BECC=(P1/P2)*AES

C     SET THE OUTPUTS FROM TYPE 291
300   OUT(1)=LFLGOUT
      OUT(2)=LLH
      OUT(3)=LLNH
      OUT(4)=COOL
      OUT(5)=BASECOOL
      OUT(6)=HEAT
      OUT(7)=BASEHEAT
      OUT(8)=LSCALE
      OUT(9)=SUNLIGHT
      OUT(10)=XTRAHEAT

C     SET THE OUTPUTS FROM ORGINAL TYPE 292
      OUT(11)=LIGHT
      OUT(12)=P

C     ECONOMIC OUTPUTS
      OUT(13)=P1
      OUT(14)=P2
      OUT(15)=AES
      OUT(16)=BECC
      OUT(17)=LATENTCOOL/3600.0
      OUT(18)=LATENTHEAT/3600.0
```

```
      OUT(19)=SYSEFF
C     CHROMATICITY OUTPUTS
      OUT(20)=U1
      OUT(21)=V1
      OUT(22)=CCT1
      OUT(23)=U2
      OUT(24)=V2
      OUT(25)=CCT2
      OUT(26)=AIRMASS
      OUT(27)=ZENA
      OUT(28)=HEXTRA
      OUT(29)=ETSum
      OUT(30)=TBEAM
      OUT(31)=BEAMA
      OUT(32)=HHOR
      OUT(33)=HOZ
      OUT(34)=SCALEFAC
      OUT(35)=LF0
      OUT(36)=LF10
      OUT(37)=LF20
      OUT(38)=LF30
      OUT(39)=LF40
      OUT(40)=LF50
      OUT(41)=LF60
      OUT(42)=LF70
      OUT(43)=LF80
      OUT(44)=LF90
      OUT(45)=LF100
      OUT(46)=TURB
      OUT(47)=CRI
      OUT(48)=W
      OUT(49)=CT5500
      OUT(50)=CT5000
      OUT(51)=CT4500
      OUT(52)=CT4000
      OUT(53)=CT3500
      OUT(54)=CT3000
      OUT(55)=CRI100
      OUT(56)=CRI90
      OUT(57)=CRI80
      OUT(58)=CRI70
      OUT(59)=CRI60
      OUT(60)=CRI50
      OUT(61)=elevation
      OUT(62)=PMBAR

1300  RETURN 1

      end subroutine type296

C
      *****************************************************************
*
C     *
                         *
```

```
C     *                                   FUNCTION DEFINTION
                         *
C     *
                               *
C
      *****************************************************************
*

C     DUFFIE & BECKMAN,EQ.11.5.1
      FUNCTION PWF(N,INF,DIS)
      DOUBLE PRECISION N,INF,DIS,PWF
      IF (DIS.EQ.INF) THEN
            PWF=N/(1+INF)
      ELSE
            PWF=(1/(DIS-INF))*(1-(((1+INF)/(1+DIS))**N))
      ENDIF
      END FUNCTION
```

# Bibliography

American Society of Heating, Refrigeration, and Air-conditioning Engineers (ASHRAE), *2001 ASHRAE Handbook - Fundamentals*, 2001.

American Society of Heating, Refrigeration, and Air-conditioning Engineers (ASHRAE), *Ventilation for Acceptable Indoor Air Quality, ASHRAE Standard 62-2001*, 2001.

Berman, S.M. (1992). Energy efficiency consequences of scotopic sensitivity. Journal of the Illuminating Engineering Society, 21, 3-14

Berry, J.L. (1983). Work efficiency and mood states of electronic assembly workers exposed to full spectrum and conventional fluorescent illumination. Dissertation Abstracts International, 44, 635B

Bielski, R.J.,Mayor, J.,&Rice,J. (1992) Phototherapy with broad spectrum white fluorescent light: A comparative study. Psychiatry Research, 43, 167-175.

Blackwell, H.R. (1985) Effects of light source spectral distribution upon visual functions. Annals of the New York Academy of Sciences, 453, 340-353

Boray, P.F., Gifford, R., & Rosenblood, L. (1989) Effects of warm white, cool white, and full spectrum fluorescent lighting on simple cognitive performance, mood, and ratings of others. Journal of Environmental Psychology, 9, 297-308.

Boyce, P.R. & Rea, M.S. (1993, August). A field evaluation of full spectrum, polarized lighting. Paper presented at the 1993 Annual Convention of the Illuminating Engineering Society of North America, Houston, TX.

Boyce, P.R. & Simons, R.H. (1977). Hue discrimination and light sources. Lighting Research and Technology, 9, 125-140.

Brainard, G.C., Sherry, D., Skwerer, R.G. (1990) Effects of different wavelengths in seasonal affective disorder. Journal of Affective Disorders, 20, 209-216

Department of Energy, *Annual Energy Outlook 2001 Market Trends – Energy Demand*, available at http://www.eia.doe.gov/oiaf/aeo/demand.html#comm, Dec. 2000.

Department of Energy, Energy Information Administration, available at http://www.eia.doe.gov/emeu/states /_states.html, 2003.

Duffie, J.A. and Beckman, W.A., *Solar Engineering of Thermal Processes*, 2nd Ed., John Wiley and Sons, 1991.

Dye, D., Wood, B.D., Fraas, L.M., Muhs, J.D., *Optical Design of an Infrared Non-Imaging Device for a Full Spectrum Solar Energy System*, International Solar Energy Conference, Kohala Coast, Hawaii Island, March 15-18, 2003.

Earl, D.D., Muhs, J.D., *Modeling and Evaluation of Chromatic Variations in a Hybrid Solar/Electric Lighting System*, International Solar Energy Conference, Kohala Coast, Hawaii Island, March 15-18, 2003a.

Earl, D.D., Maxey, C.L., Muhs, J.D., *Performance of New Hybrid Solar Lighting Luminaire Design*, International Solar Energy Conference, Kohala Coast, Hawaii Island, March 15-18, 2003b.

Fraas, L.M., Avery, J.E., Nakamura, T., *Electricity from Concentrated Solar IR in Solar Lighting Applications*, 29th IEEE Photovoltaic Specialists Conference, May 20-24, 2002.

Figueiro, M. G., Rea, M.S., Daylight and Productivity - A Possible Link to Circadian Regulation, Rensselaer Polytechnic Institute Lighting Research Center, 2003.

Figueiro, M. G., Bullough, J.D., Rea, M.S., Spectral Sensitivity of the Circadian System, Rensselaer Polytechnic Institute Lighting Research Center, 2003.

Gueymard, C., *Prediction and Performance Assessment of Mean Hourly Global Radiation*, Solar Energy, Vol. 68, No. 3, March, 2000.

Hellekson, C.J., Kline, J.A., & Rosenthal, N.E. (1986). Phototherapy for seasonal affective disorder in Alaska. American Journal of Psychiatry, 143 1035-1037.

Heschong Mahone Group, Skylighting and Retail Sales, Condensed Report, submitted to Pacific Gas and Electric Company August 20, 1999.

Hill, M.A. (1992). Light, circadian rhythms, and mood disorders: A review. Annals of Clinical Psychiatry, 4, 131-146.

Illuminating Engineering Society of North America (IESNA), *The IESNA Lighting Handbook: Reference and Application,* Illuminating Engineering Society of North America, New York, N.Y., 2000.

Kuller, R. & Wetterberg, L. (1993) Melatonin, cortisol, EEF, ECG and subjective comfort in healthy humans: Impact of two fluorescent lamp types at two intensities. Lighting Research and Technology, 25, 71-81.

Klein, S.A., et al., *TRNSYS, A Transient Simulation Program*, Solar Energy Laboratory, University of Wisconsin – Madison, USA, 2000.

Lewy, A.J., Sack, R.L., Miller, S., & Toban, T.M. (1987) Antidepressant and circadian phase shifting effects of light. Science, 235, 352-354

Maxey, L.D., Cates, M.R., Jaiswal, S.L., *Efficient Optical Couplings for Fiber-Distributed Solar Lighting*, International Solar Energy Conference, Kohala Coast, Hawaii Island, March 15-18, 2003b.

Muhs, J.D., *Hybrid Lighting Doubles the Efficiency and Affordability of Solar Energy in Commercial Buildings*, CADDET- Energy Efficient News Letter, No. 4, 2000a, p. 6 - 9.

Muhs, J.D., *Design and Analysis of Hybrid Solar Lighting and Full Spectrum Solar Energy Systems*, Proceedings of the American Solar Energy Society, Solar 2000, June16-21, 2000b, American Solar Energy Society.

Murdoch, Joseph B. Illumination Engineering - From Edison's Lamp to the Laser. New York:Macmillan Publishing Company, 1985,

National Lighting Product Information Program (NLPIP), *Dimming Electronic Ballasts, Specifier Reports*, available at http:\\www.lrc.rpi.edu, Vol.7, Number 3, October 1999.

Pande-Rolfsen, Trine, *Experimental Performance Evaluation of a Photoelectric Controlled Hybrid Lighting System*, The Norwegian University of Science and Technology, Dept. of Electrical Engineering, July 2003

Schlegel, G.O, *A TRNSYS Model of a Hybrid Lighting System*, Solar Energy Laboratory, University of Wisconsin – Madison, USA, June 2003

Schlegel, G., Burkholder, F., et. al., *Analysis of a Full Spectrum Hybrid Lighting System*, Solar Energy, Vol. 76, 2004, pp. 359-368

Tekelioglu, M., Wood, B.D., *Thermal Management of the Polymethylmethacrylate (PMMA) Core Optical Fiber for use in Hybrid Solar Lighting*, International Solar Energy Conference, Kohala Coast, Hawaii Island, March 15-18, 2003.

Typical Meterological Year 2 User's Manual, National Renewable Energy Laboratory, available at http://rredc.nrel.gov/solar/pubs/tmy2/

Veitch, J.A., Hine, D.W. & Gifford, R. (1993). End user's knowledge, preferences, and beliefs for lighting. Journal of Interior Design, 19(2), 15-26

Wurtman, R.J. (1975) The effects of light on the human body. Scientific American, 233, 68-77.